ATTACHMENT 5

CONTINUUM DYNAMICS, INC

CDI REPORT NO. 10-12NP

DESIGN AND STRESS EVALUATION OF NINE MILE POINT UNIT 2 STEAM DRYER MODIFICATIONS FOR EPU OPERATION

(NON-PROPRIETARY)

Information in this Attachment is proprietary.

Nine Mile Point Nuclear Station, LLC
July 30, 2010

CDI Report No. 10-12NP

Design and Stress Evaluation of Nine Mile Point Unit 2 Steam Dryer Modifications for EPU Operation

Revision 0

Prepared by

Continuum Dynamics, Inc.
34 Lexington Avenue
Ewing, NJ 08618

Prepared under Purchase Order No. 7708631 for

Constellation Energy Group
Nine Mile Point Nuclear Station, LLC
P. O. Box 63
Lycoming, NY 13093

Prepared by

Alexander H. Boschitsch

Approved by

Alan J. Bilanin

July 2010

This report complies with Continuum Dynamics, Inc. Nuclear Quality Assurance Program currently in effect.

Executive Summary

The stress assessment for the Nine Mile Point Unit 2 steam dryer at EPU conditions conducted in [1] using loads produced by the latest acoustic circuit model (ACM) Rev. 4.1 [2, 3] identified several locations requiring modification or reinforcement. Section 6 of [1] identifies four distinct groups of nodes that require modifications to obtain an alternating stress ratio of 2.0 at EPU conditions. Briefly, these groups consisted of the following:

(1) Nodes located on the weld connecting the lifting rod braces to the vane bank side plates. The end of each such weld has high stress despite weld reinforcement.
(2) Nodes on the weld lying on the inward edge of the middle hood reinforcement strip.
(3) The inner hood/hood support welds.
(4) All remaining nodes having alternating stress ratios between SR-a=2.65 and the CLTP target stress ratio of 2.76 (this value scales to 2.00 at EPU using the velocity-square scaling)

For Groups 1-3, modifications and reinforcement concepts were proposed, designed and analyzed on the basis of finite element calculations. For Group 1 several reinforcement concepts involving a thickening of the brace and/or local side plate were presented. For Group 2 it was proposed to attach a conforming 3/8" plate over the middle hood section lying between the existing reinforcement strip and closure plate. The Group 3 locations were successfully addressed by adding a total of four 20 lb masses on the central inner hood sections. While quantitative predictions of the stresses resulting with the modifications in place were produced, details pertaining to the designs such as the method of mass attachment or selection of the final brace reinforcement concept were not finalized. Finally, Group 4 locations were not considered in detail because the limiting alternating stress ratios are all within 4% of the target value of 2.76. Given the presence of significant noise (which does not scale with the square of steam flow speed) the prospect is high that during power ascension the alternating stress ratio remains above 2.0 and the need for reinforcement becomes redundant. Nevertheless reinforcement concepts for all members of Group 4 were presented, though stress evaluations of the concepts were either limited or qualitative in nature.

Following a summary of the main results in [1] and review of the evaluation procedures used in Sections 1 and 2, the present report continues in Section 3 by performing a more detailed and quantitative assessment of the reinforcements proposed for all limiting nodes in Groups 1-4. The section also provides additional details on the modifications including added mass dimensions, attachment and reinforcement weld sizes and operational considerations that either drive the design or are judged significant from a stress evaluation vantage point. For Group 1 a down-selection to one concept is performed and details provided for the lifting rod brace reinforcement. For Group 2 the thickness of the middle hood covering plate is reduced from 3/8" to 1/8". The inner hood vibrations are attenuated by attaching masses to these hoods. The required masses are reduced from 20 lbs to 15 lbs and details of the mass geometry are provided.

For the Group 4 locations the provisional concepts outlined in Section 6 of [1] are developed in further detail and quantitative assessments performed. Specifically:

- The bottom of the skirt/drain channel weld is reinforced with a wrap-around weld and evaluated with the aid of a sub-model raising the alternating stress ratio from SR-a=2.65 before modification up to SR-a=4.09 with the wrap around weld.
- The middle hood/hood support weld stresses with limiting SR-a=2.68 are alleviated by attaching a total of four 10 lb masses to the central sections of the middle hoods resulting in a limiting SR-a=4.05.
- The common intersections between the outer hood, hood support and cover plate with limiting SR-a=2.65 are addressed by inserting a semi-circular stress relief cutout in the hood support and re-evaluating the proximate stresses with the aid of a sub-model. The location and size of the cut-out is optimized to achieve a stress reduction factor, SRF=0.73 and limiting SR-a=2.87 at these locations. The stress relief accomplished by this modification is also of importance towards ensuring that existing flaws at these locations do not propagate further when ascending to EPU conditions.

Section 3 concludes with details of the geometry and modeling of the closure plate reinforcement ribs.

Section 4 provides summarizing tables of the post-reinforcement stress states at the limiting nodes in Groups 1-4. In addition, stress results for the complete dryer are presented to demonstrate that the complete dryer with all modifications in place meets the specified EPU target stress levels. This ensures that the modifications produced do not inadvertently introduce new high stress locations due to reshifting of stress paths and/or frequency peaks. The evaluation shows that after the modifications are made, the limiting alternating stress ratio at CLTP is SR-a=2.85 which corresponds to SR-a=2.07 at EPU. The evaluation also shows that the prior reinforcements of the middle closure plate attachment welds previously required for EPU operation are no longer necessary since the rib reinforcements made to the closure plates and the other modifications described here reduce the weld stresses to levels below the allowable limits resulting in a limiting SR-a=2.84 for these welds.

The assessment shows that with the modifications in place all locations meet the required stress margin EPU operation.

Table of Contents

1. Introduction and Purpose

Plans to qualify the Nine Mile Point nuclear plant for operation at Extended Power Uprate (EPU) operating condition require an assessment of the steam dryer stresses experienced under the increased loads. The steam dryer loads due to pressure fluctuations in the main steam lines (MSLs) are potentially damaging and the cyclic stresses from these loads can produce fatigue cracking if loads are sufficiently high. The industry has addressed this problem with physical modifications to the dryers, as well as a program to define steam dryer loads and their resulting stresses. The purpose of the stress analysis discussed here is to calculate the maximum and alternating stresses generated during Current Licensed Thermal Power (CLTP) and Extended Power Uprate (EPU) and to determine the margins that exist when compared to stresses that comply with the ASME Code (ASME B&PV Code, Section III, subsection NG).

The stress analysis of the modified NMP2 steam dryer establishes whether the existing and proposed modifications are adequate for sustaining structural integrity and preventing future weld cracking under planned EPU operating conditions. The load combination considered here corresponds to normal operation (the Level A Service Condition) and includes fluctuating pressure loads developed from NMP2 main steam line data, and weight. The fluctuating pressure loads, induced by the flowing steam, are predicted using a separate acoustic circuit analysis of the steam dome and main steam lines [4]. Level B service conditions, which include seismic loads, are not included in this evaluation.

A prior stress evaluation of the NMP2 steam dryer was performed in [1] using acoustic loads generated using a revised Acoustic Circuit Model (ACM) Rev. 4.1. The revision was motivated primarily by a desire for consistent usage of noise filtering strategies during both model calibration against available data and application of the model to plants. Other than the removal of known non-acoustic discrete frequencies (e.g., electrical noise at multiples of 60 Hz) and the application of coherence filtering (which was also invoked when processing the QC data) no other filtering methods are used. In particular, no noise subtraction using low power data is performed. Further details of the ACM Rev. 4.1 calibration activity are provided in [2]. Its application to obtain NMP2 steam dryer acoustic loads is detailed in [3]. As described in [2] re-benchmarking the ACM against available Quad Cities data produced updated estimates of the acoustic speed and damping in the acoustics description and also revised biases and uncertainties due to changes in the model, coherence-based noise filtering and comparison method. For the same reasons, acoustic peaks predicted with the Rev. 4.0 and 4.1 models will differ, with the latter load estimates generally being higher and more conservative.

Using the acoustic loads predictions obtained with prior ACM Rev. 4.0 the NMP2 steam dryer stresses were shown to remain below EPU allowable stresses [5]. No low flow-based noise subtraction was performed to achieve this result and the limiting stress was calculated by considering the frequency shifts between ±10%. Also, to meet margin the dryer model incorporated stiffened closure plates, reinforced welds on the lifting rod braces and reinforced closure plate attachment welds. When the new acoustic loads derived from recently acquired main steam line strain gage measurements[3] and processed with the ACM Rev. 4.1 analysis and were applied to the NMP2 steam dryer, several locations emerged that exceeded EPU target stress ratios of 2.0 [1]. With frequency shifting accounted for, the limiting alternating stress ratio at CLTP was determined to be SR-a=1.56 occurring on the weld connecting the lifting rod support brace to the vane bank side plate. Since flow-induced acoustic resonances are not anticipated in the steam dryer, the alternating stress ratios at EPU operation can be obtained by scaling the CLTP values by the steam flow velocity squared, $(U_{EPU}/U_{CLTP})^2=1.1756^2=1.382$. Thus, without additional modification the limiting alternating stress ratio at EPU was SR-a=1.56/1.382=1.13. Thus to qualify the dryer for EPU operation using the ACM Rev. 4.1 load estimates additional modifications are needed.

In Section 6 of [1] the locations having EPU alternating stress ratios below 2.0 were organized into four groups and modifications presented for each group. The first three groups and attendant modifications were:

Group 1: The lifting rod bracket/side plate welds. The upper and middle brackets already had weld reinforcement, but this did not reduce stresses sufficiently under the new loads. Several local reinforcements consisting of plates welded to the vane bank side plate, brace or both were proposed and analyzed. Excepting one, all reinforcements were shown successful and selection of the preferred modification concept was to be decided on the basis of ease of implementation and diver exposure time.

Group 2: The middle hood reinforcement strip incurs a high stress due to vibration of the outboard section of the middle hood. The preliminary design to alleviate this stress consists of overlaying a 3/8" curved plate over the portion of the middle hood located between the existing reinforcement strip and the closure plate. This increased the alternating stress ratios of the previous high stress nodes to above SR-a>22. Such large stress ratios imply that the required stress reduction can be achieved with a thinner plate.

Group 3: The inner hood/hood support welds that experience high stresses due to the inner hood vibrations. The originally proposed stress alleviation method consisted of placing a total of four 20 lb masses on the central inner hood panels (the two panels connecting to the central hood support) 18" below the top of the vane bank surface.

Finite element calculations carried out with these modifications in place showed that the limiting stress ratios at the nodes in Groups 1-3 all increased to above 2.76 indicating that the modifications are effective in meeting the target EPU stresses. All of the evaluations were performed using shell element-based finite element analysis that did not consider details pertaining to welding, installation or, in the case of added masses, the modification dimensions. Moreover, for Group 1 a down-selection from the various successful proposed reinforcement concepts is needed before proceeding to a more detailed definition of welds and installation procedures.

The final Group 4 contained all the remaining locations with stress ratios below 2.76. The limiting alternating stress ratio in this group was SR-a=2.65. Unlike the other groups the limiting alternating stress ratio for Group 4 is already close to (within only 4%) the allowable level, which engendered consideration of several ways to address these locations. One option is to calculate the alternating stress ratio on the basis of Curve B rather than curve C in Fig I-9.2.2

of Appendix I in Section III of the ASME B&PV Code [6]. Curve C imposes a more stringent allowable (13.6 ksi) than curve B (16.5 ksi). However, per the directions of usage specified in the flow chart in Figure I-9.2.3 of the ASME Code and the observation that the peak stresses range is below 27.2 ksi, it follows that the appropriate allowable stress is correctly inferred from Curve B. Using the associated Curve B allowable of 16.5 ksi then all locations in Group 4 achieve an alternating stress ratio at EPU of SR-a≥2.32, well above the value of 2.0 required for EPU operation.

Another option for addressing the Group 4 nodes is to monitor the locations during power ascension and halt power ascension if any alternating stress ratio drops below 2.0. This approach builds upon the observation that the main steam line strain gage measurements used to define the acoustic loads (via the ACM Rev. 4.1 analysis) contain noise contributions from various sources such as pipe bending, electrical interference, etc. While coherence filtering reduces the noise content some contributions inevitably remain, notably those that can be attributed to coherent sources (e.g., structural vibrations). Since non-acoustic sources are expected to be invariant with flow speed it follows that the stress ratios inferred from measurements at higher power levels will be below those inferred from CLTP measurements and the flow speed squared scaling, $(U_{EPU}/U_{CLTP})^2=1.382$. Supposing that the computed alternating stress at CLTP can be decomposed into an acoustic and non-acoustic contribution,

$$(Salt)_{CLTP}=(Salt)_{noise}+(Salt)_{acoustic},$$

then one expects the corresponding alternating stress at EPU to be:

$$(Salt)_{EPU}=(Salt)_{noise} + 1.382\times(Salt)_{acoustic}<1.382\times(Salt)_{CLTP}$$

Based on this simple scaling it is easy to show that if 15% or more of the alternating stress at CLTP is actually due to non-acoustic sources or noise then the corresponding stress ratio at EPU will exceed 2.0 with noise included. Despite the somewhat over-simplified argument regarding the scaling of acoustic and non-acoustic sources, this option does not compromise safety since the stresses at nodes on the dryer will be monitored during power ascension and power ascension would halt if any location exhibits an alternating stress ratio below 2.0.

The final option for addressing Group 4 nodes is to develop modifications for the various locations in the Group. For each of the three distinct locations a modification was proposed as follows:

(i) Bottoms of the drain/skirt welds. Here a wrap around weld was recommended as an easy to implement reinforcement.

(ii) The common junctions between the hood/hood support and base plate. For these locations a stress relief cut-out in the bottom of the hood stiffener was proposed as a means of reducing the stresses without the need for additional welding (welding is undesirable at these locations as they require access from underneath the dryer and would subject underwater divers to high radiation doses).

(iii) The middle hood/hood support welds. The high stresses are caused by vibration of the center panels of the middle hoods and are alleviated by adding a total of four 10 lb masses to these panels.

Instead of quantitatively definitive evaluations of these modifications, a combination of qualitative arguments and analogies were presented to show that the modifications were highly likely to succeed, particularly given that the existing alternating stress ratios are already very close to the required values. Nevertheless, a more definitive and quantitative assessment is needed prior to implementation of any such modification.

The present report is concerned with refining and providing additional details for the modifications planned in all groups 1-4 and also performing a comprehensive quantitative evaluation of all modifications. Section 3 details the modifications for each group. For Group 1 a down-selection of the various originally proposed concepts is made and implementation details for the final concept provided. The Group 2 modification originally consisted of a 3/8" thick curved reinforcement plate, which has now been reduced to 1/8". The stress evaluation performed below using this thinner plate shows that there remains ample stress margin at EPU. The Group 3 locations are addressed by adding a total of four masses to the inner hoods. In [1] 20 lb masses were used; here these have been reduced to 15 lbs since addition of these smaller masses still meets the target EPU stress margins. Finally Group 4 locations are modified as follows. High stress locations on the middle hood/hood support welds are addressed similarly to the inner hoods by adding a total of four 10 lb masses to the central sections of the middle hoods. The bottoms of the drain channel/skirt welds are reinforced by thickening the length and wrapping the weld around the junction terminus and continuing it for 1" along the interior side.

For the outer hood/hood support/cover plate junctions a stress relief cut-out hole optimized to minimize the alternating stresses is added to the support plate. The sub-models used to analyze the stress relief cut-out serve a two-fold purpose. The first is to evaluate the FIV stress with the cut-out in place. The other purpose is to assess the impact of the cut-out hole upon the growth of flaws discovered at these locations. This flaw evaluation is performed separately in [7].

In Section 4 a summary of the modifications made to the dryer is given and stress analysis is carried out with the modifications in place. To ensure that the modifications do not inadvertently introduce new high stress locations, unit solutions of the complete dryer are recomputed over the 30-250 Hz frequency range with the modifications in place including the stiffened closure plate, the masses added to the inner and middle hoods, and the 1/8" thick reinforcement plate placed over the middle hood section outboard of the closure plate. Below 30 Hz the original un-modified steam dryer unit solutions are used. This is acceptable since the dynamic response of the dryer below this frequency is small; it is also conservative since no credit is taken for the stress reductions realized by these modifications. All other reinforcements such as reinforcing the drain channel/skirt weld are localized and are evaluated using stress reduction factors (SRFs) to adjust the local stresses.

A stress evaluation using the modified steam dryer is performed using the harmonic analysis described in [1] showing that the limiting alternating stress ratio on the dryer is SR-a=2.85. This evaluation is performed with reinforcements made to the closure plate attachment welds. These reinforcements were required at an earlier point in the NMP2 steam dryer stress evaluation process (when noise was filtered using low power data). In light of the additional modifications made since this earlier evaluation, it was questioned whether the closure plate weld reinforcements are still required. Therefore a second stress evaluation was performed without this weld reinforcement. This calculation shows that while the closure plate attachment weld now contains the limiting location the associated alternating stress ratio is SR-a=2.84 which meets the required EPU stress margin and is only slightly lower than the limiting value

(SR-a=2.85) when the attachment welds are reinforced. This implies that the closure plate attachment weld reinforcements are redundant when the other steam dryer modifications are implemented.

2. Methodology & Evaluation Procedures

The overall harmonic analysis used to predict the stresses resulting from acoustic loads is described in [1]. [[

(3)]]

[[2.1 (3)]]

[[

(3)]]

[[

(3)]]

2.2 Sub-Modeling

[[

(3)]]

[[

(3)]]. A compilation of the sub-modeled locations together with the calculated stress reduction factors is given in Table 1 and associated Figure 1 with a brief discussion of these locations provided below.

List of Sub-Models

Several sub-models have been used in the current and prior NMP2 steam dryer stress evaluations and these are assembled here for convenience. The first set of sub-models was developed for four locations on the welds connecting the closure plates to the rest of the steam dryer. The first two are on the vertical weld joining the closure plate to the vane bank. The first node is at the top of this weld and the second one lies 13.5" below it. The other two locations are on the curved weld connecting the closure plate to the curved hood. Again the first location is at the top of this weld and the second one lies 14.5" below it. In both cases, the stresses at the top location result from a combination of membrane and bending stresses whereas the stresses at the lower locations are predominantly due to bending. The stresses are induced by a closure plate response dominated by a (1,2) mode (i.e., the mode shape resembles the first mode of a beam in the horizontal direction and the second mode in the vertical sense) in the 125-135 Hz frequency range which explains the high stress at the lower locations on the welds.

Preliminary sub-model evaluations showed that to meet EPU target stresses it was necessary to increase the weld size (the top 18" of these welds were increased) and all final stress reduction factors (SRFs) obtained with the sub-models pertain to these reinforced welds. The acoustic loads driving these high stresses and used to develop the sub-models were originally obtained with the prior ACM Rev. 4.0 and filtered using low-flow noise subtraction. The use of low-flow noise subtraction has since met with increasing scrutiny and opposition by the staff. To proceed, it was decided to re-evaluate the acoustic loads and stress *without* low-flow noise subtraction. This led to higher stresses in general and the weld reinforcements were insufficient by themselves to achieve adequate stress levels. The closure plates were therefore reinforced using stiffening ribs. This modification in combination with the reinforced welds resulted in EPU stress ratios above the target value of 2.0 [5]. In 2010, the ACM Rev. 4.1 analysis was developed in response to staff concerns over differences in the signal processing methods used when benchmarking and when applied to plants. The resulting changes in the stresses necessitated additional modifications as summarized in [1] and below. One particular and beneficial consequence of reinforcing the closure plates and other components in the steam dryer, particularly the middle hood, is that most of the closure plate weld reinforcements are no longer necessary an adequate stress margin is met using the existing welds as shown in Section 4.

The next sub-model examined the weld connecting the support braces for the lifting rods to the vertical plates on the outer vane banks. The high stress location occurs at one end of the weld line and is characterized by a re-entrant junction membrane stress concentration in the brace. As with the closure plate welds, these welds were found to require reinforcement to meet target stress ratios for EPU using the prior ACM Rev. 4.0 model *without* low-flow noise subtraction [5]. However, even with the weld increased from its current ¼" size to ½" the required margins were not met when the ACM Rev. 4.1 loads were imposed. Therefore in Section 6 of [1] several additional reinforcement concepts were proposed and analyzed. Further analysis and down-selection to the final concept is carried out in Section 3.1.

The sixth sub-model considers the weld connecting the hood and hood support. This sub-model was originally developed to address a high stress developing in this weld due to hood vibration. Since it is not accessible no reinforcement of the weld can be performed at this location and the sub-model analysis was carried out to determine the SRF for the existing weld. The SRF determined in [9] was 0.77. This value closely matches that expected for this full penetration weld since the product of the SRF (0.77) and fillet weld factor (1.8), $0.77 \times 1.80 = 1.39$, agrees to within 1% with the weld factor for a full penetration weld (1.4). Therefore, rather than using the sub-model result, the weld factor (1.4) for a full penetration weld is used for this weld. This yields a slightly more conservative analysis. As with the sub-models above, while the SRF for this location was sufficient to meet the EPU stress margin when using the ACM Rev. 4.0 for acoustic loads predictions, it was insufficient when proved adequate for the subsequent predictions using ACM Rev. 4.1. These locations are therefore addressed by an alternate means consisting of placing small masses on the vibrating inner and middle hoods.

The seventh and eight sub-models were developed to more accurately characterize the stresses at the ends of the tie bars landing on the top plates of the vane banks. These locations involve large welds that are not accounted for in the shell model. All of the preceding sub-models were used to evaluate existing welds in their existing or reinforced configurations, arising when applying ACM Rev. 4.0 acoustic loads. The remaining sub-models were developed to address high stress locations arising in response to ACM Rev. 4.1 acoustic loads.

The ninth sub-modeled location is at the bottom end of the weld joining the drain channel to the skirt. This site experiences an increase in stress under the ACM Rev. 4.1 loads such that the EPU stress margin is no longer achieved under the existing weld configuration. To regain the necessary EPU stress margin the weld is reinforced by adding a weld that increases the size of the bottom 4" of the existing weld from 0.125" to 0.25", wraps around the bottom of the drain channel and extends up 1" on the interior side. The modification and associated sub-model analysis are detailed in Appendix A.

Finally sub-modeling is used to analyze the common junction between the outer hood, hood support and cover plate. This sub-model serves two purposes. The first is to establish whether the existing flaws discovered at this location will propagate during EPU operation (see Section 2.3). The other is to design and evaluate a stress relief cut-out added to the hood support to attenuate the stress intensity at the existing high stress location. The sub-model analysis for this location is presented in Appendix A.

Table 1. Summary of stress reduction factors obtained using sub-model analysis.

	Location	Stress Reduction Factor	Notes
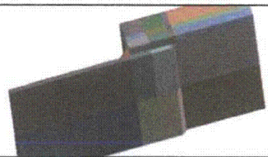	1. Top of vertical closure plate/vane bank weld	0.62 [1]	Used, but not needed if all other modifications are implemented.
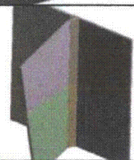	2. 14.5" below location 3 on the same weld	0.71 [1]	Used, but not needed if all other modifications are implemented
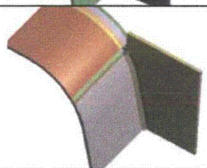	3. Top of closure plate/hood weld	0.86 [1]	Used, but not needed if all other modifications are implemented
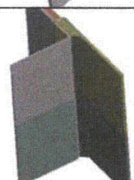	4. 13.5" below location 1 on the same weld	0.88 [1]	Used, but not needed if all other modifications are implemented
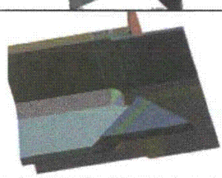	5. Lifting rod support brace/vane side plate junction (assuming an increased 1/2" weld)	0.60 [12]	Used to calculate baseline results in the absence of the additional reinforcements discussed in Section 3.1.

Note: For locations 1-4 it is assumed that an inner weld has been to the top 18" of the welds joining the closure plate to the hoods or vane banks, thereby replacing the existing single-sided fillet weld by one that is double sided. Also, an increased ½" weld is assumed for location 5.

Table 1 (cont.). Summary of stress reduction factors obtained using sub-model analysis.

	Location	Stress Reduction Factor	Notes
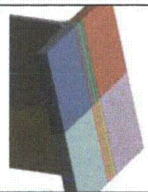	6. Hood/hood support.	0.77 [9]	Since this weld is a full penetration weld with weld factor of 1.4, the SRF is replaced by the slightly more conservative value of 1.4/1.8=0.78.
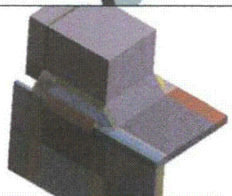	7. Side plate/top plate	0.70 [12]	
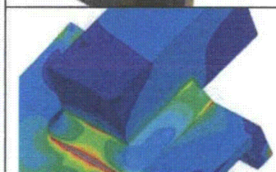	8. Tie bar/top vane bank plate.	0.71 [12]	
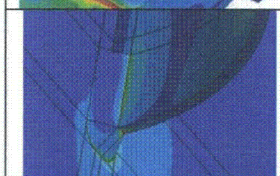	9. Bottom of skirt/drain channel weld with reinforced wrap-around weld.	0.65 Appendix A	
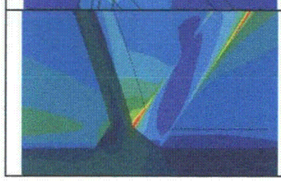	10. Bottom of outer hood/hood support weld (no stress relief cut-out)	(Not evaluated) Appendix A	Model transmitted to SIA for detailed stress evaluation.

	Location	Stress Reduction Factor	Notes
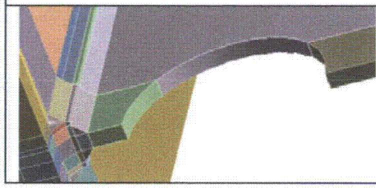	11. Bottom of outer hood/hood support weld with stress relief cut-out.	0.73 Appendix A	Same as 10, but with stress relief cut-out on the bottom edge of the hood support.

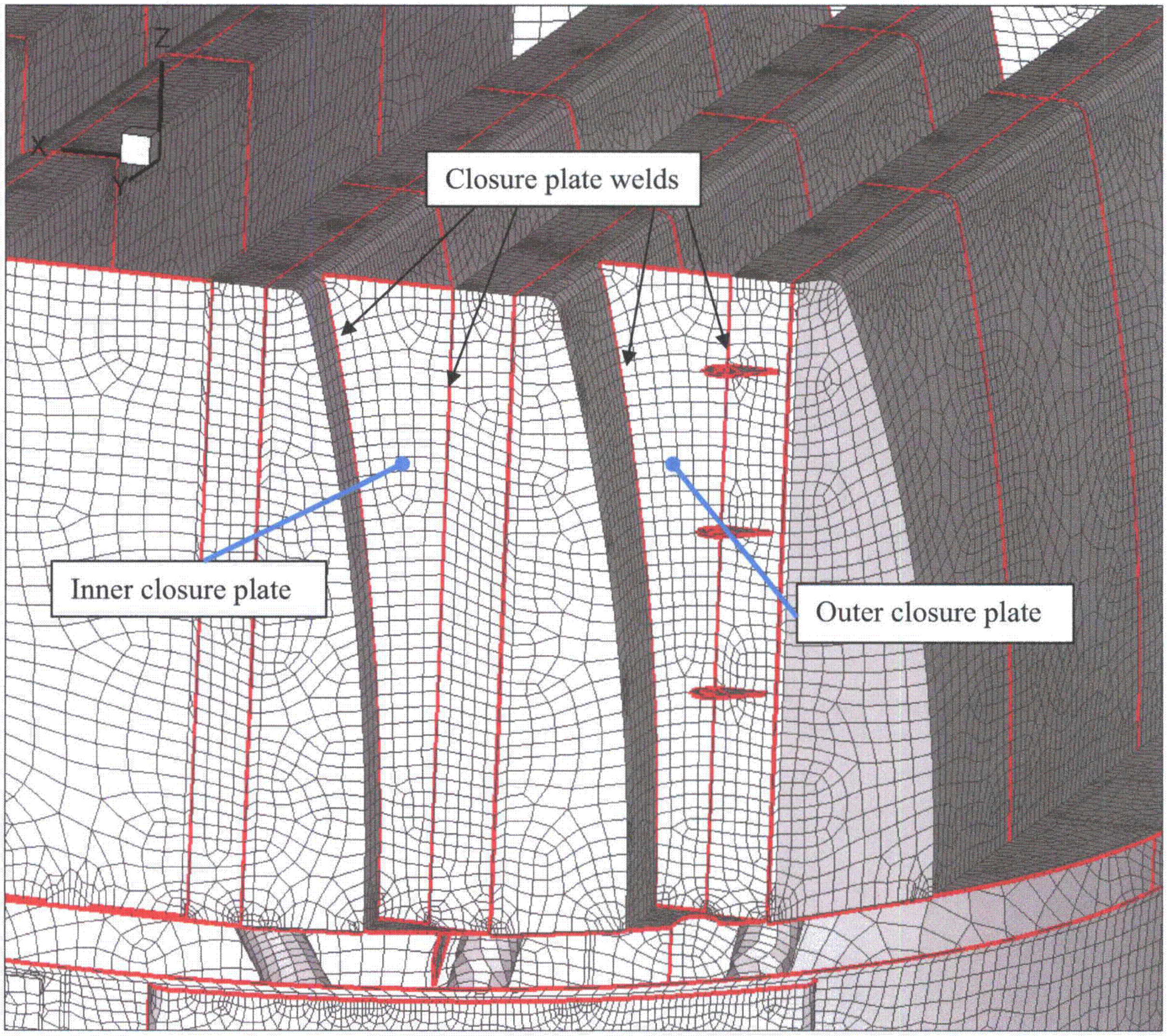

Figure 1a. Closure plates and associated attachment welds which are reinforced and examined with sub-model (note lifting rods and other components modeled with solid elements are omitted for clarity). Sub-models on the perimeter are locations 1-4 in Table 1.

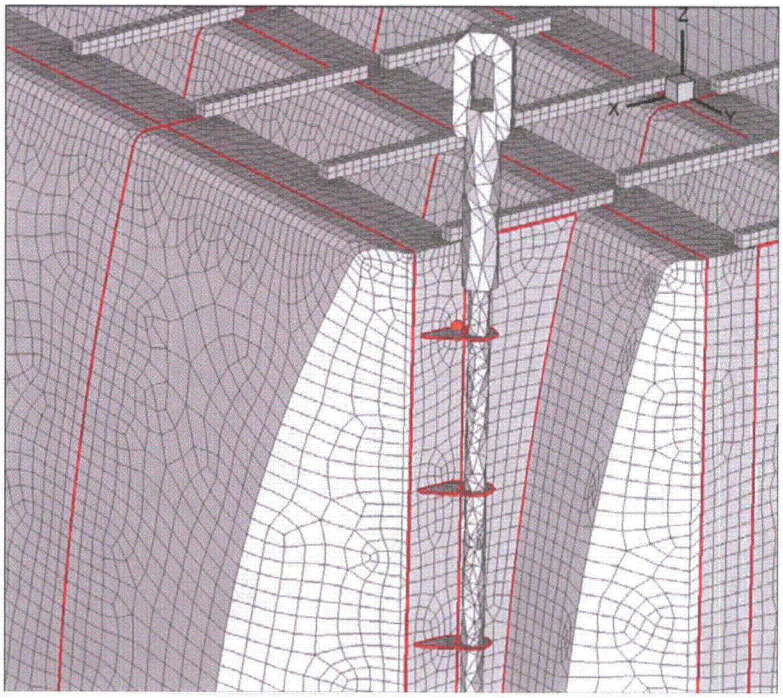

Figure 1b. Location of node on inner hood/hood support/middle base plate weld analyzed with sub-model in [12]. Sub-model corresponds to location 5 in Table 1.

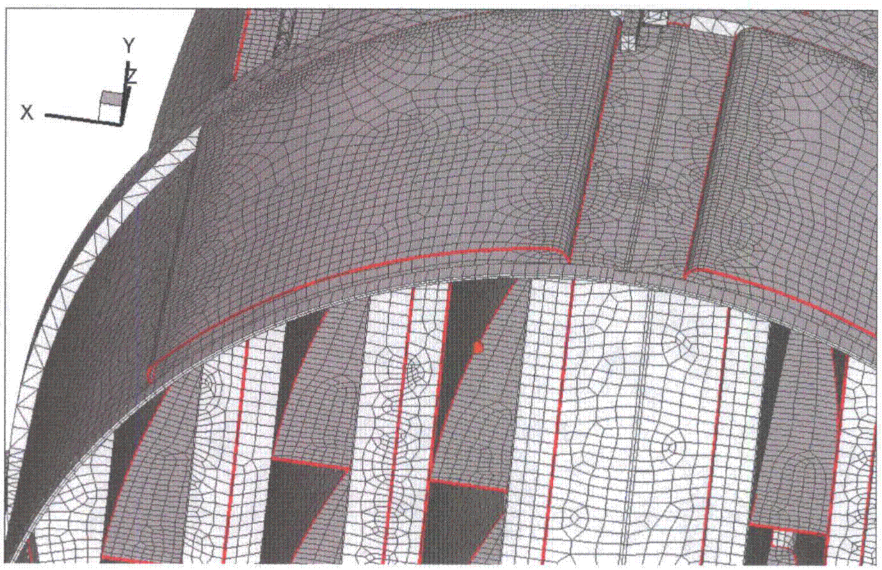

Figure 1c. Location of node on hood/hood support weld analyzed with sub-model analysis procedure in [9]. Sub-model corresponds to location 6 in Table 1.

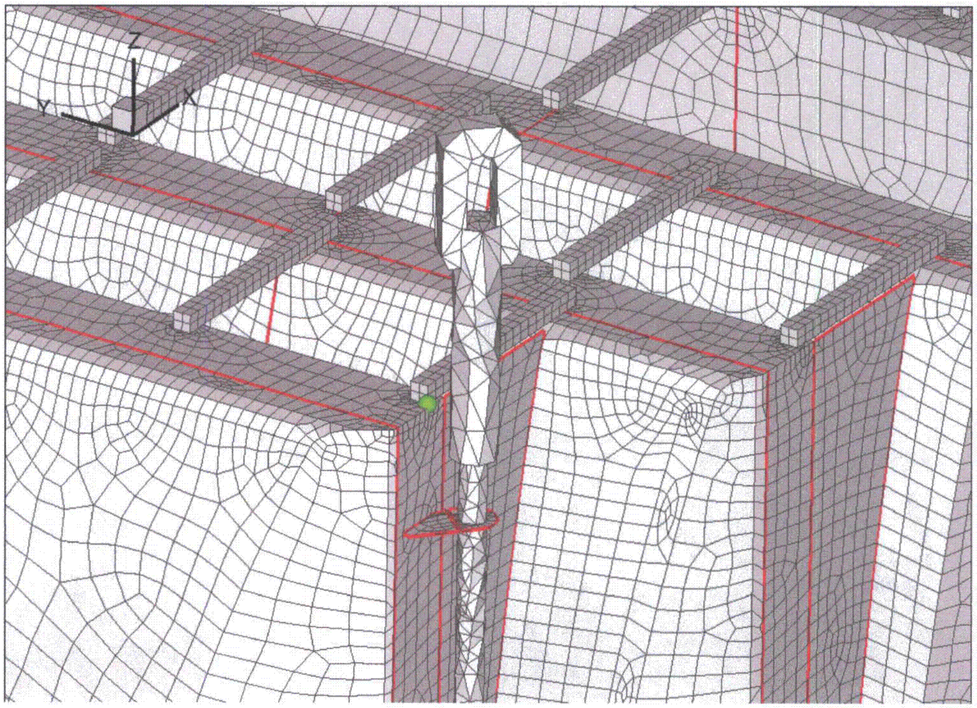

Figure 1d. Location of node on side plate/top plate weld analyzed with sub-model analysis procedure in [12]. Sub-model corresponds to location 7 in Table 1.

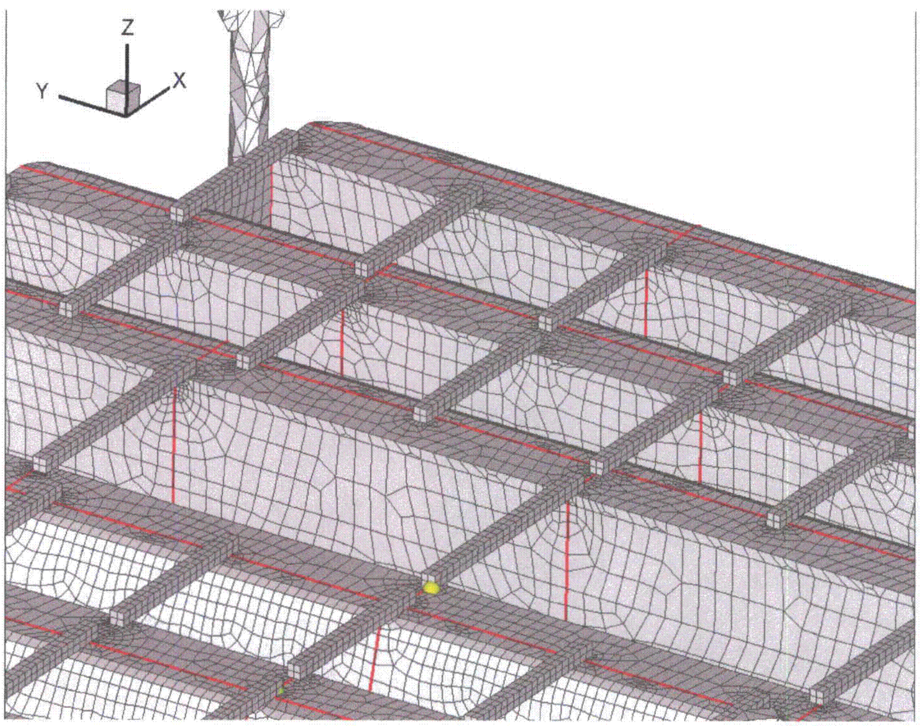

Figure 1e. Location of node on tie bar/top vane bank plate weld analyzed with sub-model analysis procedure in [12]. Sub-model corresponds to location 8 in Table 1.

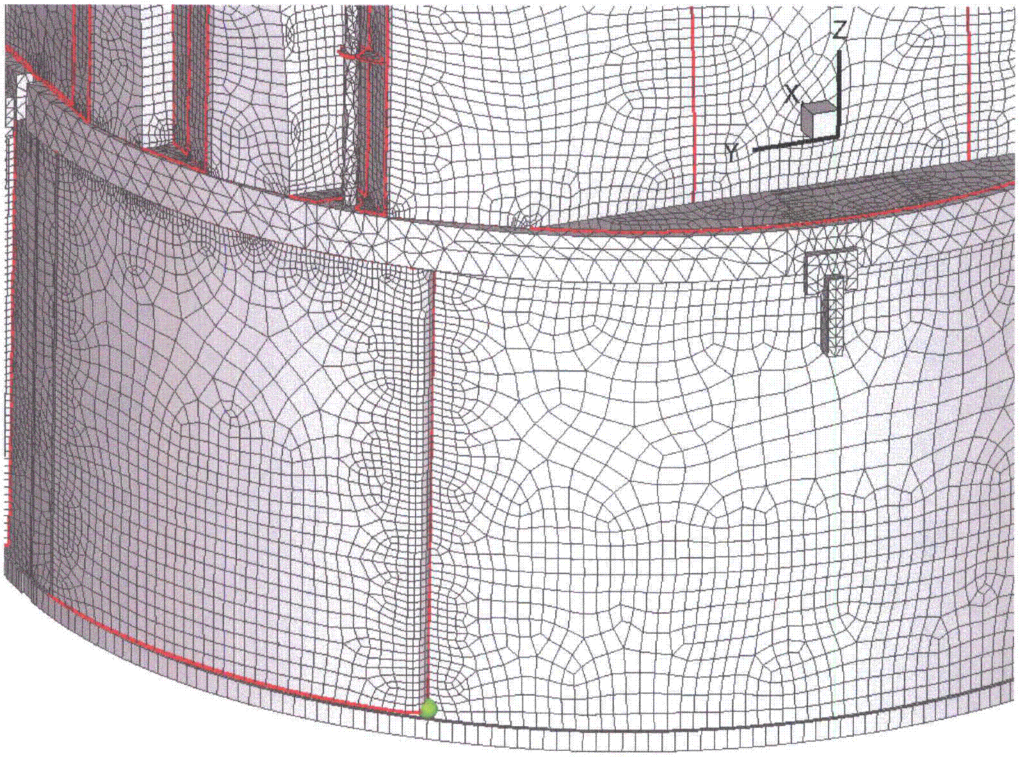

Figure 1f. Location of node on bottom of drain channel/skirt weld analyzed with sub-model analysis procedure in Appendix A. Sub-model corresponds to location 9 in Table 1.

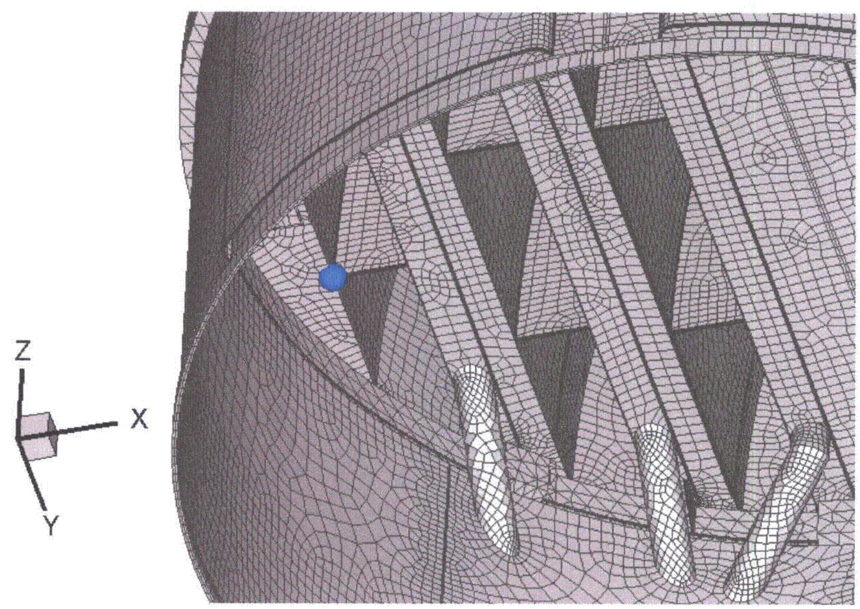

Figure 1g. Location of node on outer hood/hood support/cover plate analyzed with sub-model analysis procedure in Appendix A. Sub-model corresponds to locations 10 and 11 in Table 1.

2.3 Flaw Evaluation

As part of the steam dryer stress assessment for EPU operation an evaluation of existing flaws discovered in the outer hood/hood support/base plate junctions is required to establish whether or not flaw propagation will occur at EPU conditions. If growth of the existing indications cannot be readily ruled out then a modification to the existing locations is required. Performing the flaw evaluation and designing the stress relief cutout required the combined use of several analysis methods which are summarized here. The flaw growth assessment is performed jointly by CDI and Structural Integrity Associates (SIA). CDI provided a high resolution sub-model that includes details of the local welds together with the perimeter loads and inertial and body forces as described above. CDI also conducted supporting calculations to estimate the RMS stresses and determine whether the behavior at these locations is symptomatic of load- or displacement-controlled stresses. Finally a modified sub-model of this location with a circular cutout in the hood support was developed as a contingency repair in the event that arresting of further crack growth at EPU operation cannot be assured under the current (unmodified) configuration. The sizing and placement of the circular cut-out was also developed herein. With these results, SIA conducted the flaw evaluation using a combination of analytical methods and finite element modeling using crack elements as described in [7].

The sub-model and attendant boundary forces and moments as well as acoustic and dynamic inertial loads are developed using the method described in Section 2.2. The intersection box defining the sub-model encompasses 6" of the bottom edge of the hood support, extends 9" upward from this edge bottom edge of the hood support and extends 3" in all other directions relative to the high stress location. The extended length (3" longer than typical for sub-models) in the vertical direction is necessary to allow the examination of hood/hood support weld stresses over a sufficient length to determine whether crack growth will occur. The extended length of the sub-model (also by 3") horizontally along the hood support is needed to accommodate the stress relief cut-out and evaluate its impact on the stress field near the high stress region.

[[

(3)]]

Load- or Displacement-Controlled Stresses

The detailed flaw evaluation requires an assessment of whether the stress at the crack is primarily load- or displacement-controlled as this distinction warrants different criteria for establishing crack growth. In a load-controlled configuration the applied load essentially remains constant as the structure displaces. In a displacement-controlled configuration the forces experienced by the load are relieved as the structure displaces.

The distinction can be explained by way of example and reference to Figure 2 which depicts a structure similar to the hood support. The structure contains a flaw as shown and the right hand edge is either: (i) loaded with a constant force or (ii) required to move by a specified displacement. The former case would arise if the edge is directly loaded; the second situation arises when the hood response is dominated by the response of adjacent structures. Suppose that the displacement at the location indicated is monitored as the flaw length is increased. In a load-controlled configuration – case (i) - the monitored displacement is expected to increase as the flaw grows. Conversely in the displacement-controlled setting the monitored displacement will only be weakly affected by the flaw length and will either remain approximately the same or decrease with increasing flaw size.

For the outer hood/hood support/cover plate junction it is noted that the 1/4" outer hood support connects to the much thicker (1/2") outer hoods on the left edge and to the massive outer vane banks on the right edge. Since the outer hoods connect directly to the vane banks it can be surmised that acoustic forcing of the outer hoods will produce motions in the combined outer hood + vane bank assembly. Because of the comparatively stiff outer hoods and massive vane banks (compared to the hood support), the motions of this assembly is anticipated to be only weakly affected by a flaw at this junction.

To verify this behavior for a complex structure such as the dryer where multiple load paths exist, a practical means of establishing whether the forces transmitted to the hood support plates are displacement-limited is required. To this end the global finite element model is used and elements along the hood/hood support weld line progressively disconnected to simulate flaws of different lengths. Thus one begins with the fully connected model and evaluates the displacements at selected locations on the hood support and connected components when subjected to the ACM Rev. 4.1 acoustic loads. These locations are chosen to lie between 3-9 inches away from the high stress location as shown in Figure 3. The lowest finite element in the hood support that is adjacent to the outer hood/hood support weld is then disconnected. The nearest middle hood/hood support is similarly disconnected and the displacements at the same locations recalculated. Next this process is repeated by disconnecting the two lowest finite elements along the weld (i.e., the one disconnected previously and the one immediately above it also adjacent to the weld) and re-evaluating the displacements; then disconnecting the three lowest elements, etc. The displacements are then plotted as a function of disconnection length to see whether the displacements generally increase with disconnection length which is indicative of load-controlled behavior, or whether the displacements remain constant or reduce with disconnection length which implies displacement-controlled response. These plots are presented in Figure 4. From these plots the response at the outer hood/hood support/cover plate is consistent with displacement-controlled behavior as all displacements tend to reduce with crack length or plateau to constant values.

At the middle hood/hood support/base plate junction, the displacement amplitudes all decrease gradually or plateau except for the middle hoods themselves whose amplitudes continue to grow. This is indicative of a vibration mode that continues to grow as the restraint provided by the hood support is reduced. For the hood support itself however, where the dominant stress occur, the displacements at 2A and 2B are generally level or diminishing with crack length (see Figure 4) indicating that the hood support stress is also displacement-controlled.

The stress at the flaw tip is also recorded as a function of crack length to corroborate whether or not the stress is displacement-controlled. Generally, one would expect to observe a reduction in this stress as the crack is extended. This observation is indeed borne out as shown in Figure 5. This plot records the maximum unit solution stress at the flaw tip as a function of displacement length where the maximum is taken over all frequencies and MSL forcings.

Finally, it is noted that the displacement-controlled stress behavior at all hood/hood support/base plate junctions is supported by field observations at explained at length in [7]. Essentially, for a load-controlled stress state the observed flaws would have grown to considerably longer lengths. Instead, the flaws which are believed to have been initiated by residual stresses, have grown to approximately 2" on the outer hood supports and 0.5" at the middle and some inner hood supports and stopped. This is fully consistent with a displacement-controlled stress situation and also corroborates the analysis conducted in [7] which predicts crack growth to approximately 2" during the first operational cycle and subsequent arrest of the crack as the crack tip stress field diminishes. While the evaluation in [7] focuses on the outer hood support, this evaluation constitutes the bounding flaw assessment for all (outer, middle and inner) hood support junctions given that the highest junction stresses occur on the outer hood supports and all locations evidence displacement-controlled stress behavior near the flaws.

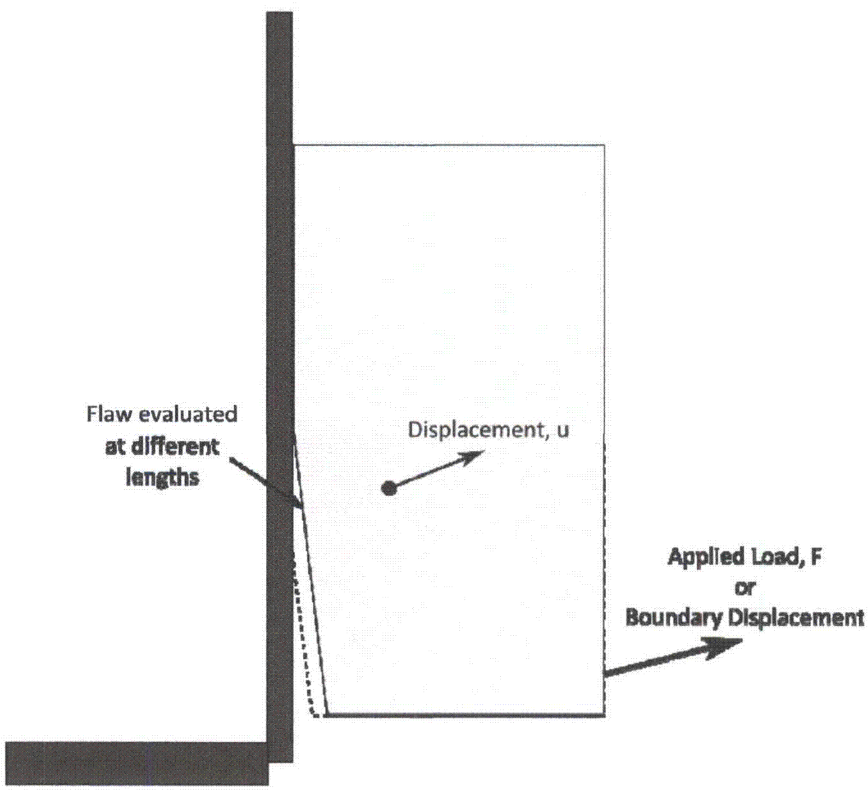

Figure 2. Conceptual arrangement of hood support geometry for the determining whether the limiting stresses are load- or displacement-controlled.

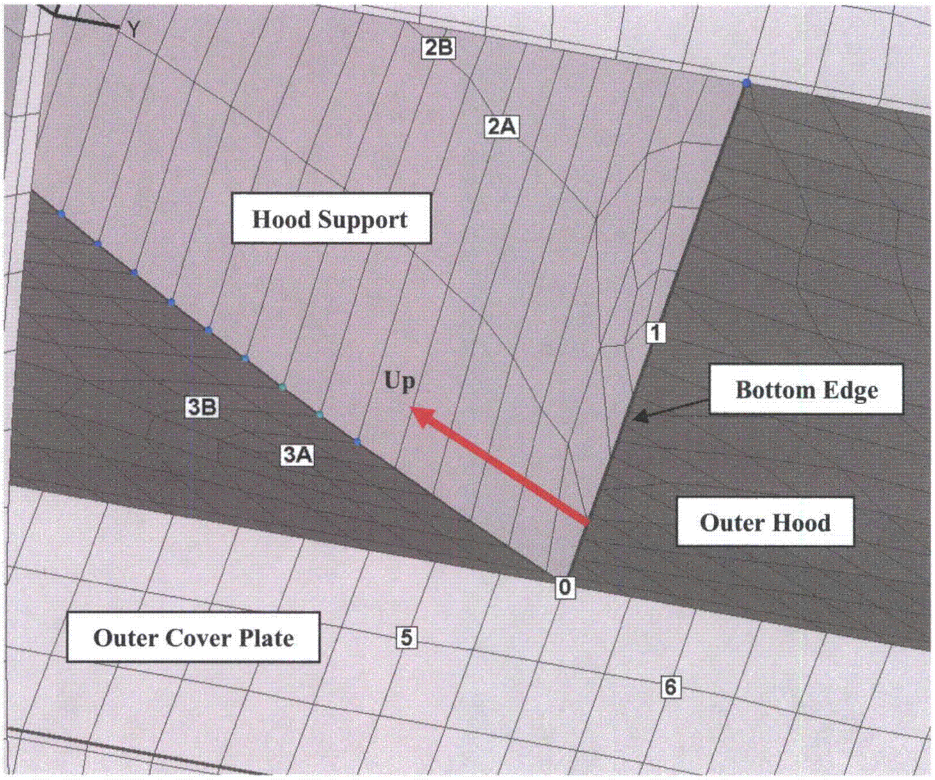

Figure 3. Depiction from below of locations near the outer hood/hood support/cover plate high stress point where displacements are recorded. Location 0 lies at the high stress location. Location 1 lies on the bottom edge of the hood support whereas locations 2A and 2B lie approximately 9" and 13" respectively above location 1. Locations 3A and 3B reside on the outer hood at approximately the same heights as 2A and 2B; Locations 4A and 4B are similarly placed on the outer hood and are located behind the hood support and thus obscured by the hood support in this view. Finally locations 5 and 6 are on the outer cover plate. Precise values are given in Table 2. Analogous locations are erected about the middle hood/hood support junction.

Table 2. Coordinates of Locations 0-6 in Figure 3.

Index	node	x	y	z
0	95267	-102.75	28.39	0
1	14954	-94.875	28.39	0
2A	14789	-93.7966	28.39	10.0558
2B	14840	-93.7159	28.39	13.6998
3A	79184	-102.624	23.9483	9.44825
3B	78999	-102.495	23.689	13.4162
4A	77836	-102.617	33.8335	9.70184
4B	77835	-102.48	34.3628	13.8147
5	48374	-105.543	24.76	0
6	48388	-106.358	32.0303	0

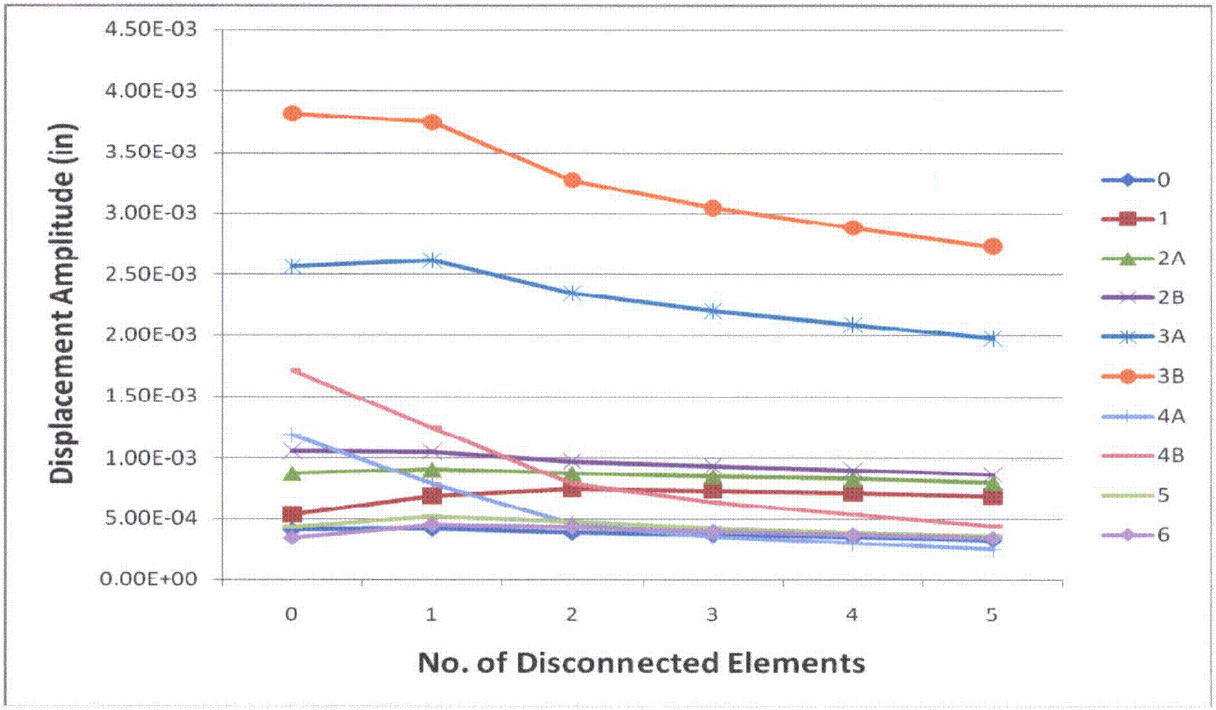

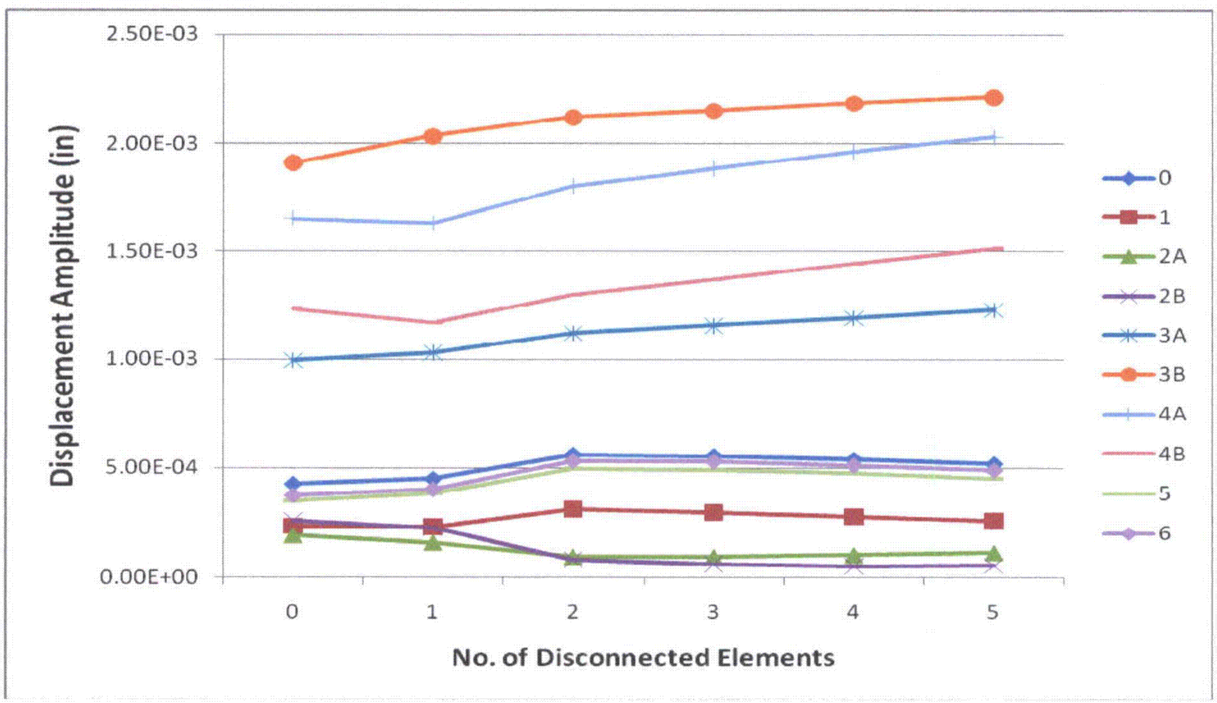

Figure 4. Variation of displacement amplitudes at the locations depicted in Figure 3 as a function of the number of disconnected elements along the hood/hood support weld line. Top – outer hood; bottom – middle hood.

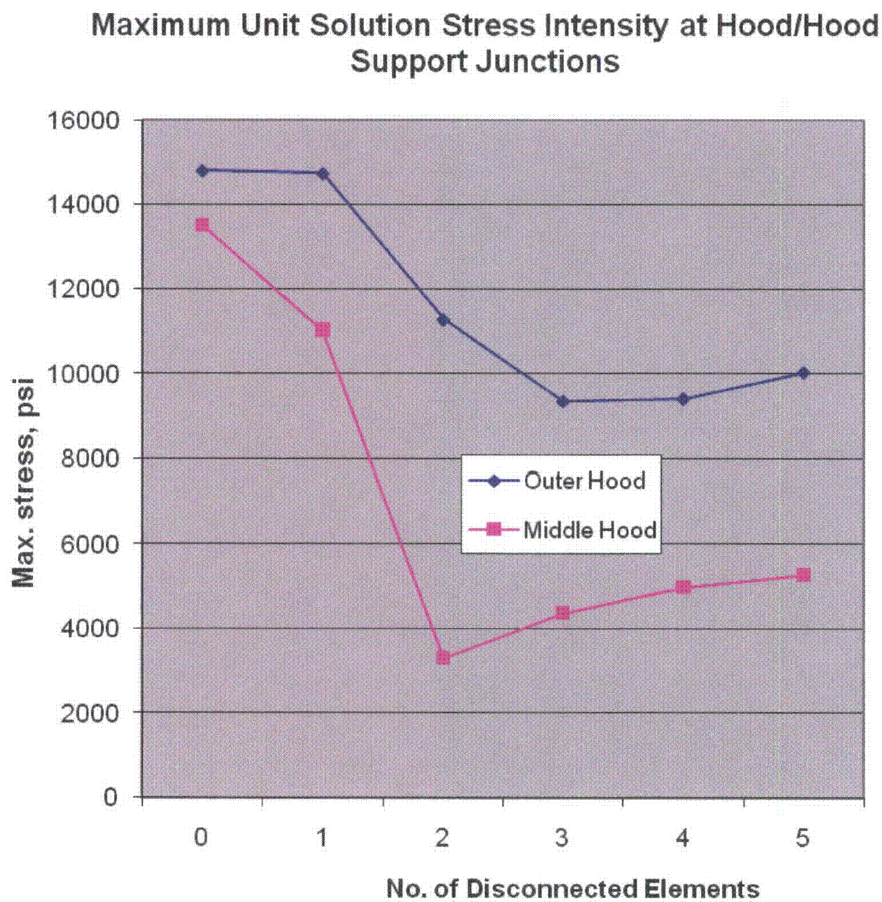

Figure 5. Variation of the maximum unit solution stress at the tip of the disconnection line as a function of the number of disconnected elements. The maximum of the stress intensity is taken over all MSL loadings and frequencies.

Sizing and Positioning the Stress Relief Cut-Out Hole

If the flaw evaluation shows insufficient margin a means of reducing the stress is needed. The option considered here is the insertion of a semi-circular stress relief cutout hole. Another option considered previously was to reinforce the existing welds, but this entails access from underneath the dryer exposing the diver to significant radiation dose. A cut-out hole on the other hand can be machined remotely by electrical discharge machining (EDM) thus limiting diver dose to at most the time required to attach the EDM device to the hood support. Insertion of the cut-out, while reducing the stress at the current high stress location, can introduce new high stress regions – for example on the cut-out hole perimeter due to stress concentration. The cut-out hole is optimized by adjusting the position and radius of the hole to minimize the overall stress ratio. The optimization process is carried out using a shell-based sub-model to expedite the overall design process. A series of such sub-models with different cut-out holes parameterized in terms of radius, R, and distance, d, from the existing high stress location is generated and loaded with the distributed forces and moments inferred from the global model. For each configuration the limiting stress is calculated. This is the higher of the limiting stress intensity on the weld multiplied by 1.8 and the stress on the perimeter of the cut-out hole. By plotting this stress (or the inverse quantity, the stress ratio) against the parameters, d and R, an optimizing combination is readily obtained. The optimized stress relief cut-out geometry is then applied to the solid element-based sub-model for a final evaluation of the SRF which is the ratio of the limiting stress with the cut-out divided by the value without the cut-out. Additional details of this process are provided in Appendix A.

3. Proposed Modifications to Meet EPU Stress Margins

The dryer analyzed in Section 5 [1] identified several locations with alternating stress ratios below the EPU target of 2.00 when subjected to the ACM Rev. 4.1 acoustic loads. To achieve the desired EPU stress margins several modification were proposed and analyzed in Section 6 of the same report. These evaluations were carried out using a combination of sub-modeling techniques and finite element analyses conducted over limited frequency ranges. In most cases geometrical details of the reinforcement and weld size information were either not finalized or were omitted. Also, for some locations (e.g., Group 1) several reinforcement concepts were proposed but no final down-select carried out. The purpose of the present section is to develop more definitive specifications of the required modifications and carry out more extensive stress assessments where warranted.

In Section 6 of [1] the locations whose alternating stress ratios at EPU fall below2.0 were organized into four distinct groups as follows:

- Group 1: The lifting rod bracket/side plate welds. The upper and middle brackets already have weld reinforcement, but this does not reduce stresses sufficiently under the new loads.
- Group 2: The middle hood reinforcement strip incurs a high stress due to vibration of the outboard section of the middle hood.
- Group 3: The inner hood/hood support welds that experience high stresses due to the inner hood vibrations.
- Group 4: The remaining points which are readily modified to achieve SR-a>2.76 as discussed further below.

The locations and stress states calculated using only the baseline modifications listed in [5] (reinforce closure plates, reinforced closure plates and increased lifting rod brace welds) are given in Table 3 together with the stress estimates obtained after implementing the modifications in [1].

Below, these groups are discussed in further detail.

Table 3. List of locations from Table 9b in [1] with alternating stress ratios below 2.76 re-ordered into groups.

Location	GROUP	SRF	node	Pm	Pm+Pb	Sa	SR-P	SR-a	% Freq. Shift	Dom. Freq. [Hz]
1. Side Plate/Brace	1	0.6(5)	89649	4022	5464	4413	2.31	1.56	-5	139.7
3. Side Plate/Brace	1	1	89646	3460	4435	3947	2.69	1.74	5	103.3
7. Side Plate/Brace	1	0.6(5)	89652	2656	3752	2924	3.5	2.35	-5	139.7
2. Hood Reinforcement/Middle Hood	2	1	98275	414	4626	4229	3.01	1.62	10	109.0
8. Hood Reinforcement/Middle Hood	2	1	90126	1090	3925	2918	3.55	2.35	10	109.0
9. Hood Reinforcement/Middle Hood	2	1	98268	665	2992	2889	4.66	2.38	-7.5	146.1
10. Hood Reinforcement/Middle Hood	2	1	90949	1071	2776	2673	5.02	2.57	2.5	190.7
4. Hood Support/Inner Hood	3	1(b)	95636	1160	3228	3172	4.32	2.17	-10	51.2
5. Hood Support/Inner Hood	3	1(b)	95650	1126	3277	3027	4.25	2.27	-10	51.2
6. Hood Support/Inner Hood	3	1(b)	95642	1270	3023	3017	4.61	2.28	2.5	44.1
11. Hood Support/Outer Base Plate/Middle Backing Bar	4	1(b)	95428	4516	4994	2593	2.06	2.65	5	48.6
14. Hood Support/Outer Cover Plate/Outer Hood	4	1(b)	95267	4892	5223	2538	1.9	2.71	-10	60.5
12. Submerged Drain Channel/Submerged Skirt	4	1	93430	820	6224	2591	2.24	2.65	5	51.8
15. Submerged Drain Channel/Submerged Skirt	4	1	84597	1167	4640	2527	3	2.72	2.5	104.0
13. Hood Support/Middle Hood	4	1(b)	96022	905	2750	2562	5.07	2.68	-5	53.4

Notes.

(a) Node numbers are retained for further reference.

(1-8) Appropriate stress reduction factor for the welds and modifications listed in Table 1 have been applied. The number refers to the particular location and corresponding stress reduction factor in Table 1.

(b) WF=1.4

3.1 Lifting Rod Support Brackets (Group 1)

Without any modification other than an increase in the existing weld size from ¼" to ½" which, from sub-modeling [12] allows imposition of a stress reduction factor of 0.6, the limiting alternating stress locations occur on the lifting rod support brackets (see Figure 6) with an alternating stress ratio of SR-a=1.56. The stresses are highly localized (only one node on each such bracket is affected) which is indicative of development of stress singularities at this re-entrant corner. The dominant frequencies for these locations are found to lie about the 98 Hz (for the lowest bracket) and 130-140 Hz (middle and upper brackets) frequency ranges. If the lower brackets are modified using the same weld reinforcement planned for the middle and upper brackets then their limiting alternating stress ratio increases to 2.90. However, the middle and upper brackets are still below target stress ratios and further weld reinforcement appears unlikely by itself to achieve the necessary stress reductions. Instead a more substantial structural reinforcement is required.

The localized nature of the stress concentration calls for a corresponding localized reinforcement. Several such concepts were proposed in [1]. There it was shown that increasing the local thickness – specifically that of all elements with at least one node on the vertical plate/brace weld line – from 0.375" to 0.75" satisfactorily reduced the stress and did not significantly impact the modal properties or stresses elsewhere on the steam dryer. Of the various concepts considered, Concept 2 was recommended as it provided substantial stress reduction while requiring less severing, grinding and re-welding than some of the other concepts. This configuration shown in Figure 7 consists of a 2" radius, 0.375" thick circular disk welded to the vertical plate and a small reinforcement plate, shaped to match the re-entrant corner contour as shown, is welded onto the support bracket to increase the effective thickness and thereby reduce the membrane stress. By examining the maximum stress in the unit solution stresses over the 128–145 Hz frequency range (which brackets the dominant frequencies for this location in the global solution) it was shown that this reinforcement reduces the maximum stress by a factor of 0.18 (Table 11 of [1]).

The design finalized here builds upon the semi-circular disc concept 2 but is modified to eliminate and cutting of existing welds. It consists of a 2.5" wide by 3" high 3/8" thick rectangular plate with a 1.5" long and 1" wide slot cut out as indicated in Figure 8. The dimensions are selected so that the plate can slide over the existing 0.25" brace attachment weld (W1). Note that the total width of the existing 0.25" double sided fillet weld is 2x0.25" (two fillets) plus 0.375" (brace plate thickness) or 0.875". The larger 1" slot accommodates possible irregularities in the actual weld. The length of the slot is sized so that the plate can slide up to the existing weld (again accounting for possible irregularities in the wrap around portion of the existing weld) and leave sufficient room for a 0.375 fillet weld (W2) around its perimeter. The plate and slot has ¼" rounded fillets. The installation process begins by sliding this plate over the brace and attaching it to the vertical plate by a 3/8" fillet weld as indicated in Figure 8. Next a ½" weld (W4) is created as shown in Figure 9 to attach the 3/8" brace reinforcement plates. These welds are continued to the right along the entire length of the vertical plate/brace joint wrapping around the end. This allows continued used of the SRF=0.6 for this reinforced weld line. The attachment is completed by adding a ¼" weld W5 to attach the brace reinforcement plates to the brace. A top view of the brace reinforcement plate is shown in Figure 10. The plate is 5" long by 1.25" wide and trimmed at a 47.5 deg. angle as indicated so that the edge is parallel to the existing weld joining the two plates comprising the lifting rod brace.

This reinforcement is used for the middle and top lifting rod braces. For the lowest braces adequate stress margin is achieved by increasing the existing weld size to ½" allowing application of the SRF=0.6 stress reduction factor to this weld as shown in [12].

Prior to final design and installation it is require that available photographs of the as-built lifting rod brace installations be reviewed to ensure that there is adequate clearance relative to existing welds and to ensure proper fitting of the new components. For example, reference to the photograph in Figure 11 suggests that proper fitting of the vertical plate will entail milling out a step on the face adjacent to the vertical plate to accommodate the closure plate and its attachment weld.

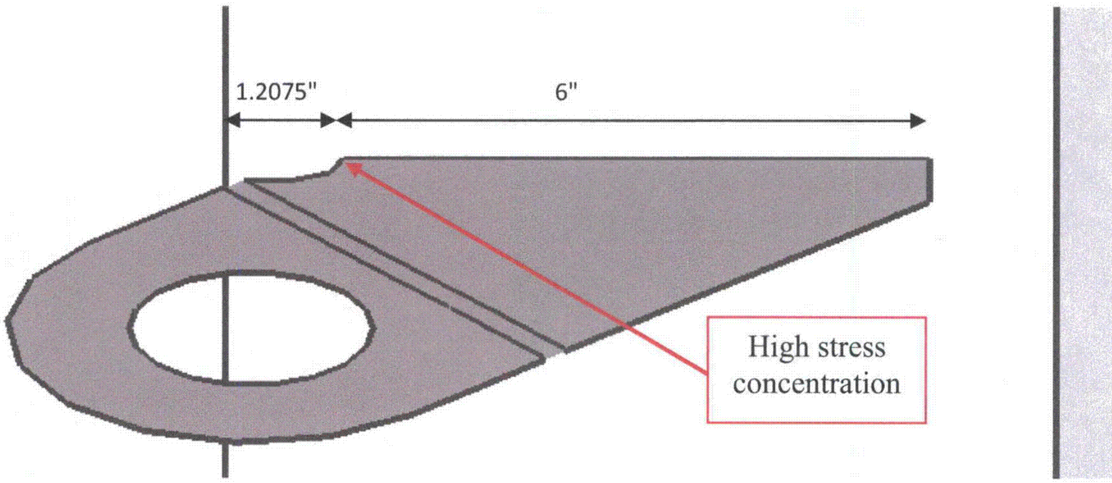

Figure 6. Basic geometry of lifting rod brace. The lifting rod slides through the circular hole and the brace is attached to the vane bank vertical plate.

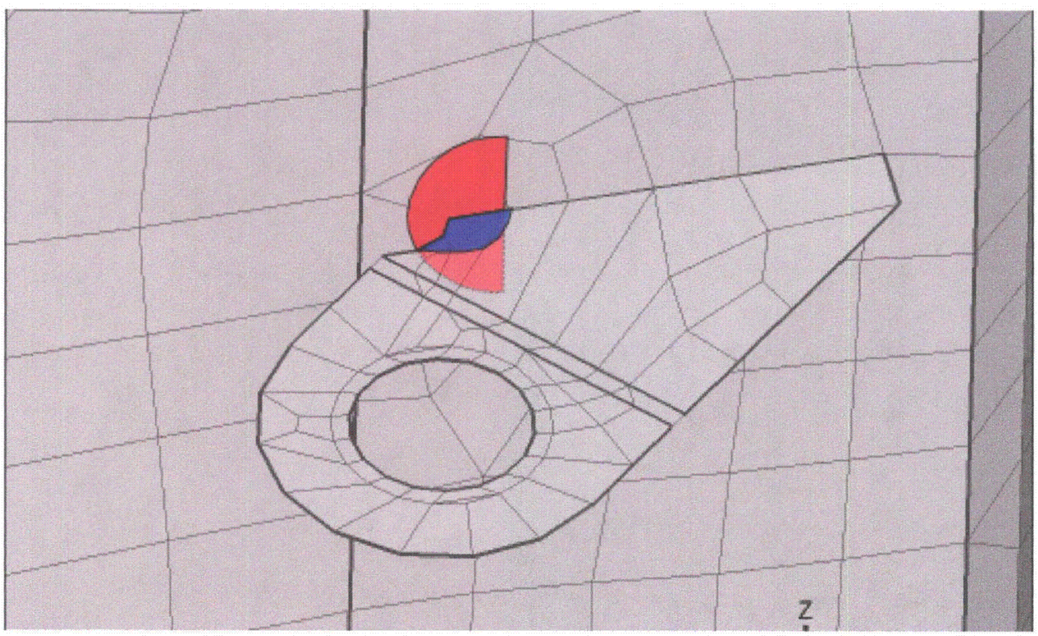

Figure 7. Reinforcement concept 2: Partial reinforcement – semi-circular plate one side plate (red) and reinforcement of re-entrant corner on support bracket (blue)

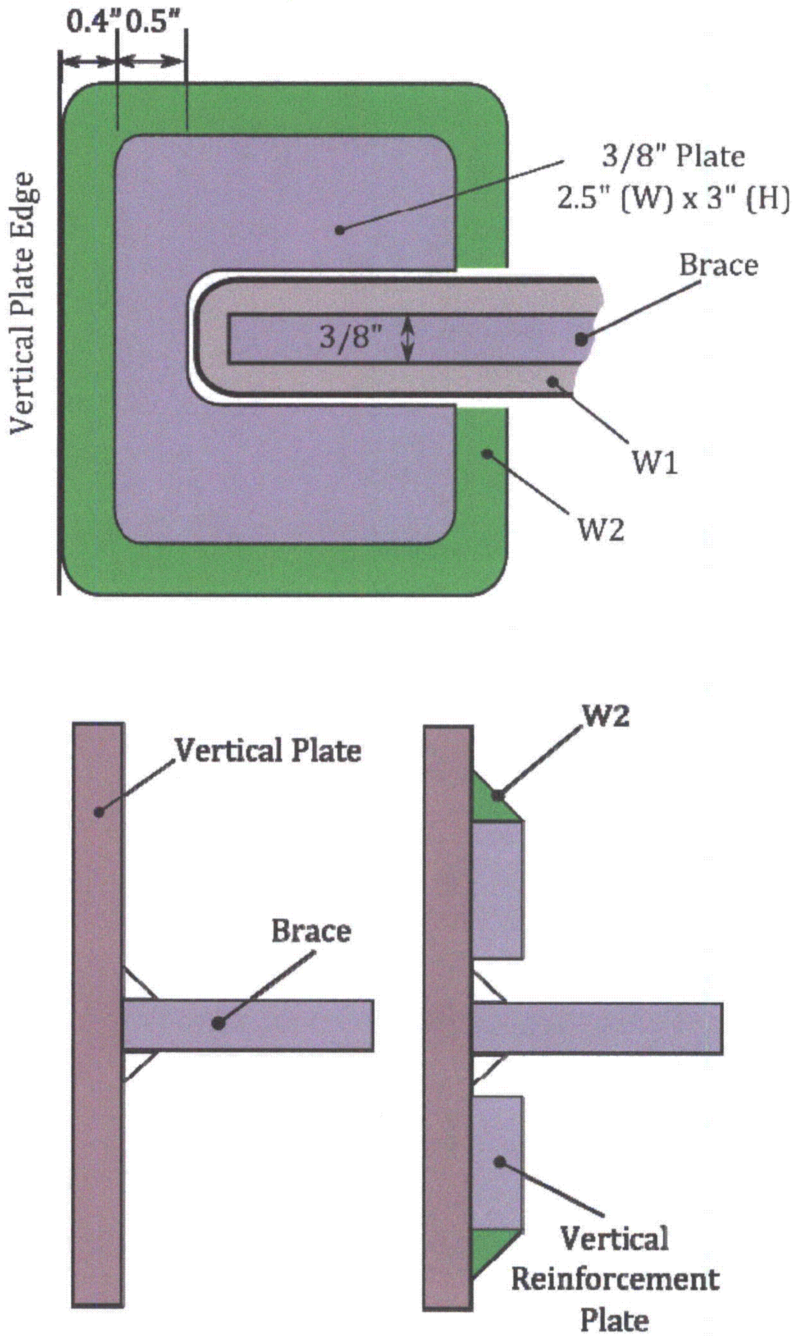

Figure 8. Schematic of reinforcement. W1 is the existing 0.25" weld; W2 is the new 0.375" weld for attaching the vertical reinforcement plate.

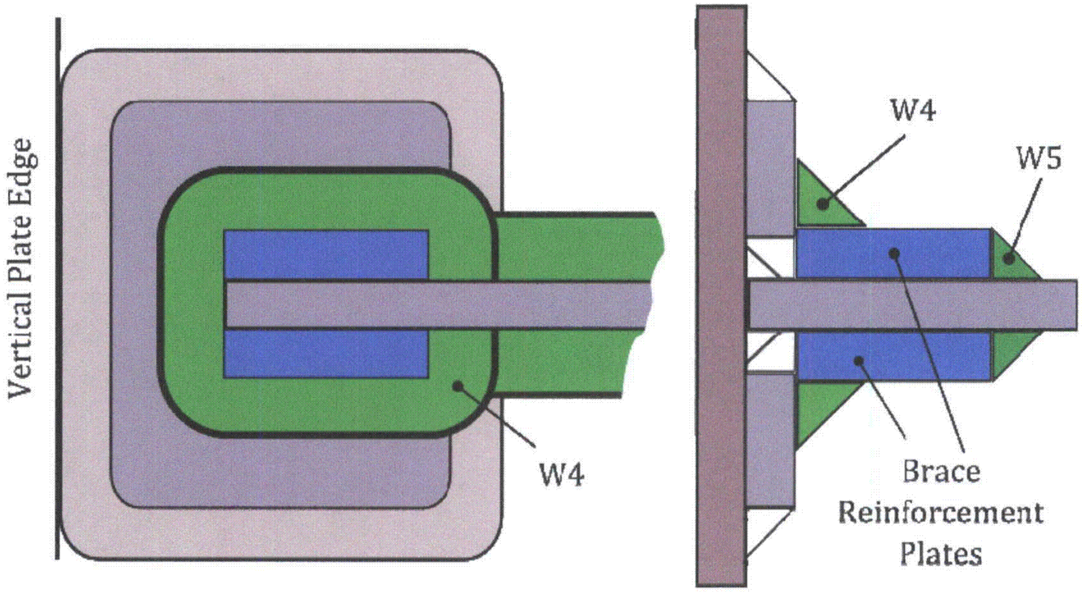

Figure 9. Additional welds. The 0.5" fillet weld, W4, attaches the 3/8" brace reinforcement plates to the vertical reinforcement plate. The weld continues on over the existing brace attachment weld. W5 attaches the brace reinforcement plates to the existing brace.

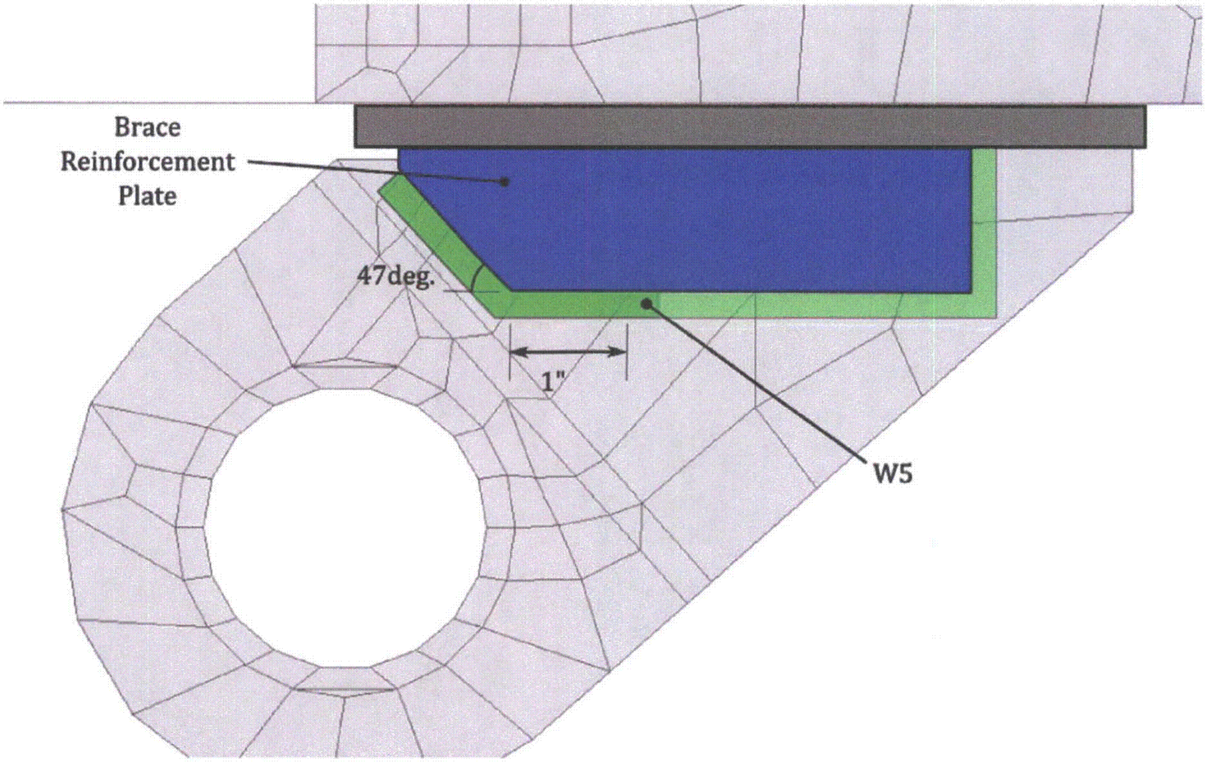

Figure 10. Depiction of brace reinforcement plate.

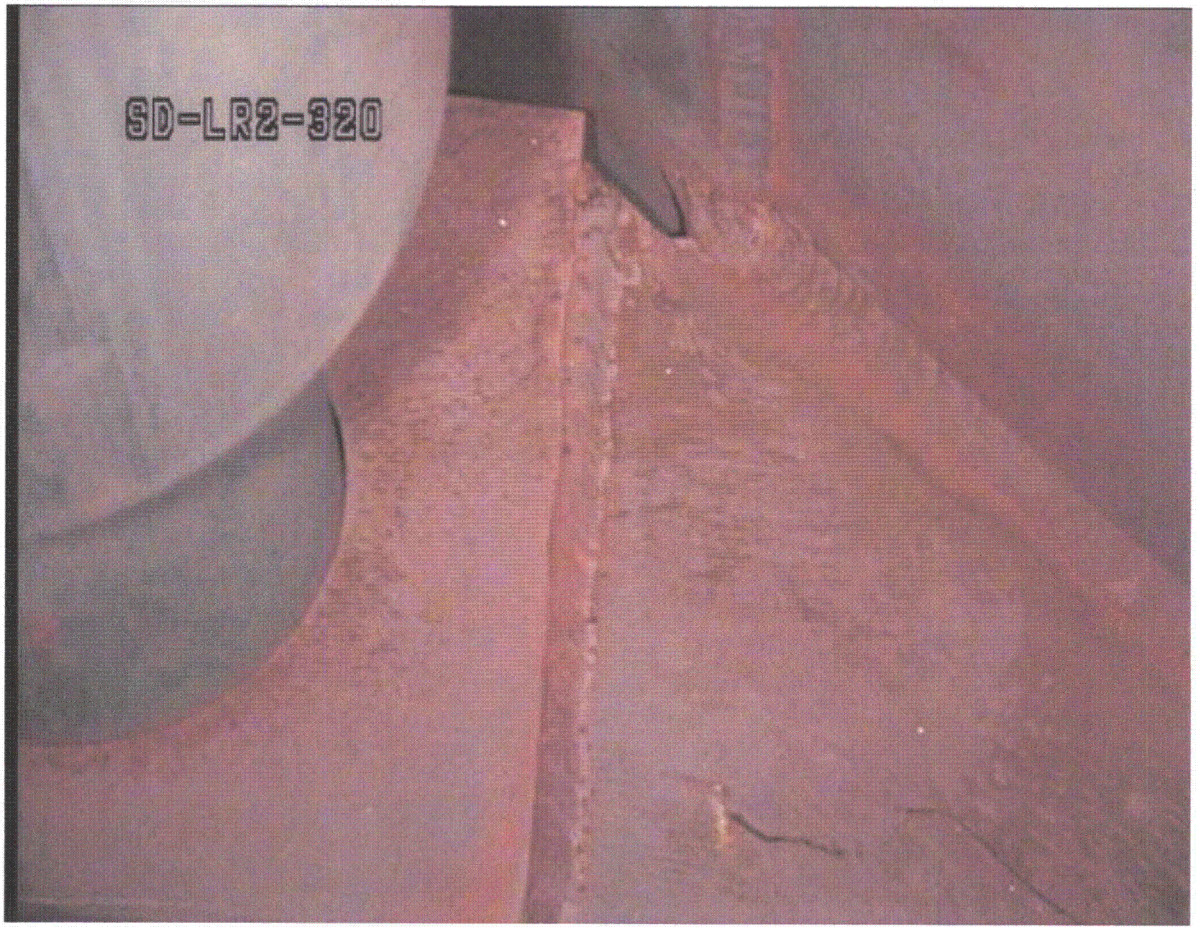

Figure 11. As built lifting rod brace.

3.2 Middle Hood/Reinforcement Strip (Group 2)

Application of the Rev. 4.1 acoustic loads induces a strong response on the section of the middle hood lying between the closure plate and the vertical reinforcement strip (see Figure 12), and generates stresses along this strip that exceed target levels (SR-a=1.62). This strip was previously added to address indications on the outboard section of the middle hood. The high stresses occur on the 1/8" middle hood rather than within the much thicker strip (additional 3/8") and are dominated by a 109.0 Hz signal which, at the +10% shift, excites a structural response at 119.9 Hz.

In Section 6 of [1] it was reasoned that a local modification was unlikely to rectify the high stress, but merely shift its location slightly. Therefore, to reduce the stress it was proposed to suppress the active oscillation by covering this section of the middle hood with a 3/8" curved plate welded about its perimeter to the hood and closure plate. Manufacture of the plate is straightforward and creating the attachment weld does not pose accessibility challenges. However, since each such plate would weigh approximately 90 lbs and stress evaluations showed that all previously limiting locations on the hood acquired very high alternating stress ratios (SR-a>20) after the modification it was surmised that adequate stress reduction could easily be achieved using thinner reinforcement plates.

Therefore the steam dryer stress evaluation is repeated by replacing the previous 3/8" curved reinforcement plate by one that is 1/8" thick thus increasing the effective thickness of the hood section to ¼". Unit solution stresses of the complete steam dryer with this modified middle hood section (and also the other planned reinforcements – reinforced closure plate and added masses on the inner and middle hoods as discussed below) are developed in the 30-250 Hz frequency range. This range: (i) encompasses the frequency where stresses are highest and (ii) ensures that any higher order modes occurring at higher frequencies are fully accounted for. Recalculation of the stresses at the Group 2 locations in Table 3 results in the considerably lowered stress in Table 4. Though more than adequate, this level of reinforcement seems excessive and a re-evaluation of the dryer using a ¼" or 1/8" rather than 3/8" curved plate over the middle hood section is recommended. The stress results for the previous high stress locations are listed in Table 4 and seen to maintain ample margin for EPU operation.

It is recommended that the panels be trimmed to size such that the plate edges reach to within 1/8" of the existing welds on the closure plate and the reinforcement strip. A 3/16" inch fillet weld is then applied around the perimeter of the reinforcement plate.

Table 4. Group 2 CLTP stresses after adding 1/8th reinforcement plate over the middle hood section lying between the existing reinforcement strip and closure plate.

Location	node	Pm	Pm+Pb	Sa	SR-P	SR-a	% Freq. Shift	Dom. Freq. [Hz]
2. Hood Reinforcement/Middle Hood	98275	200	497	362	28.07	18.96	0	135.4
8. Hood Reinforcement/Middle Hood	90126	981	1462	381	9.47	18.05	5	51.2
9. Hood Reinforcement/Middle Hood	98268	352	597	377	23.34	18.24	2.5	135.4
10. Hood Reinforcement/Middle Hood	90949	993	1112	321	9.36	21.36	-5	140.9

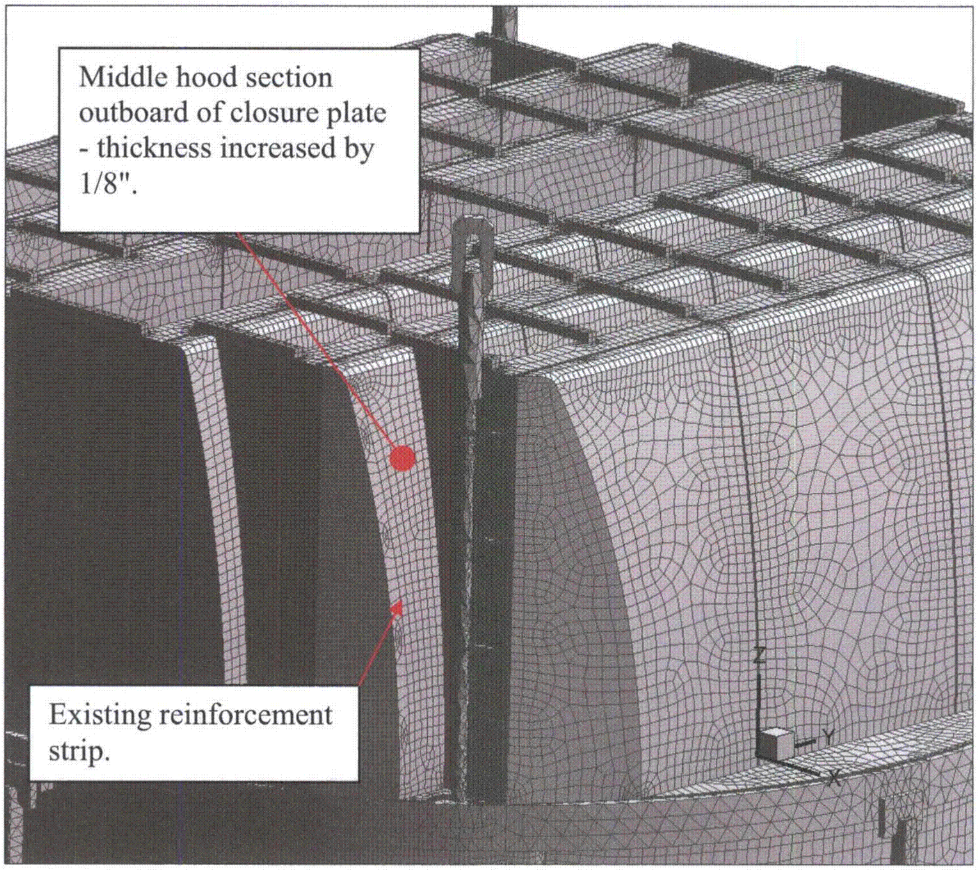

Figure 12. Middle hood section subject to modification and existing reinforcement strip.

3.3 Inner Hoods/Hood Support (Group 3)

In its present configuration the inner hoods and to a lesser extent also the middle hoods, show a strong stress response on the hood/hood support welds at 41 Hz and 51-54 Hz. The stresses result from strong vibrations of the central sections of the inner and middle hoods. Since the acoustic loads on these hoods are relatively low, these vibrations are caused by transmission of loads from other steam dryer components such as the directly forced outer hoods. Previous sub-model analysis of the hood/hood support weld yielded a stress reduction factor of SRF=0.77 (this corresponds very closely to the ratio, 1.4/1.8=0.78 expected for the full penetration weld joining the hood and hood supports). Even with this SRF however, the stresses exceed EPU target levels. Since the welds, particularly at higher elevations, are difficult to access and reinforce it is necessary to pursue alternate modifications. One option is to stiffen the hood panels and suppress vibrations by adding reinforcement strips at the modal displacement response peaks. This would generally result in similar response modes occurring at upward-shifted natural frequencies. However, examination of the MSL signals in the vicinity of 52 Hz indicates that these signals increase with frequency so that an upward shift in the hood frequencies would place these frequencies into a range with stronger MSL signals.

Therefore the option proposed here is to add small masses on the inner hoods. Specifically one such mass is added to each of four central inner hood sections as indicated in Figure 13. Each mass is located 18" below the top of the vane bank surface since this is approximately the reach length of a submerged diver welding the masses to the inner hoods. The addition of the masses lowers the natural response frequencies and reduces the modal amplitudes (since the generalized masses of the participating modes are reduced). In Section 6 of [1] it had been proposed to utilize 20 lb masses. While this successfully reduced the stresses in the high stress regions, it is desirable to minimize the size and weight of these masses while still meeting the required stress margins. Therefore the stress evaluation was repeated using 15 lb masses attached to the inner hoods. These masses were added into the global model and unit solutions regenerated over the 30-250 Hz frequency range (in conjunction with the other modifications to the dryer including the thickened closure plates, middle hood masses and middle hood reinforcement described for Group 2). The stresses at the high stress regions when applying the ACM Rev. 4.1 loads are summarized in Table 5. While the stress ratios are somewhat less than obtained previously using 20 lb masses, all locations still meet the required margins.

Using a density of 0.284 lb/in^3 for stainless steel it follows that the volume of the 15 lb mass is 52.8 in^3. It is here proposed to use a rounded 8"x8" 1" thick rectangular mass with two interior slits – a lower 6" slit and an upper 3" slit - added for additional weld support (see Figure 14). The mass is attached with a ¼" weld around the top and side edges (the bottom edge is considered inaccessible to diver reach) and the same sized weld around the interior perimeters of the two slits. The bottom face of the mass facing the hood is milled to accommodate the hood curvature (radius of curvature is 353") at 18" below the top of the vane bank. The upper 3" and lower 6" slots are added to allow for additional attachment welds which are placed along the interior slot perimeters. The slots are angled as shown to facilitate access with welding rods. Note that the outer perimeter welds should be sufficient to secure the masses under vibration, the interior slot welds being added for additional conservatism.

Table 5. Group 3 CLTP stresses after modification

Location	SRF	node	Pm	Pm+Pb	Sa	SR-P	SR-a	% Freq. Shift	Dom. Freq. [Hz]
4. Hood Support/Inner Hood	1(b)	95636	902	2270	2236	6.14	3.07	-10	51.2
5. Hood Support/Inner Hood	1(b)	95650	787	2124	1917	6.56	3.58	-10	51.2
6. Hood Support/Inner Hood	1(b)	95642	975	2435	2433	5.72	2.82	-10	51.2

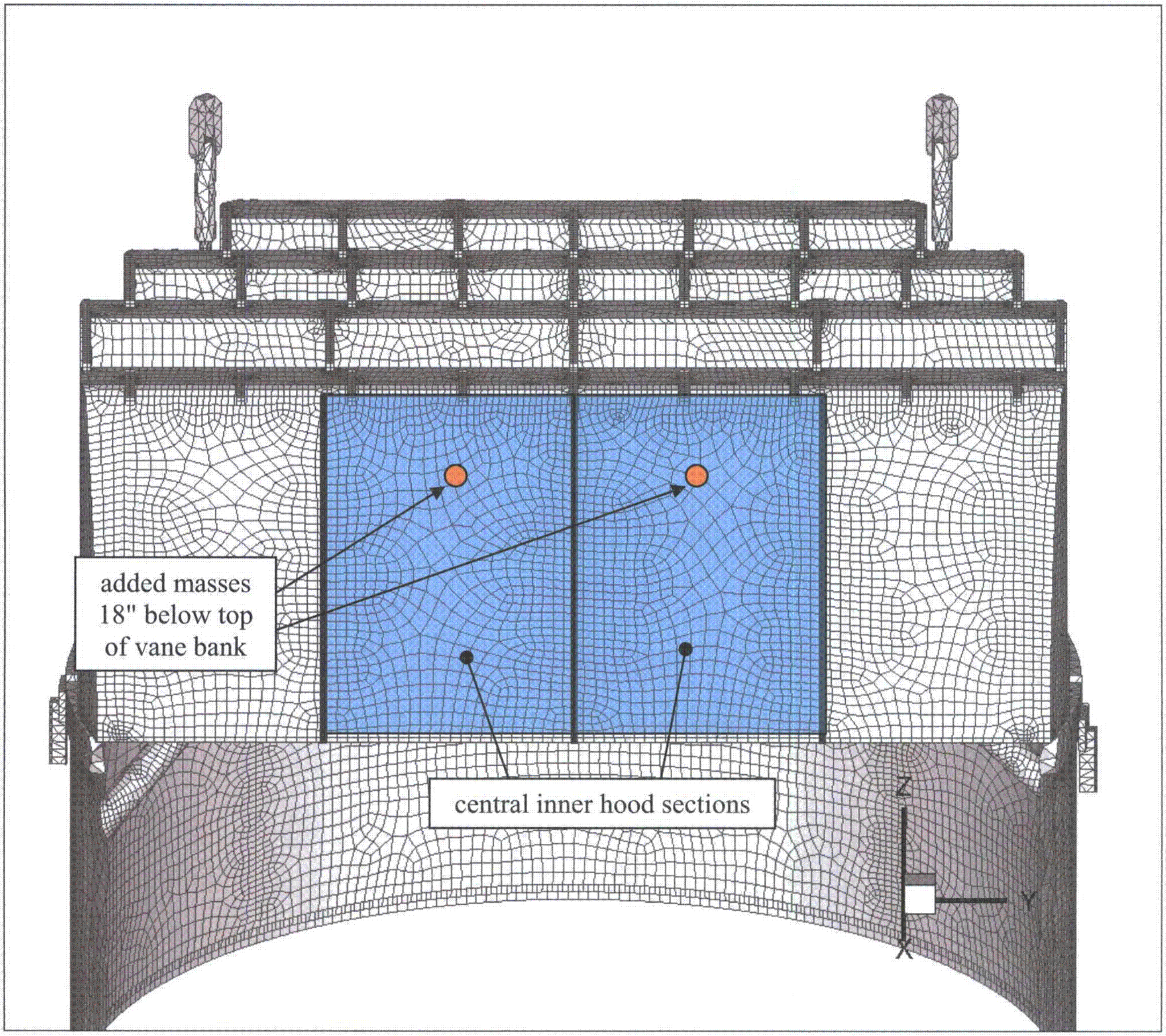

Figure 13. The inner hood sections (blue) whose response contributes to the high stresses on the central hood support/inner hood weld. Middle and outer hoods excluded from view to expose inner hood surfaces. Proposed masses are added 18" below the top of the vane bank.

[[

(3)]]

3.4 Group 4 Locations

The stresses in the remaining group 4 do not change significantly with the modifications described above for groups 1-3. All of these locations were identified as having stress ratios of 2.65 or higher before the modifications above are implemented [1]. It was argued in [1] that there is a strong likelihood that no additional modifications are needed for at least two reasons. First, significant measurement noise is present that contributes to the stress predictions. Since these contributions are not expected to increase with power increase, the stress ratios resulting from acoustics plus noise will increase at a somewhat lesser rate than inferred from a pure acoustics load. During power ascension, these locations can be processed using the actual measured signals at increased power levels and the exact same ACM Rev. 4.1 loads model and stress evaluation procedures utilized above. If the resulting stress ratios for these locations remain above 2.00 the power ascension process can continue; if the stress ratio reduces to below 2.00 then power ascension is halted and the modifications outlined below would be implemented in the subsequent outage. Secondly, all stress ratios were calculated on the basis of curve C of Fig I-9.2.2 in Appendix I in Section III of the ASME B&PV Code. However, according to the flow chart in Figure I-9.2.3 of the ASME Code use of curve B is permitted. No credit is taken for this higher allowable so that all reported alternating stress ratios are conservative by a 21.3% margin. Application of Curve B would result in all Group 4 locations meeting the EPU stress margin.

This reasoning notwithstanding it is still required to identify designs that meet the required stress margin at EPU assuming a velocity squared scaling of the stresses and the curve C-based endurance limit. In [1] modifications were scoped out for the group 4 locations. Here these modifications are developed in more extensive detail and assessed quantitatively.

For locations 11 and 14 in Table 3 involving the common intersection between the hood, hood support and base plate a stress relief cut-out hole in the hood support is proposed. A detailed evaluation of this modification is developed in Appendix A showing that the stress reduction factor achieved with the cut-out hole is SRF=0.73. A previous evaluation using a weld reinforcement at this location yielded a stress reduction factor of 0.63 [13]. A weld reinforcement however, is undesirable as the location must be accessed from underneath the dryer, exposing the diver to a hazardous radiation dose. The semi-circular stress relief cut-out hole, on the other hand, can be generated using electrical discharge machining (EDM) that can be implemented remotely thus reducing diver dose to at most the period required to attach the device to the hood support. When the circular cut-out is considered by itself the limiting stress ratio (at CLTP) at these locations increases from 2.65 to 2.65*0.78/0.73=2.83 which is above the target value (2.76 at CLTP). Here the factor of 0.78 is due to the prior usage of the full penetration weld factor of 1.4 (1.4/1.8=0.78) and 0.73 is the SRF developed in Appendix A. When the application of the SRF=0.73 is also considered in combination with the other repairs it is observed that the stress ratio at the middle hood/hood support/base plate junction (location 11 and node 95428) increases to SR-a=4.27. This is because the addition of 10 lb masses to the middle hoods (see below) also reduces the stress at this junction. Therefore if these masses are added to the middle hoods then no stress relief cut-out is needed at these junctions. For the outer hoods on the other hand (location 14 in Table 3, node 95267), the other modifications made to the steam dryer slightly reduce the alternating stress ratio from SR-a=2.71 to 2.69. Application of the SRF=0.73 increases this result to SR-a=2.87.

The bottom of the submerged drain channel/skirt weld (locations 12 and 15 in Table 3) is easily accessible and can be reinforced by adding a wrap-around reinforcement weld to alleviate the stress. In [1] a stress reduction factor of SRF=0.58 applicable to this reinforcement pertaining and calculated in [8] was provisionally applied. The sub-modeling technology and characteristic loads used to derive that factor are somewhat different than the ones here. Therefore a sub-model was developed specifically for the NMP steam dryer at this location using the sub-modeling method described in Section 2.2. This sub-model is detailed in Appendix A and provides a stress reduction factor of SRF=0.65 with the provision that the existing bottom 4" of weld are increased to a thickness of 0.25" and the weld wraps around the bottom of the drain channel and 1" up on the interior side of the junction. When the stress reduction factor is invoked in conjunction with all other dryer modifications, the stress ratios increase to the values in Table 6 showing a limiting value of SR-a=4.09 for these locations which is well above the allowable level.

The final entry in Table 3 involves the middle hood/hood support welds and arises due to vibrations of the middle hoods. The stresses at these locations are addressed by adding a total of four 10 lb masses on the central sections of the middle hoods. These function in a manner similar to the masses employed for the inner hoods. However, because a lesser reduction is needed the masses are smaller than those proposed for the inner hoods. The detailed design is the same as for the inner hoods except that the thickness of the rectangular plate is reduced from 1" to 11/16". The middle hood masses are placed at the same 18" depth measured from the top of the vane bank as the inner hood masses. The impact on stress of adding these masses in and also the other reinforcements including the reinforced closure plates, inner hood masses and reinforced middle hood section outboard of the closure plate is quantified by generating unit solutions with all modifications implemented over the 30-250 Hz frequency range as described in Section 2.1 and applying the ACM Rev. 4.1 loads. With these modifications the alternating stress ratio at this location increases from SR-a=2.68 to SR-a=4.05.

The resulting changes in the stress ratios for the Group 4 locations when implementing all steam dryer modifications are summarized in Table 6.

Table 6. Alternating stress ratios for group 4 locations before and after modifications.

Location	Modification	node	SR-a	
			Pre-modification	Post-Modification
11. Hood Support/Outer Base Plate/Middle Backing Bar	Cut-out in hood support (SRF=0.73, Appendix A)	95428	2.65	4.27
14. Hood Support/Outer Cover Plate/Outer Hood	Cut-out in hood support (SRF=0.73)	95267	2.71	2.87
12. Submerged Drain Channel/Submerged Skirt	Wrap around weld (SRF=0.65)	93430	2.65	4.18
15. Submerged Drain Channel/Submerged Skirt	Wrap around weld (SRF=0.65)	84597	2.72	4.09
13. Hood Support/Middle Hood	Added 10 lb mass	96022	2.68	4.05

3.5 Modification of Closure Plates

The presently installed closure plates are 1/8 in thick and contain a structural mode near 128 Hz. This mode is a second order mode in the vertical direction and first order in the horizontal direction. In preliminary analyses of the dryer these plates were found to respond strongly to a 135.7 Hz component in the acoustic signal which when shifted by -10% during frequency shifting, couples closely to the closure plate frequency. The response mode induces high stresses along the lateral welds connecting the closure plate to the vane bank (a straight vertical weld) and to the adjacent hood (a mostly vertical weld, but curved to accommodate the hood geometry). The highest stresses generally occur at the top of this weld. However, significant stresses also develop on these weld lines between 10-20 inches below the top of the weld. This corresponds to the weld locations nearest the maximum displacement of this mode. In preliminary stress assessments made for the dryer where noise was filtered from the signal on the basis of low power measurements, several locations on the closure plate welds emerged as having stress ratios that do not meet target levels at EPU. These locations were addressed by performing a sub-model analysis to obtain a more accurate representation of the local stress field. In some cases, addition of an interior weld or thickening of the existing weld (see Section 2.2) was required to achieve acceptable stress ratios.

With the more recent acoustic loads processed with the ACM Rev. 4.1 (and where low power subtraction is <u>not</u> performed) the closure plate weld reinforcements are insufficient to achieve the target EPU stress margin. Rather than pursue further weld reinforcement, which is limited in regard to both access (finite arm reach limits the length of weld that can be produced on the interior side of the closure plate) and prospect for improvement (making weld legs significantly larger than the plate thickness does not necessarily improve the stresses), it was decided to reinforce the closure plate itself to simultaneously reduce stresses and separate structural mode and peak acoustic frequencies.

[[

(3)]]

With the closure plate reinforcement and other steam dryer modifications it is useful to inquire whether the previous closure plate attachment weld reinforcements described in Section 2.2 remain necessary. To this end the evaluation in Section 4 is done twice, one with and one without the weld reinforcements.

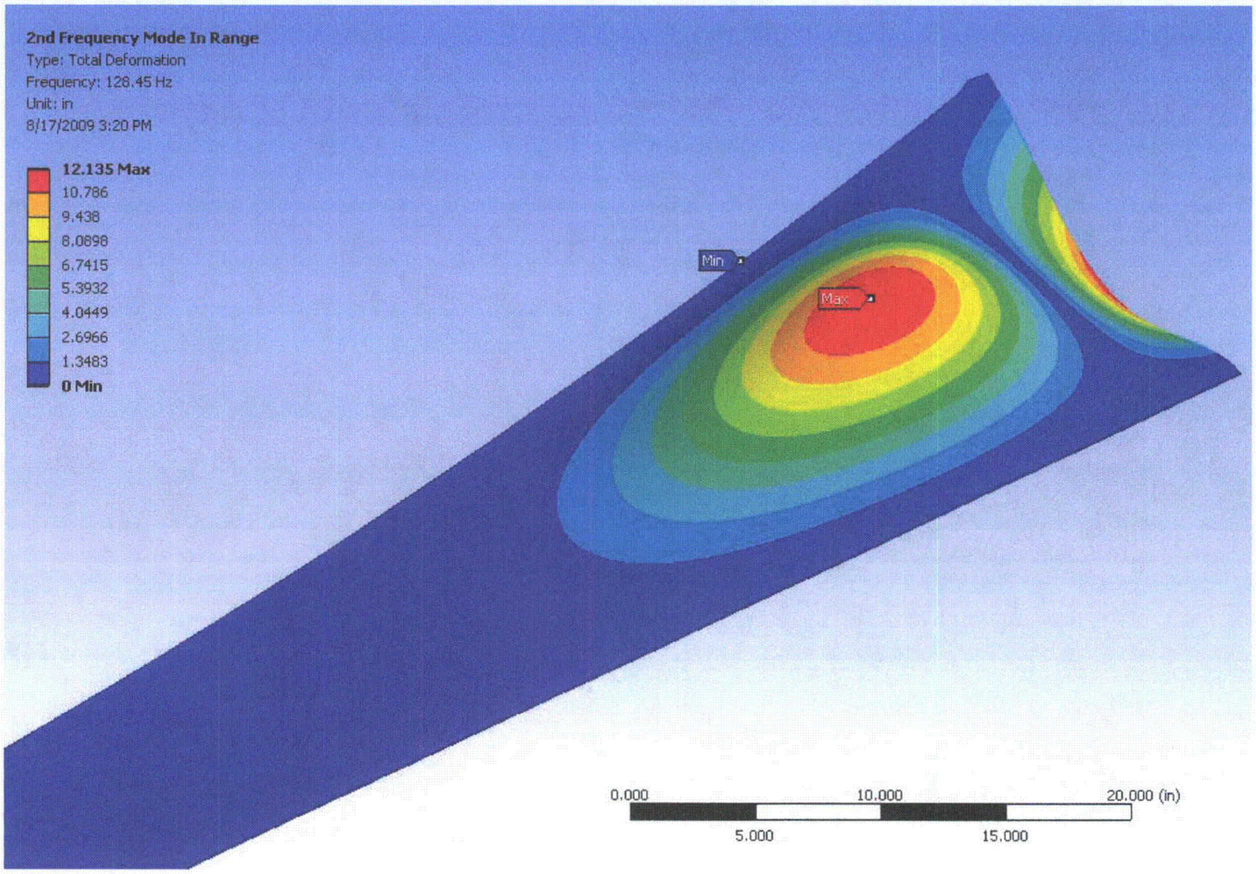

Figure 14: Second mode shape (f=128.45 Hz) of unmodified closure plates

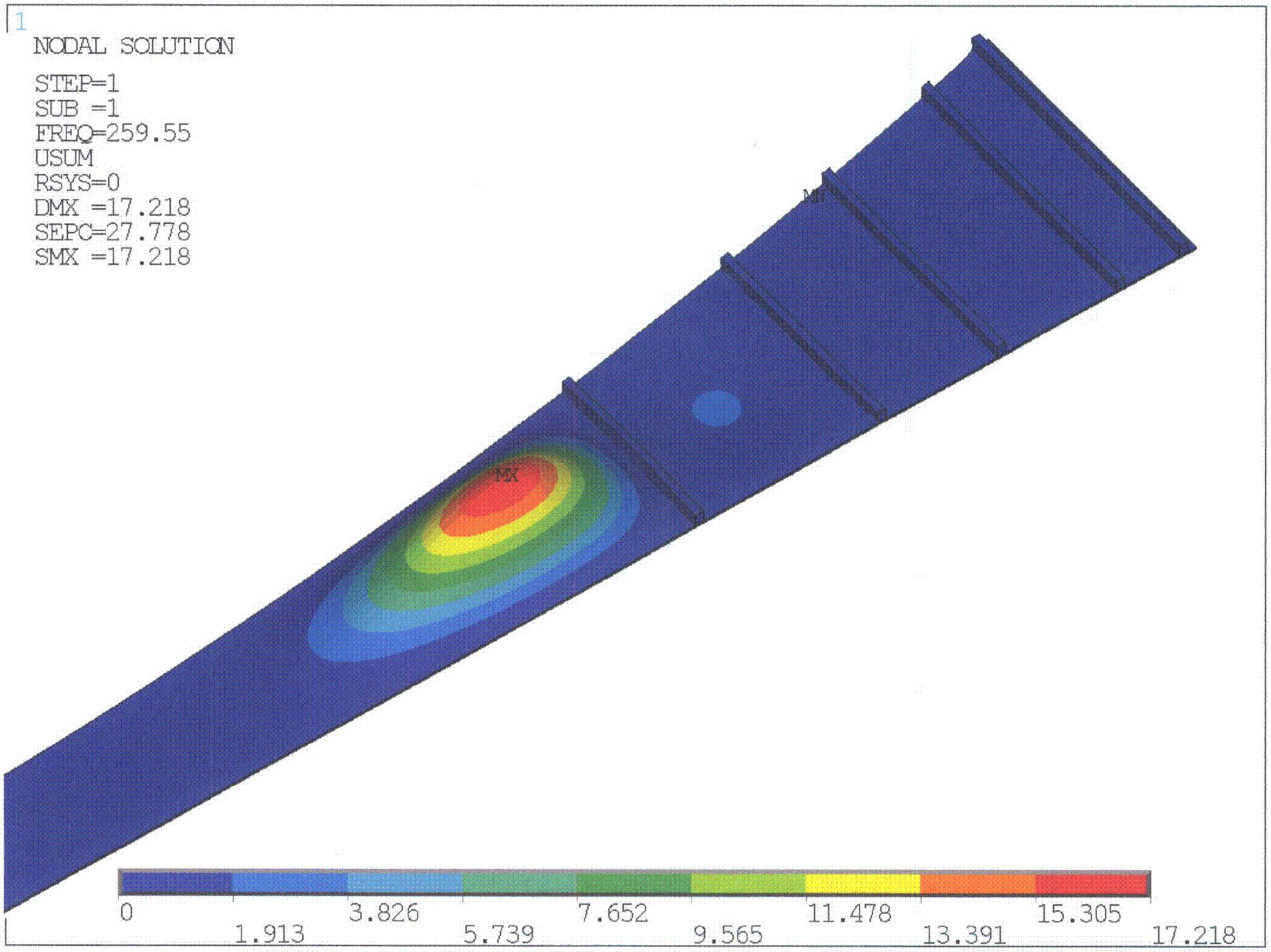

Figure 15: Fundamental mode shape (f=259.6 Hz) of modified closure plate.

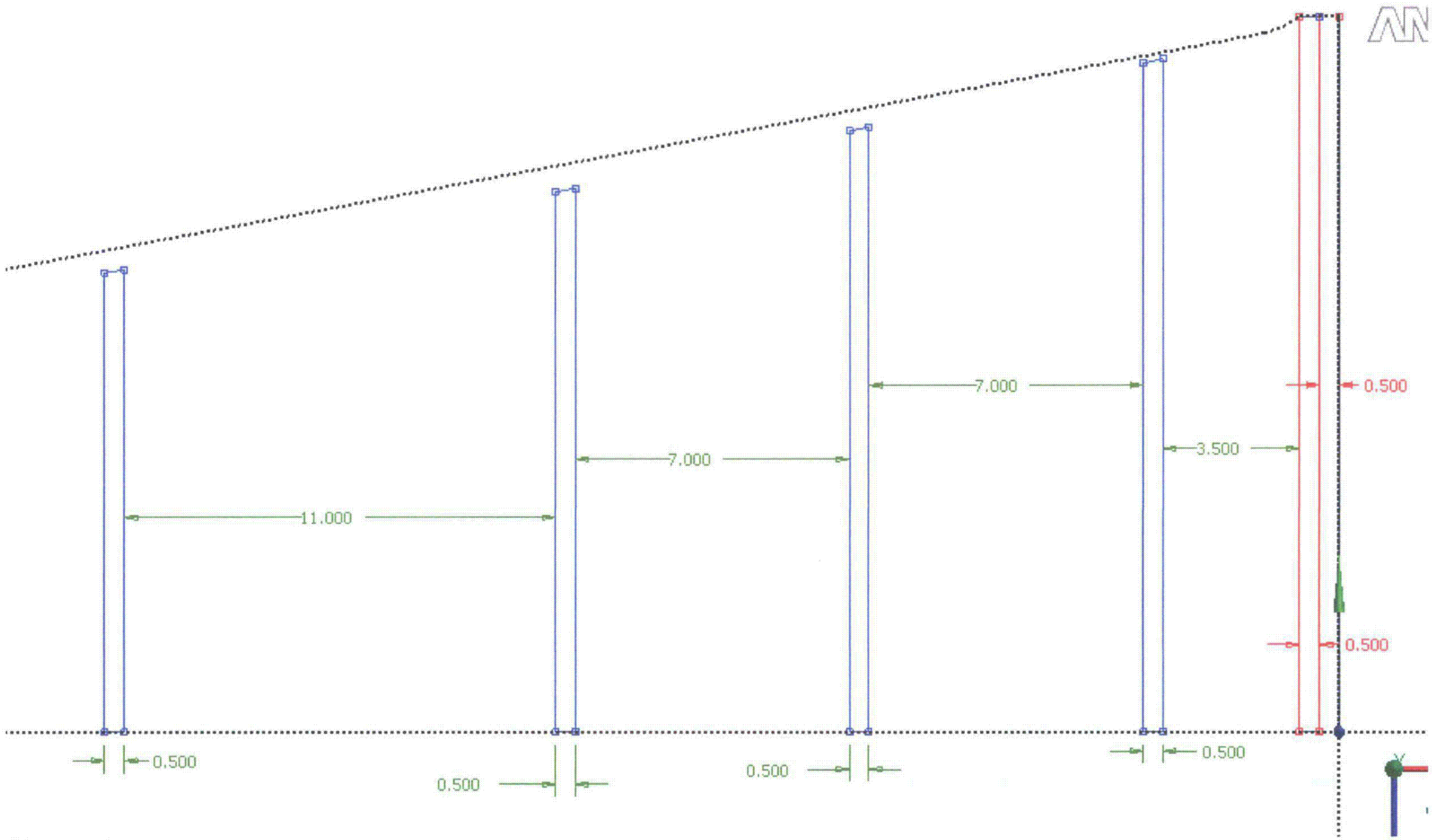

Figure 16. Closure Plate Modification – Geometry (0.5"w x 0.75"h Beam (from [14])

4. Reanalysis with All Modifications

In this section the NMP2 steam dryer is re-evaluated with all of the modifications described above in place. This calculation is intended to confirm that the modifications do not give rise to new high stress locations and are effective in achieving the required stress margins. The dryer modifications are summarized in Table 7. To implement the modifications 1, 5, 6 and 9 unit solutions are regenerated over the 30-250 Hz frequency range with these modifications in place. Below 30 Hz the unit solutions for the original unmodified dryer are used. Since the original dryer had no significant stress response below 30 Hz, the splitting of the unit solutions in this manner is acceptable. For the remaining locations stress reduction factors are appropriate since they involve localized reinforcements that do not affect the overall modal properties of the dryer, The unit solutions and are combined with the MSL signals in the manner described in [1].

The acoustic loads applied to the steam dryer are obtained using the most recent and complete strain gage signals [3] and processed using the ACM Rev. 4.1 analysis with associated biases and uncertainties updated to reflect the new revision as described in [2]. The applied load includes all biases and uncertainties for both the ACM (summarized in [15]) and the FEM. For the latter there are three main contributors to the bias and uncertainty. The first is an uncertainty (25.26%) that accounts for modeling idealizations (e.g., vane bank mass model), geometrical approximations and other discrepancies between the modeled and actual dryer such as neglecting of weld mass and stiffness in the FEA. The second contributor is a bias of 9.53% accounting for discretization errors associated with using a finite size mesh, upon computed stresses. The third contributor is also a bias and compensates for the use of a finite discretization schedule in the construction of the unit solutions. The frequencies are spaced such that at 1% damping the maximum (worst case) error in a resonance peak is 5%. The average error for this frequency schedule is 1.72%.

The lowest stress ratios obtained by comparing the stresses against allowable values, accounting for stress type (maximum and alternating) and location (on or away from a weld), are reported in Table 8 for the limiting locations in Groups 1-4 and in Table 9 for the entire steam dryer. The stress ratios are grouped according to type (SR-P for maximum membrane and membrane+bending stress, SR-a for alternating stress) and location (away from welds or on a weld). These results correspond to the limiting values over all frequency shifts between -10% and +10%. The same blanking procedure described in Section 5 of [1] is used here to prepare this table.

Table 8 records the alternating stress ratios for the locations Table 3 prior to and after all modifications are in place. All locations in the post-modification configuration meet the target stress margins required for EPU operation. The lowest alternating stress ratio in the list is 2.87 and occurs on the inner hood/hood support weld and is reflects the fact that the inner hood masses have been reduced from 20 lbs to 15 lbs. The highest post-modification margins are achieved on the weld attaching the reinforcement strip on the middle hood section outboard of the closure plate showing the effectiveness of the curved 1/8th inch laid over this section in eliminating the high stress points.

Results from the stress evaluation of the entire dryer show that the limiting alternating stress ratios on a weld involve the outer hood. The limiting value of SR-a=2.85 occurs on the weld where the outer joins to the outer cover plate. The location is positioned very near the dryer symmetry plate (y=0) or half way between the outer two hood supports. It also is close to the man way access plate welded to the outer plate and corresponds to node 17 in Table 9b of [1] which is depicted in Figure 15j of that same reference. The next highest location corresponds to the outer hood/hood support/cover plate junction. The introduction of the stress relief cut-out increases the stress ratio to 2.88. Peak stress ratios are virtually unchanged from the values presented previously; specifically the limiting value of SR-P=1.25 is identically the same and occurs at the same location as in Table 9b of [1].

In order to assess whether the closure plate attachment welds require reinforcement in light of all the other modifications made to the dryer, the stress evaluation is repeated but without the closure plate weld SRFs applied. These are the first four entries in Table 1. The resulting list of limiting alternating stress ratio locations is given in Table 10. Results for locations on the closure plate welds are highlighted in gray. It is seen that while a node on the closure plate weld now becomes the limiting location on the dryer the associated alternating stress ratio is nevertheless above 2.76 so that the EPU target stress margin is still met. The implication is that no reinforcement of these welds is needed to achieve the required stress margin. The limiting location is at the top of the closure plate/middle hood weld.

Table 7. Summary of modifications made to the NMP2 steam dryer.

Reinforcement / Modification	Details	FEA Implementation
1. Add reinforcement ribs to all (8) closure plates.	Section 3.5	Closure plates are thickened to obtain dynamically equivalent structure a described in Section 3.5
2. Reinforce closure plate attachment welds.	Section 2.2 Also [1]	SRFs listed for locations 1-4 in Table 1 applied to these welds.
3. Increase weld of the lowest lifting rod brace/vertical plate welds to 0.5"	Section 3.1 Also [12]	Apply SRF=0.6 corresponding to location 5 in Table 1 to these welds.
4. Reinforce middle and upper lifting rod braces to eliminate stress concentration on weld to vertical plate.	Section 3.1	Apply stress reduction factor of 0.18 to this location based on FEA reductions shown for Concept 2 in Table 11 of [1])
5. Add 1/8" thick plate over the middle hood section lying between the closure plate and existing reinforcement strip.	Section 3.2	Thicken the existing plate by 1/8".
6. Add total of four 15 lb masses to the central sections of the inner hoods.	Section 3.3	Place 15 lb point masses on the inner hoods at the mass centers.
7. Add stress relief cut-out at the bottom edge of the outer hood supports.	Section 3.4; Appendix A	Apply SRF=0.73 to the outer hood/hood support/cover plate junctions.
8. Reinforce the bottom of the drain channel/skirt weld with thickened wrap-around weld.	Section 3.4; Appendix A	Apply SRF=0.65 to the stresses at these locations.
9. Add total of four 10 lb masses to the central sections of the middle hoods.	Section 3.4	Place 10 lb point masses on the middle hoods at the mass centers.

Note. Modifications 1, 5, 6 and 9 are implemented into the FE model and associated unit solutions regenerated over the 30-250 Hz frequency range for subsequent combination with MSL signals.

Table 8. Post modification stress ratios for the limiting locations in Table 3

Location	GROUP	SRF	node	SR-a	% Freq. Shift	Dom. Freq. [Hz]	SR-a Post Mod.(d)
1. Side Plate/Brace	1	0.6(5)	89649	1.56	-5	139.7	5.77
3. Side Plate/Brace	1	1	89646	1.74	5	103.3	3.33
7. Side Plate/Brace	1	0.6(5)	89652	2.35	-5	139.7	8.03
2. Hood Reinforcement/Middle Hood	2	1	98275	1.62	10	109.0	19.74
8. Hood Reinforcement/Middle Hood	2	1	90126	2.35	10	109.0	18.39
9. Hood Reinforcement/Middle Hood	2	1	98268	2.38	-7.5	146.1	18.66
10. Hood Reinforcement/Middle Hood	2	1	90949	2.57	2.5	190.7	21.38
4. Hood Support/Inner Hood	3	1(b)	95636	2.17	-10	51.2	3.10
5. Hood Support/Inner Hood	3	1(b)	95650	2.27	-10	51.2	4.23
6. Hood Support/Inner Hood	3	1(b)	95642	2.28	2.5	44.1	2.94
11. Hood Support/Outer Base Plate/Middle Backing Bar	4	1(b)	95428	2.65	5	48.6	4.27
14. Hood Support/Outer Cover Plate/Outer Hood	4	1(b)	95267	2.71	-10	60.5	2.88
12. Submerged Drain Channel/Submerged Skirt	4	1	93430	2.65	5	51.8	4.18
15. Submerged Drain Channel/Submerged Skirt	4	1	84597	2.72	2.5	104.0	4.09
13. Hood Support/Middle Hood	4	1(b)	96022	2.68	-5	53.4	4.05

Notes.

(a) Node numbers are retained for further reference.

(1-11) Appropriate stress reduction factor for the welds and modifications listed in Table 1 have been applied. The number refers to the particular location and corresponding stress reduction factor in Table 1.

(b) WF=1.4

Table 9. Locations with minimum stress ratios for CLTP conditions with frequency shifts. Stress ratios at every node are recorded as the lowest stress ratio identified during the frequency shifts. Stress ratios are grouped according to stress type (maximum – SR-P; or alternating – SR-a) and location (away from a weld or at a weld). Bold text indicates minimum stress ratio of any type on the structure.

Stress Ratio	Weld	Location	Location (in.)			node(a)	Stress Intensity (psi)			Stress Ratio		% Freq. Shift
			x	y	z		Pm	Pm+Pb	S_{alt}	SR-P	SR-a	
SR-P	No	1. Inner Side Plate	3.1	119	0.5	37229	7567	9032	680	2.23	18.17	5
"	"	2. Thin Vane Bank Plate	-15.6	-118.4	0.6	2558	4883	5306	275	3.46	44.91	-2.5
"	"	3. Support/Seismic Block	10.2	123.8	-9.5	113286	4574	4574	1555	3.7	7.95	10
SR-a	No	1. Brace	32.9	-27.2	69.8	70703	1077	4365	4334	5.81	2.85	5
"	"	2. Inner Hood	31.1	-33.7	78.1	70266	1249	3867	3815	6.56	3.24	2.5
"	"	3. Inner Hood	79.6	85.5	75.8	37811	3789	3834	3606	4.46	3.43	-7.5
SR-P	**Yes**	**1. USR/Support/Seismic Block**	**-6.9**	**-122.3**	**-9.5**	**113554**	**7416**	**7416**	**1094**	**1.25**	**6.28**	**10**
"	"	2. Side Plate Ext/Inner Base Plate	16.3	119	0	94143	7005	9899	546	1.33	12.58	2.5
"	"	3. Tie Bar	49.3	108.1	88	141275	6234	6234	1145	1.49	6	-5
"	"	4. Inner Side Plate/Inner Base Plate	-2.3	-119	0	99200	4514	8181	781	1.7	8.79	7.5
"	"	5 Thin Vane Bank Plate/Hood Support/Inner Base Plate	24.1	-59.5	0	85191	5217	5250	1567	1.78	4.38	-7.5
"	"	6. Hood Support/Middle Base Plate/Inner Backing Bar/Inner Hood(b)	-39.9	0	0	85723	5184	5463	1942	1.79	3.54	2.5
"	"	7. Side Plate/Top Plate	17.6	119	88	91215	981	7675	1942	1.82	3.54	0
"	"	8. Closure Plate/Backing Bar/Inner Hood	39.9	108.6	0.5	93062	5017	5075	693	1.85	9.91	5
"	"	9. Hood Support/Outer Base Plate/Middle Backing Bar	-71.3	0	0	95428	4939	5341	2202	1.88	3.12	5
"	"	10. Outer Cover Plate/Outer Hood	102.8	-58.1	0	94498	1065	7287	1008	1.91	6.81	2.5
"	"	11. Hood Support/Middle Base Plate/Inner Backing Bar/Inner Hood(b)	-39.9	59.5	0	90468	4670	4812	1615	1.99	4.25	0
"	"	12. Hood Support/Outer Cover Plate/Outer Hood(11)	-102.8	28.4	0	95267	4537	4881	2386	2.05	2.88	5

Notes.

(a) Node numbers are retained for further reference.

(1-11) Appropriate stress reduction factor for the welds and modifications listed in Table 1 have been applied. The number refers to the particular location and corresponding stress reduction factor in Table 1.

(b) WF=1.4

Table 9 (cont.). Locations with minimum stress ratios for CLTP conditions with frequency shifts. Stress ratios at every node are recorded as the lowest stress ratio identified during the frequency shifts. Stress ratios are grouped according to stress type (maximum – SR-P; or alternating – SR-a) and location (away from a weld or at a weld).

Stress Ratio	Weld	Location	Location (in.)			node(a)	Stress Intensity (psi)			Stress Ratio		% Freq. Shift
			x	y	z		Pm	Pm+Pb	S_{alt}	SR-P	SR-a	
SR-a	Yes	1. Outer Cover Plate/Outer Hood	-102.8	-1	0	95236	1200	2864	2414	4.87	2.85	5
"	"	2. Hood Support/Outer Cover Plate/Outer Hood(11)	-102.8	28.4	0	95267	4537	4881	2386	2.05	2.88	5
"	"	3. Hood Support/Inner Hood(b)	-36.8	0	46.9	95644	922	2471	2371	5.64	2.9	0
"	"	4. Top Thick Plate/Inner Hood/Top Plate	24.1	-30.6	88	85512	792	2376	2320	5.87	2.96	2.5
"	"	5. Hood Support/Outer Base Plate/Middle Backing Bar	71.3	0	0	98067	4651	4952	2318	2	2.96	0
"	"	6. Thick Vane Bank Plate/Thin Vane Bank Plate/Side Plate/Side Plate Ext/End Plate	-24.1	119	11.6	90170	827	2579	2277	5.41	3.02	5
"	"	7. Hood Support/Inner Hood(b)	32.4	0	72.5	99540	628	2564	2273	5.44	3.02	5
"	"	8. Hood Support/Inner Hood(b)	-38.2	0	34.9	95638	904	2267	2232	6.15	3.08	-2.5
"	"	9. Side Plate/Top Plate	-80.2	-85.2	88	93031	515	2700	2221	5.16	3.09	2.5
"	"	10. Entry Bottom Perf/Side Plate/End Plate	24.1	119	23.7	91154	1286	2855	2148	4.88	3.2	-5
"	"	11. Closure Plate/Middle Hood(3)	60.2	-85.2	87	89317	1068	4417	2081	3.16	3.3	5
"	"	12. Side Plate/Brace(5)	79.7	85.2	31.2	89646	1986	2230	2064	4.68	3.33	2.5
"	"	13. Hood Support/Inner Hood(b)	-36.5	59.5	48.8	90430	809	2201	2039	6.33	3.37	-2.5
"	"	14. Hood Support/Middle Hood(b)	-63.8	0	72.5	96037	463	2275	2034	6.13	3.38	-2.5
"	"	15. Outer Cover Plate/Man Way Overlap	-106.5	12.5	0	87488	760	2631	2002	5.3	3.43	5

Notes
(a) Node numbers are retained for further reference.
(1-11) Appropriate stress reduction factor for the welds and modifications listed in Table 1 have been applied. The number refers to the particular location and corresponding stress reduction factor in Table 1.
(b) WF=1.4

Table 10. Locations with minimum alternating stress ratios for CLTP conditions with frequency shifts with all closure plate attachment weld SRFs (locations 1-4 in Table 1 restored to unity. Stress ratios at every node are recorded as the lowest stress ratio identified during the frequency shifts. Grayed lines correspond to closure plate attachment welds.

Stress Ratio	Weld	Location	Location (in.)			node(a)	Stress Intensity (psi)			Stress Ratio		% Freq. Shift
			x	y	z		Pm	Pm+Pb	S_{alt}	SR-P	SR-a	
SR-a	Yes	1. Closure Plate/Middle Hood	60.2	-85.2	87	89317	1242	5136	2419	2.71	2.84	5
"	"	2. Outer Cover Plate/Outer Hood	-102.8	-1	0	95236	1200	2864	2414	4.87	2.85	5
"	"	3. Hood Support/Outer Cover Plate/Outer Hood(11)	-102.8	28.4	0	95267	4537	4881	2386	2.05	2.88	5
"	"	4. Hood Support/Inner Hood(b)	-36.8	0	46.9	95644	922	2471	2371	5.64	2.9	0
"	"	5. Top Thick Plate/Inner Hood/Top Plate	24.1	-30.6	88	85512	792	2376	2320	5.87	2.96	2.5
"	"	6. Hood Support/Outer Base Plate/Middle Backing Bar	71.3	0	0	98067	4651	4952	2318	2	2.96	0
"	"	7. Thick Vane Bank Plate/Thin Vane Bank Plate/Side Plate/Side Plate Ext/End Plate	-24.1	119	11.6	90170	827	2579	2277	5.41	3.02	5
"	"	8. Hood Support/Inner Hood(b)	32.4	0	72.5	99540	628	2564	2273	5.44	3.02	5
"	"	9. Hood Support/Inner Hood(b)	-38.2	0	34.9	95638	904	2267	2232	6.15	3.08	-2.5
"	"	10. Side Plate/Top Plate	-80.2	-85.2	88	93031	515	2700	2221	5.16	3.09	2.5
		11. Closure Plate/Inner Hood	-28.8	-108.6	-87	95975	3570	5524	2153	2.52	3.19	2.5
"	"	12. Entry Bottom Perf/Side Plate/End Plate	24.1	119	23.7	91154	1286	2855	2148	4.88	3.2	-5
"	"	13. Top Thick Plate/Side Plate/Closure Plate	47.1	-108.6	87.2	96096	2497	4103	2125	3.4	3.23	2.5
"	"	14. Side Plate/Brace(5)	79.7	85.2	31.2	89646	1986	2230	2064	4.68	3.33	2.5
"	"	15. Hood Support/Inner Hood(b)	-36.5	59.5	48.8	90430	809	2201	2039	6.33	3.37	-2.5
"	"	16. Hood Support/Middle Hood(b)	-63.8	0	72.5	96037	463	2275	2034	6.13	3.38	-2.5
"	"	17. Outer Cover Plate/Man Way Overlap	-106.5	12.5	0	87488	760	2631	2002	5.3	3.43	5

Notes

(a) Node numbers are retained for further reference.

(1-11) Appropriate stress reduction factor for the welds and modifications listed in Table 1 have been applied. The number refers to the particular location and corresponding stress reduction factor in

(b) WF=1.4

5. Conclusions

The modifications described in Section 3 and summarized in Table 7 to allow operation of the NMP2 steam dryer at EPU conditions have been evaluated using a harmonic stress analysis. The analysis calculates the stresses arising when the steam dryer is subjected to acoustic loads inferred from strain gage measurements on the main steam lines and a calibrated acoustic circuit model (ACM, Rev. 4.1) that uses these measurements to obtain the acoustic loads on the dryer. The ANSYS FEA package is then used to acquire the dryer stress response resulting from these acoustic loads and post-processed to obtain the limiting alternating stress ratios.

The results account for all biases and uncertainties identified for both the ACM Rev. 4.1 and the FEA harmonic analysis. Additional conservatisms in the model include: (i) use of frequency shifting to obtain the limiting stress at a location (the highest stress or lowest stress ratio must always be used); (ii) the requirement to meet a target EPU stress ratio of 2.0; (iii) usage of the most conservative endurance limit curve C (13.6 ksi) in Fig I-9.2.2 of Appendix I in Section III of the ASME B&PV Code [6], rather than the permissible curve B (16.5 ksi) thus effectively imposing an additional 21.3% margin; and (iv) the additional safety margins (approximately a factor of two) inherent to the endurance limit Curves, C and B.

The stress evaluation shows that the limiting alternating stress ratio on the dryer with all modifications implemented is SR-a=2.85 and occurs on the outer hood/cover plate junction. The next highest alternating stress ratio (SR-a=2.88) occurs on the outer hood/hood support/cover plate junction and is addressed using a stress relief cut-out hole. Previous steam dryer stress evaluations indicated the need for reinforcement of the closure plate attachment welds to sustain the stresses induced by closure plate vibrations. With the steam dryer modifications proposed in the current evaluation, these closure plate weld reinforcements are no longer necessary. Without these reinforcements the limiting alternating stress ratio on a weld reduces slightly to SR-a=2.84 which remains above the target EPU stress margin.

In light of the aforementioned conservatisms, these stress ratios are expected to qualify the steam dryer for EPU operation both with and without reinforcement of the closure plate attachment welds.

6. References

1. Continuum Dynamics, Inc. (2010) *Stress Assessment of Nine Mile Point Unit 2 Steam Dryer Using the Acoustic Circuit Model Rev. 4.1.* C.D.I. Report No. 10-11P (Proprietary), June.
2. Continuum Dynamics, Inc. (2010) *ACM Rev. 4.1: Methodology to Predict Full Scale Steam Dryer Loads from In-Plant Measurements.* C.D.I. Report No. 10-09P (Proprietary), June.
3. Continuum Dynamics, Inc. (2010) *Acoustic and Low-Frequency Hydrodynamic Loads at CLTP Power Level on Nine Mile Point Unit 2 Steam Dryer to 250 Hz Using ACM Rev. 4.1.* C.D.I. Report No. 10-10P (Proprietary), June.
4. Continuum Dynamics, Inc. (2007) *Methodology to Predict Full Scale Steam Dryer Loads from In-Plant Measurements, with the Inclusion of a Low Frequency Hydrodynamic Contribution.* C.D.I. Report No. 07-09P (Proprietary).
5. Continuum Dynamics, Inc. (2009) *Stress Assessment of Nine Mile Point Unit 2 Steam Dryer at CLTP and EPU Conditions, Rev. 1.* C.D.I. Report No. 09-26P (Proprietary), December.
6. *ASME Boiler and Pressure Vessel Code, Section III, Subsection NG (2007).*
7. Structural Integrity Associates, Inc. (2010) *Flaw Evaluation of Indications in the Nine Mile Point Unit 2 Steam Dryer Vertical Support Plates Considering Extended Power Uprate Flow Induced Vibration Loading (Rev. 0).* SIA Calculation Package No. 1000814.401, July.
8. Structural Integrity Associates, Inc. (2008) *Shell and Solid Sub-Model Finite Element Stress Comparison, Rev. 2.* Calculation Package, 0006982.301, Oct. 17.
9. Continuum Dynamics, Inc. (2008) *Stress Assessment of Browns Ferry Nuclear Unit 2 Steam Dryer with Outer Hood and Tie-Bar Reinforcements, Rev. 0.* C.D.I. Report No. 08-20P (Proprietary).
10. Structural Integrity Associates, Inc. (2008) *Comparison Study of Substructure and Submodel Analysis using ANSYS.* Calculation Package, 0006982.304, December.
11. Continuum Dynamics, Inc. (2009) *Response to NRC Round 23 RAI EMCB 201/162 part c.* January.
12. Continuum Dynamics, Inc. (2009) *Compendium of Nine Mile Point Unit 2 Steam Dryer Sub-Models Away From Closure Plates* C.D.I. Technical Note No. 09-16P (Proprietary), August.
13. Continuum Dynamics, Inc. (2010) *Sub-model analysis of the Nine Mile Point steam dryer high stress location at node 85723, hood - base plate - hood support – backing bar junction.* C.D.I. Letter Report, April.
14. Structural Integrity Associates, Inc. (2009) *Nine Mile Point Unit 2 Steam Dryer Closure Plates Analysis Results.* SIA Letter Report No. 0900895.401 Revision 0, August 21.
15. Continuum Dynamics, Inc. (2008) *Acoustic and Low Frequency Hydrodynamic Loads at CLTP Power Level on Nine Mile Point Unit 2 Steam Dryer to 250 Hz, Rev. 2.* C.D.I. Report No. 08-08P (Proprietary).
16. ASME, ed. K.R. Rao, *Companion Guide to the ASME B&PVC, 2nd ed.* 2006.
17. Hechmer, J.L. and G.L Hollinger, *3D Stress Criteria, Guidelines for Application, WRC Bulletin 429.* 1998: New York.
18. Westinghouse (2010) *Indication Notification Form NMP2-RFO-12-INF-10-20, Rev. 0.*

Appendix A. Sub-model Analyses of Outer Hood/Hood Support/Cover Plate and Drain Channel/Skirt Junctions

Several locations on the steam dryer are examined using sub-modeling as described in Section 2.2. Table 1 summarizes the sub-models used to generate the stress tables in prior stress reports [1, 5] for the Nine Mile Point steam dryer and in the present evaluation. The current evaluation involved three additional sub-models (locations 9-11 in Table 1) that are detailed below. These are:

- outer hood/hood support/outer cover plate junction (node 95267)
- same location, but with a stress relief cut-out to reduce the high stress location
- drain channel/skirt junction (node 93430)

[[

(3)]]

A1. Outer Hood/Hood Support/Outer Cover Plate Junction (Node 95267)

A sub-model analysis at the outer hood location was performed on the 6" by 6" by 9" box, see Fig. A1-1. In the global shell model and shell sub-model no weld details were modeled. In the solid sub-model all welds and spacer plate are modeled explicitly. The dimensions of welds and spacer plate are estimated from available drawings (GE drawing 795E258 dwg section H-H and M-M) and the photographs in the flaw evaluation report in [18]. The various component thicknesses in the sub-model are as follows: 0.5" for the hood, 0.25" for the hood support, 0.375" for the outer cover plate and 0.25" for the spacer plate. All weld legs are 0.18". The width of the spacer plate is 0.75" and the weld along the bottom of the spacer plate is 1" long. There is a weld wrap around the bottom of the spacer plate, but no such wrap around the bottom of the hood support.

Stress intensity contours in the shell sub-model are shown in Fig. A1-2. Note, that the stresses at the hot spot are higher than in the global shell model due to finer grid resolution. Stresses in the shell sub-model are best compared to the global model at the nodes next to the hot spot, i.e. 1"-2" away from the singularity, where matching is performed in least-square procedure.

Solid sub-model results are shown in Fig. A1-3. Strong singularities are present at the abrupt weld ends and the linearization technique failed to provide any stress reduction compared to the global shell model.

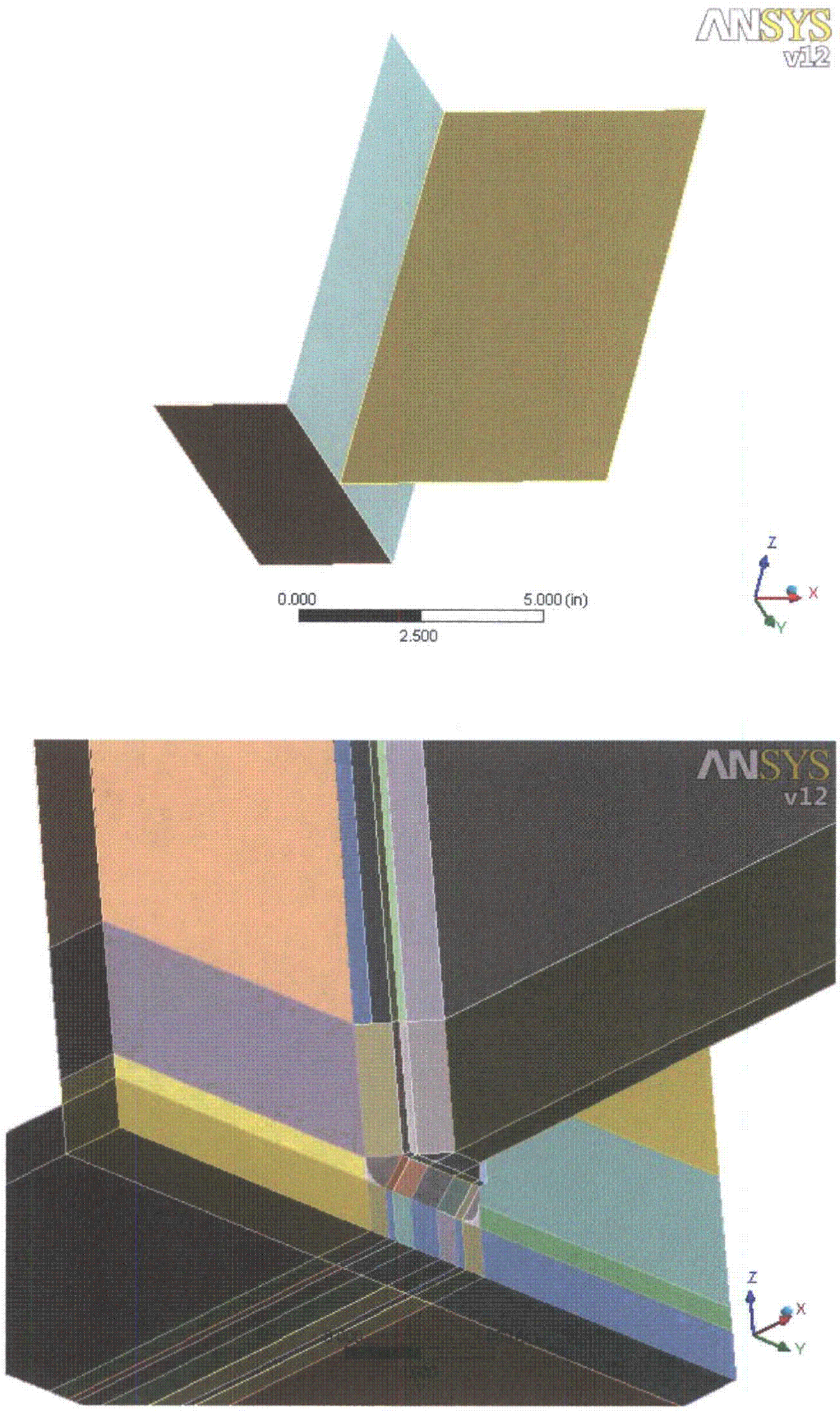

Figure A1-1. Shell sub-model (top) and solid sub-model (bottom).

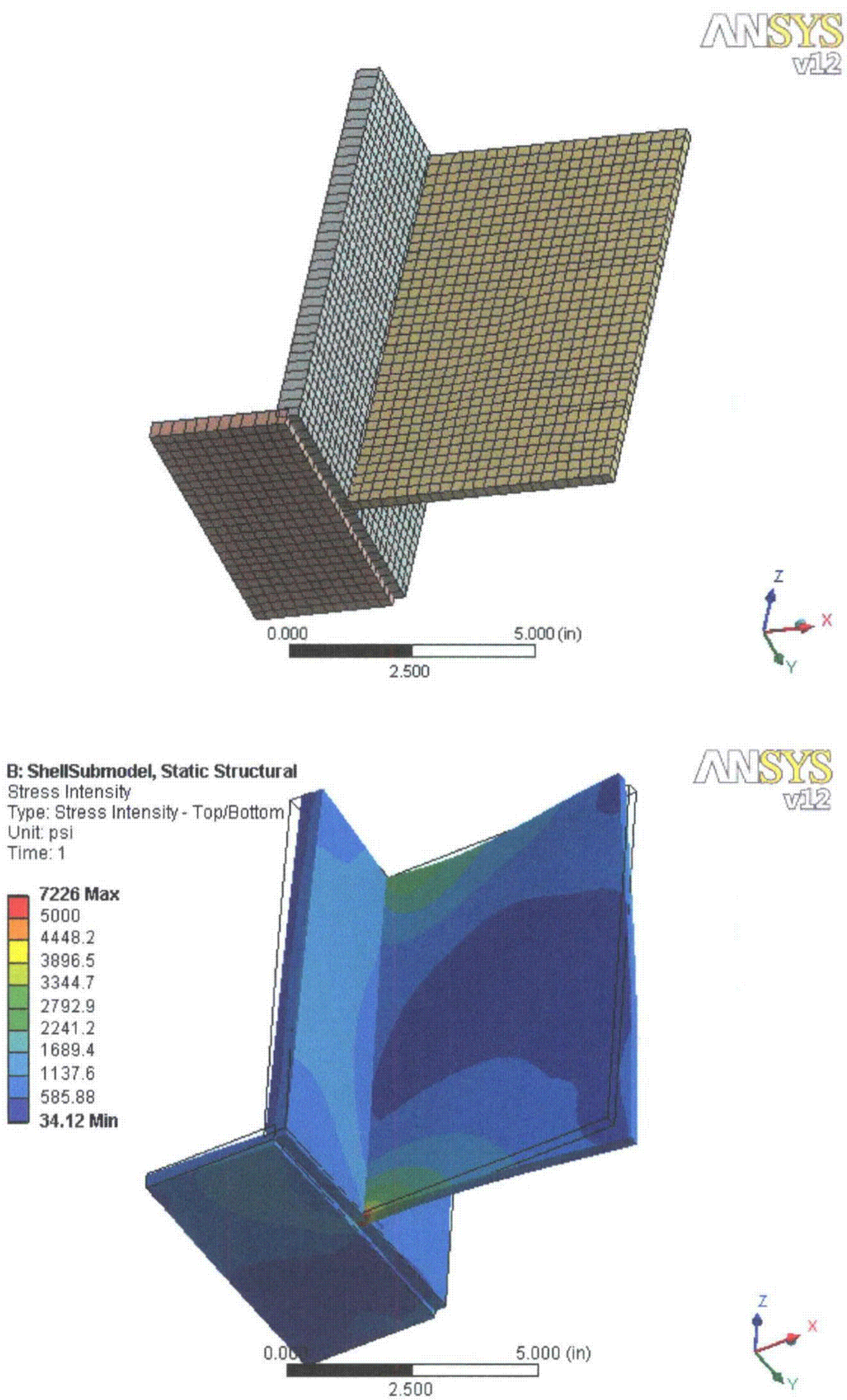

Figure A1-2. Shell sub-model. Grid (top) and stress intensity contours (bottom). Deformation are shown relative to the undeformed structure indicated by the wireframe (displacements are exaggerated for clarity)

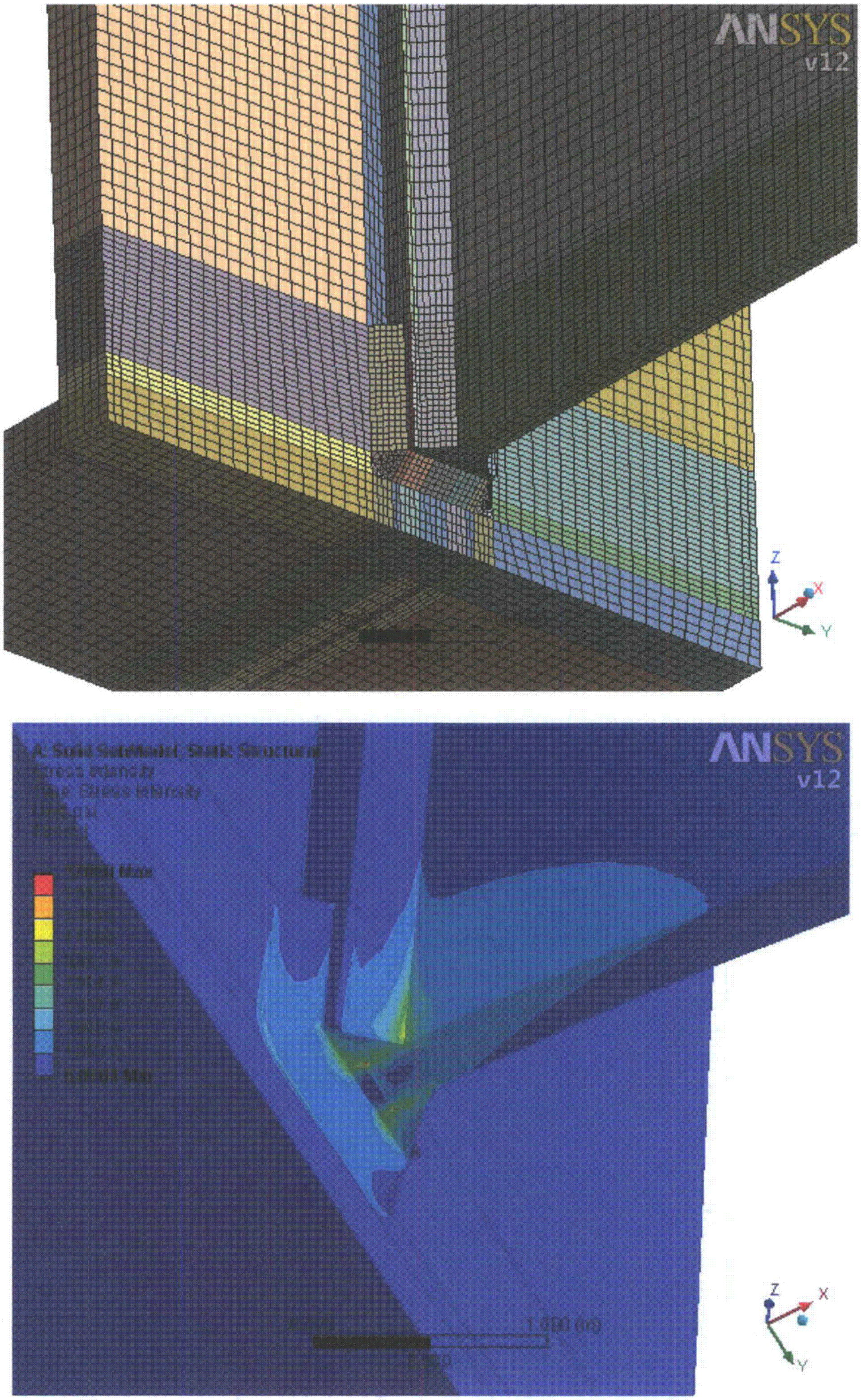

Figure A1-3. Solid sub-model. Grid (top), stress intensity contours (bottom)

A2. Hood Support/Outer Hood/Outer Cover Plate Junction with Stress Relief Cut-Out (Node 95267)

As shown in the previous section, excessive stresses are calculated at the end of the weld at the hood support/outer hood junction. To reduce these stresses a cut-out in the vicinity of the stress concentration is introduced. The resulting geometry is shown in Fig. A2-1.

A parametric study was performed to find the optimum cut-out placement. The two independent parameters are the radius of the cut-out and the distance from the cut-out to the weld line. The value being optimized is the maximum of the stress intensity at the existing high stress location (the 1.8 weld factor is applied to obtain this stress) and the stress intensity on the perimeter of the cut-out where stress concentration occurs. Typically, stresses are redistributed in the vicinity of the junction in such a way that weld stresses are reduced, but the shear stresses at the cut-out edge are increased and minimizing the higher of these two stresses is tantamount to making both stresses equal. In FEA parametric calculations the distance from the cut-out and the radius were varied and stresses computed in a shell element sub-model with nominal 0.25" resolution. For each parameter set, a normalized stress, Σ, was calculated by taking the higher of the stresses at the hot spot (multiplied by 1.8) and the hole perimeter and dividing this value by the stress needed to achieve a 2.76 stress ratio (this limiting stress is given by 13,600/(1.1*2.76)=4480 psi where 13000 psi is the allowable fatigue stress, 1.1 accounts for differences in the Young's modulus and 2.76 is the target stress ratio).

Figure A2-2 reveals that there are optimum parameters for the cut-out to minimize stresses both at the weld line and at the cut-out edge. The optimal radius is 1.5" and the optimal distance to the weld line is approximately 0.5". In this configuration the optimum normalized stress, Σ, was determined to be 0.695 which corresponds to a weld stress (before the application of the 1.8 weld factor) of 0.695*4480/1.8=1730 psi. Comparing this value to the computed global shell stress of 2993 psi leads to a stress reduction factor (SRF) of 1730/2993= 0.58. From Fig. A2-2 the location appears to be robust in a sense that small variations in the radius and the distance still keep stresses well below the limiting values.

The stress distribution in the shell sub-model for the optimal cut-out is shown in Fig. A2-3. These stress contours can be directly compared to the unmodified configuration in Fig. A1-2. As expected, the highly localized stress in the unmodified configuration is redistributed and the stresses on the weld line are much lower. Meanwhile, stresses at the cut-out edge have increased, but still are within the required limits.

To compare solid sub-models with and without the cut-out the optimum stress relief cut-out configuration was implemented in the solid sub-model. Note that in the solid sub-model the edge of the stress relief cut-out hole is located 0.5" from the toe of the fillet weld connecting the hood support to the spacer plate. The resulting stress distribution is shown in Fig. A2-4. To quantify the stress reduction in the solid sub-model, a number of linearization paths through the singular locations at the weld end were considered as shown in Fig. A2-5. The results are summarized in Table A2-1. Based on Table A2-1, the conservative stress reduction factor at the weld end due to stress relief cut-out is 0.73. This is more conservative than the factor of 0.58 obtained from the shell sub-model. It is noted however, that the linearization paths (or SCLs) adopted in the solid model pass through stress singularities and thus are overly conservative as indicated in [16, 17] and discussed above. Other contributors to the difference in shell and solid sub-model SRF predictions include the more detailed geometrical details retained in the solid model and reference point used to measure the hole location (in the shell model the center plane of the hood is used, whereas in the solid mode the weld toe is used – these distinctions do not arise in the shell element representation, but are relevant in the solid model description). On account of these factors, the more conservative result is used so that the SRF for this location is **0.73.**

Table A2-1. Linearized stresses in the solid sub-models.

Linearization path	Stress with no modification	Stress with relief cut-out	Stress reduction
A	5150	2327	0.45
B	9251	6516	0.70
C	7444	5150	0.69
D	8309	6064	0.73
E	6698	4778	0.71

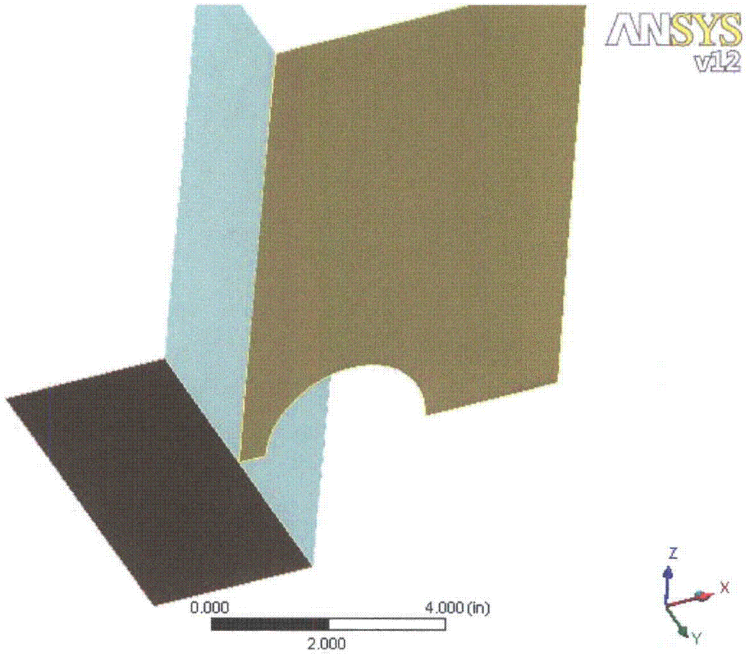

Figure A2-1. Shell sub-model with circular stress relief cut-out.

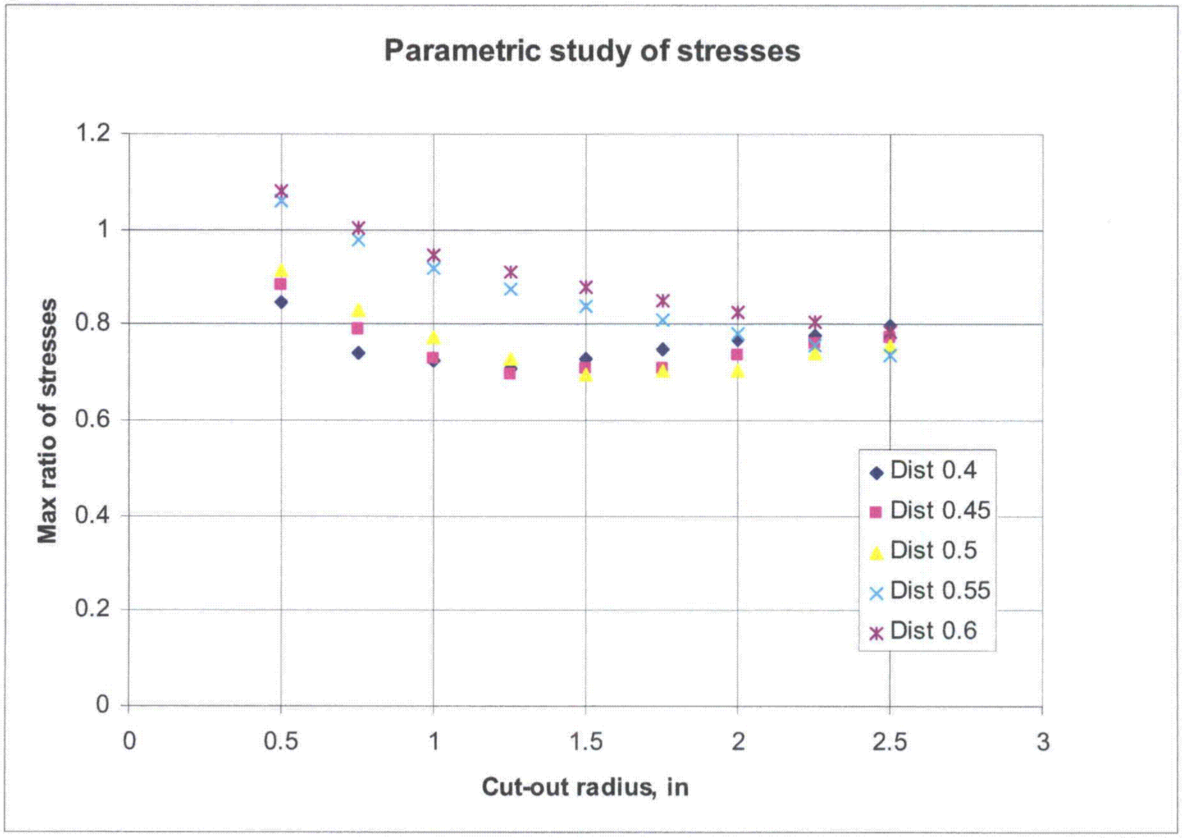

Figure A2-2. Parametric study of stresses in the shell sub-model with the cut-out. 'Dist' refers to distance from the cut-out to the weld line in inches. Normalized Stress' refers to the maximum of the stresses at: (i) the original high stress location on the weld and (ii) the perimeter of the cut-out hole. This value is normalized by the stress needed to obtain a stress ratio of 2.76.

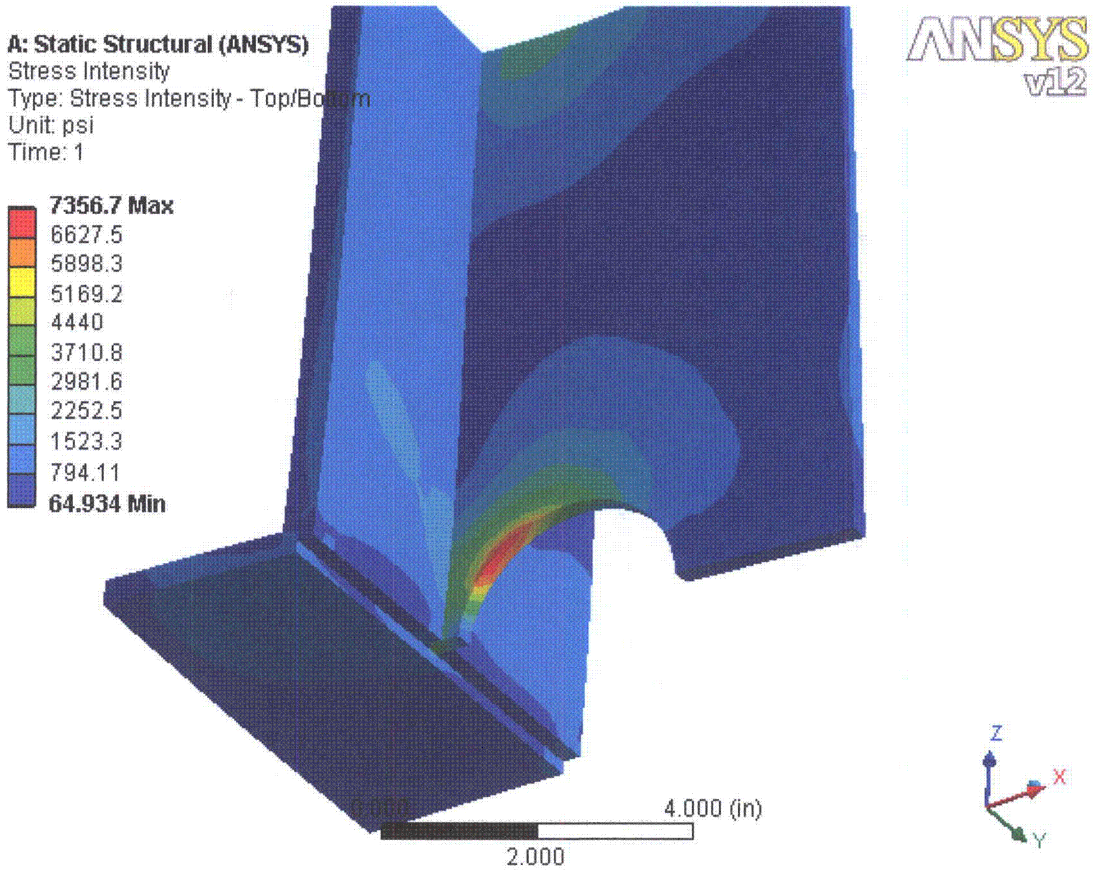

Figure A2-3. Stress intensity contours in the optimal cut-out configuration. Factor α is not applied.

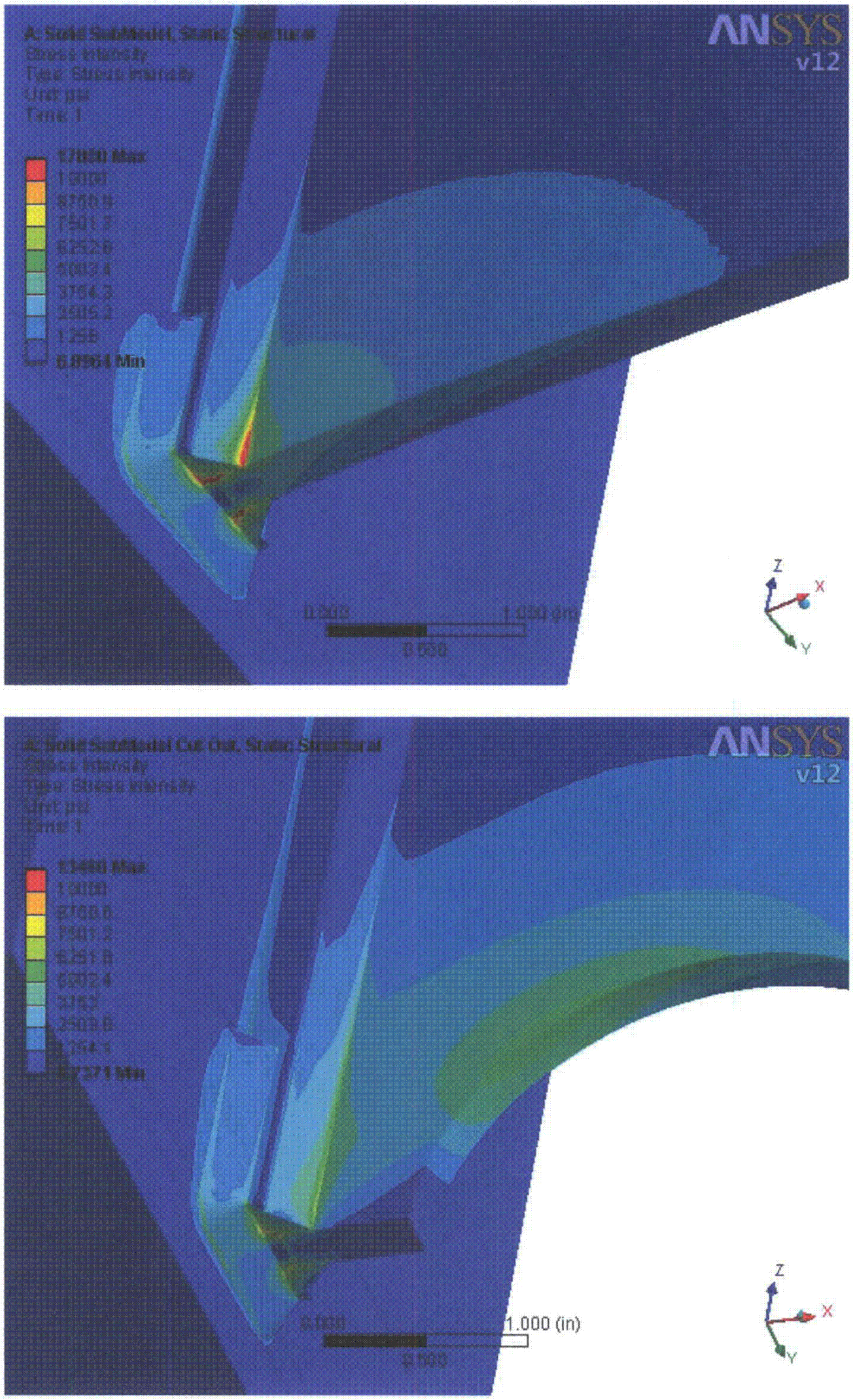

Figure A2-4. Stress distribution in the solid sub-model with and without the cut-out, optimized in the shell sub-model. Stress contours are at the same levels for direct comparison.

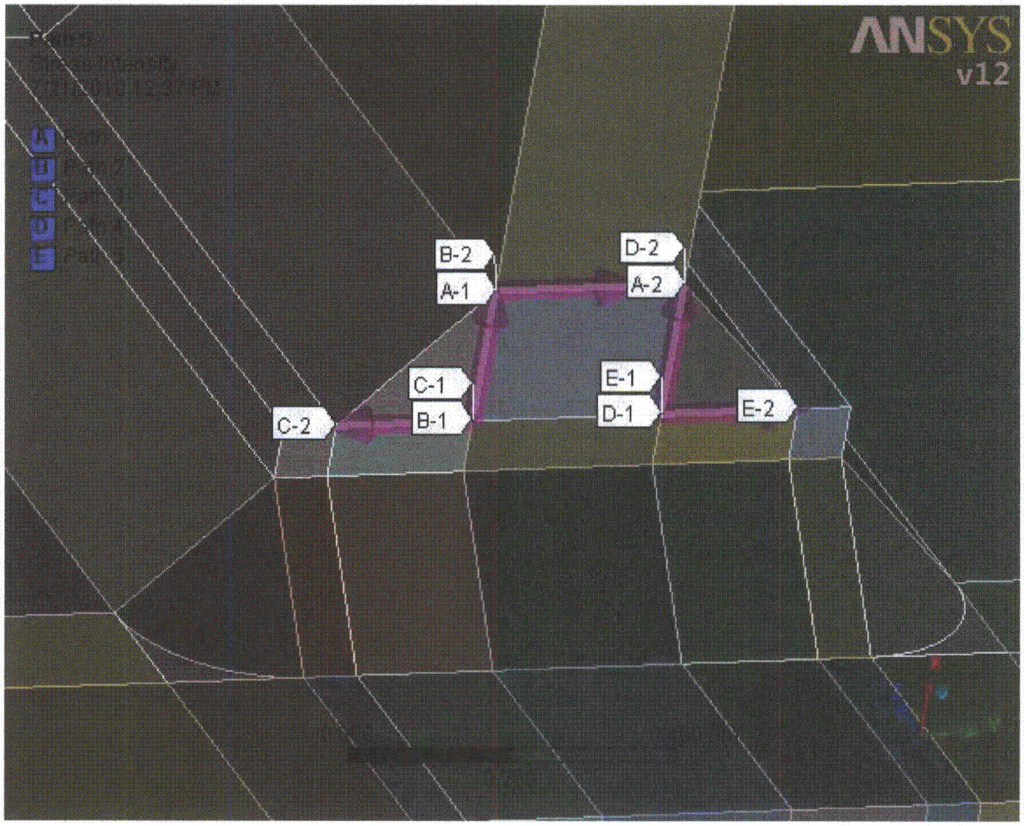

Figure 2-5. Stress linearization paths for comparison in the solid sub-models with and without the cut-out.

A3. Drain Channel/Skirt Junction (Node 93430)

Stresses exceeding target stress margins at EPU occur at the bottom of the drain channel connection to the skirt. A sub-model was excised from the global model by means of an intersection box placed about the high stress point. The sub-model boundaries consist of the intersection lines obtained where the box intersects the global shell model and the forces and moments on these boundaries are derived by integrating the stresses as described at the beginning of this Appendix. The stress contours resulting from the application of these perimeter loads together with the equivalent dynamic inertial loads, are shown in Fig. A3-1.

The same forcing was then applied to the solid sub-model with an explicitly modeled 0.125" fillet weld connecting the drain channel and skirt. The one-sided fillet weld was modeled with a wrap ending at the bottom of the drain channel. The resulting stress contours are shown in Fig. A3-2 which shows that the weld wrap around shifts the high stress location at the weld root to a location higher up along the weld line. A localized stress singularity is also visible at the end of the weld as seen in Fig. A3-2.

The linearized stresses are required for fatigue evaluation and the linearization paths used for this purpose are shown in Fig. A3-3 and the resulting linearized stresses tabulated in Table A3-1. Note, that the calculated linearized stress through the singularity is significantly higher than along other paths. However the paths near the singularity and in the weld wrap end do not adhere to ASME guidelines for linearization path choice and result in overly conservative stresses. In particular it is noted that these paths are not perpendicular to either the stress flow or the plate surfaces and thus should not be considered valid. Nevertheless, they are retained here to ensure that the results remain conservative.

To reduce the local stresses through the weld a second solid element-based sub-model with: (i) an increased 0.25" weld and (ii) a wrap-around weld extended for 1 inch inside the drain channel, was prepared and analyzed. The resulting stress intensity contours are shown in Figs. A3-4 and A3-5. The latter figure in particular shows that the stresses at the weld root are significantly reduced due to the addition of the thickened and extended wrap-around weld. Linearization paths are erected at the highest stress region as shown in Fig. A3-6. The linearized stresses are extracted and reported in Table A3-2.

Note, that reinforcing the weld provides a robust reduction of the linearized stresses with a stress reduction factor of 0.64, including linearization paths through singularity. If one excludes path A which passes through a singularity and thus does not constitutes a valid linearization path per [16, 17] then all the linearized stresses in the 0.25" weld model are lower than the global stress of 2575 psi. Of the remaining valid paths, the largest linearized stress at path B would yield stress reduction factor of SRF=1683/2575=0.65. Thus, upon reinforcement of the weld in the manner described, the conservative value of **SRF=0.65** can be used at this location.

Table A3-1. Linearization results for 0.125" weld.

SCL path	ANSYS linearized M+B stress intensity
A	6534
B	2800
C	2288
D	1995
E	2863
F	2730
G	2227
H	2625

Table A3-2. Linearization results for 0.25" weld.

SCL path	ANSYS linearized M+B stress intensity	Corresponding path and stress in the 0.125" weld model	Stress reduction relative to the 0.125" weld model
A	4064	A: 6534	0.62
B	1683	B: 2800	0.60
C	1468	C: 2288	0.64
D	1228	E: 2863	0.43
E	1187	F: 2730	0.43

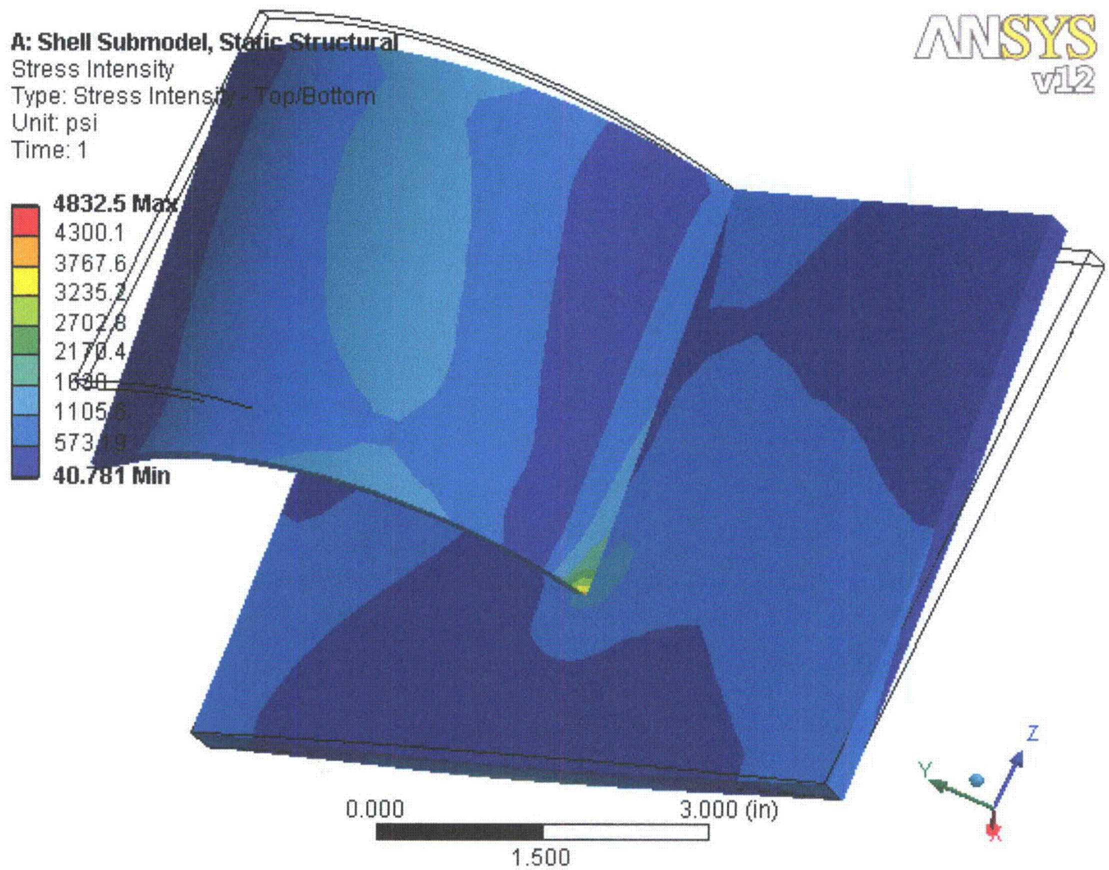

Figure A3-1. Stress intensity in the shell sub-model of the skirt/drain channel connection. The wireframe represents the undeformed structure. Displacements are exaggerated for clarity.

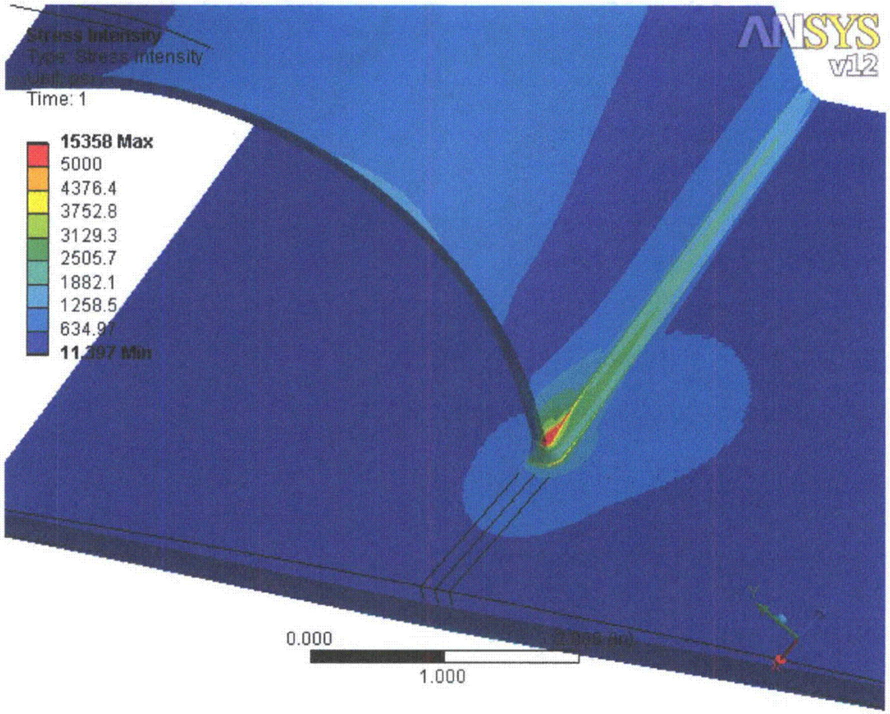

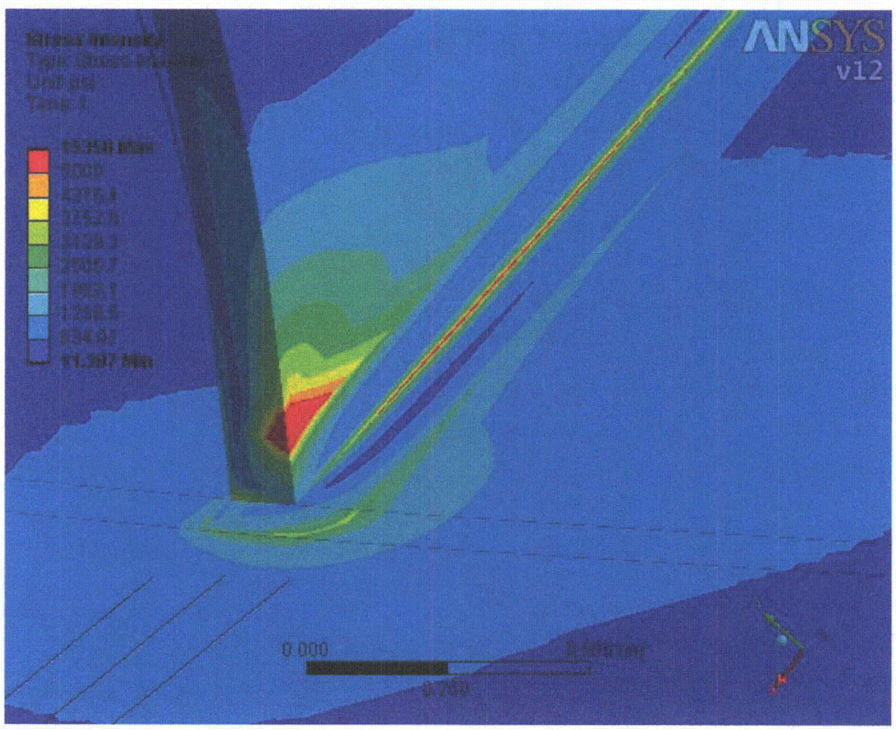

Figure A3-2. Stress intensity contours in the solid sub-model with 0.125" fillet weld. In the bottom picture the weld elements are removed to show high stresses at the weld root.

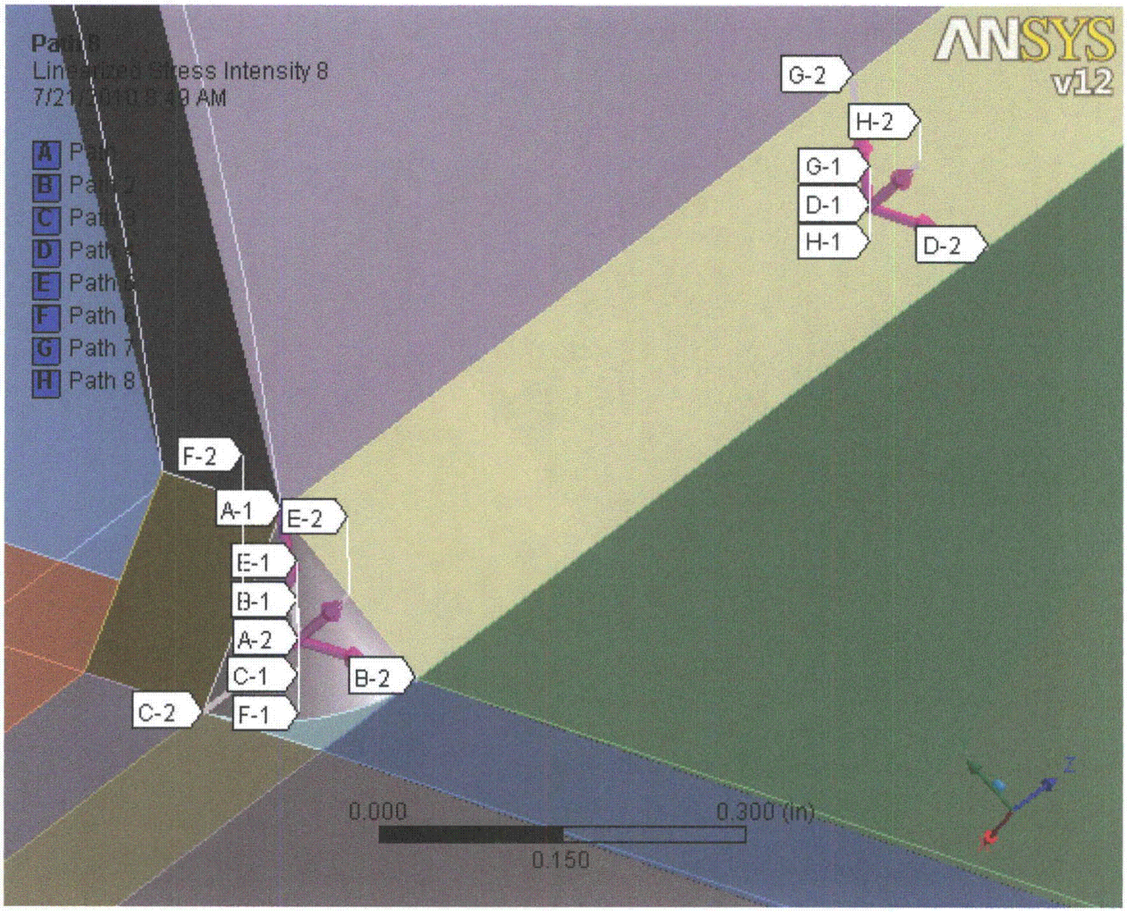

Figure A3-3. Linearization paths through the welds. Paths A-C,E,F pertain to the end of the weld and paths D,G-H are located at the weld section with largest root stress.

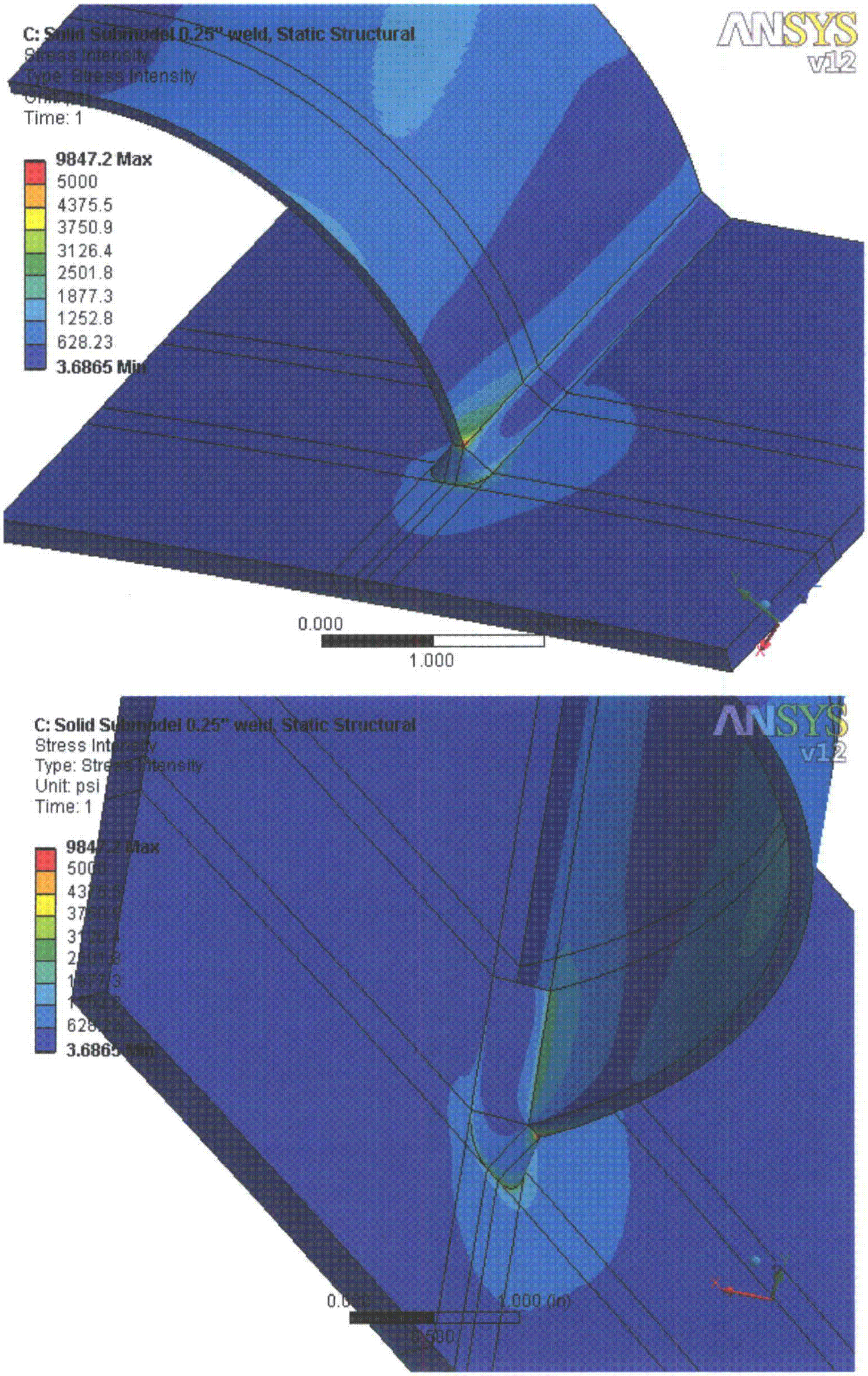

Figure A3-4. Stress intensity contours with increased 0.25" weld.

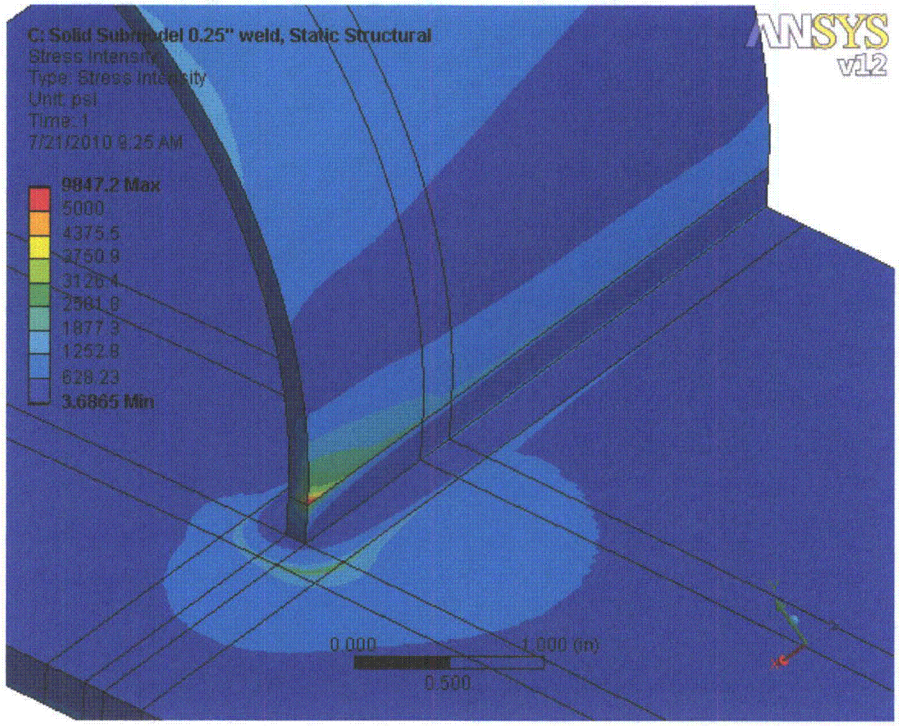

Figure A3-5. Stress intensity contours in the solid sub-model with 0.25" fillet weld. Weld elements are removed to show stresses at the weld root.

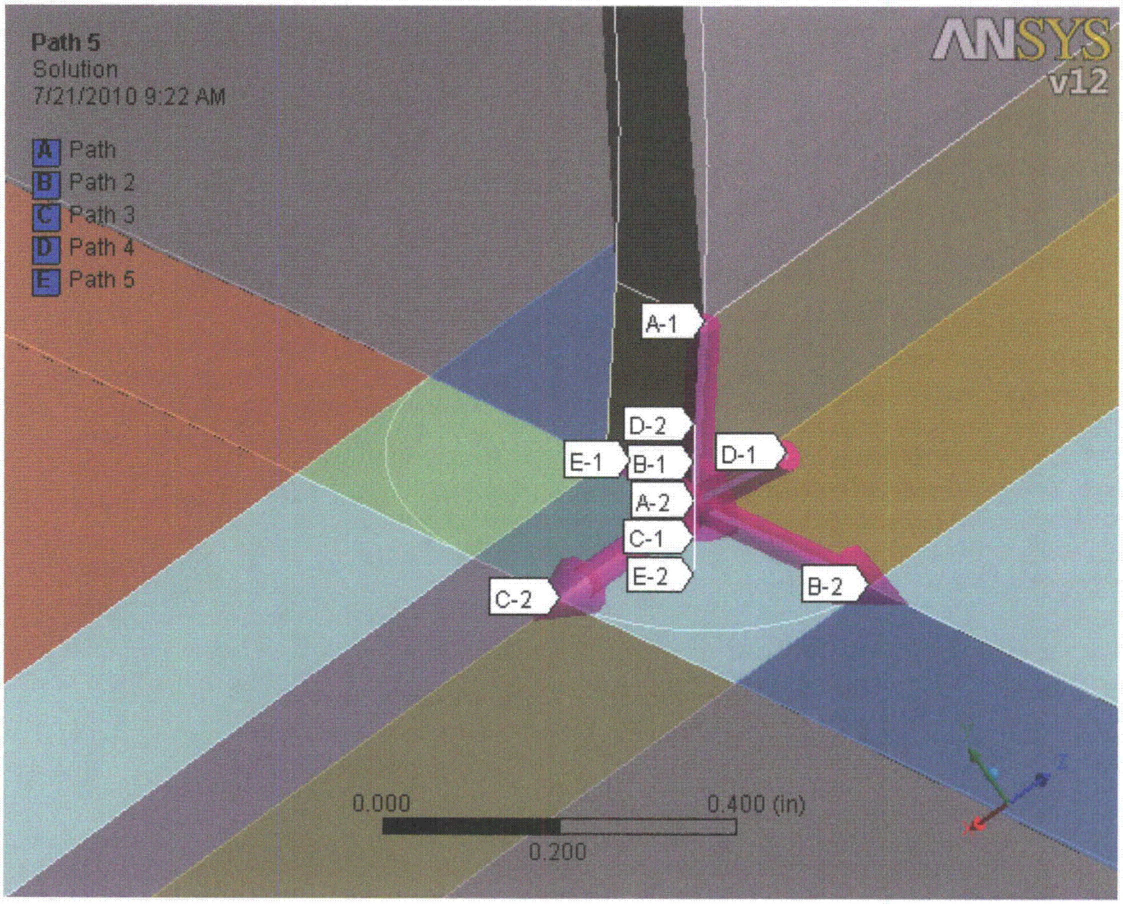

Figure A3-6. Stress linearization paths through the high stress region in the weld.

ATTACHMENT 6

AFFIDAVIT JUSTIFYING WITHHOLDING PROPRIETARY INFORMATION FROM GE-HITACHI NUCLEAR ENERGY AMERICAS LLC

Nine Mile Point Nuclear Station, LLC
July 30, 2010

GE-Hitachi Nuclear Energy Americas LLC

AFFIDAVIT

I, James F. Harrison, state as follows:

(1) I am Vice President, Fuel Licensing, Regulatory Affairs, GE-Hitachi Nuclear Energy Americas LLC ("GEH"), and have been delegated the function of reviewing the information described in paragraph (2) which is sought to be withheld, and have been authorized to apply for its withholding.

(2) The information sought to be withheld is contained in GEH letter, GE-PPO-1GYEF-KG1-546, G. Carlisle, GEH to Theresa Darling, Constellation Energy Nuclear Group, "NMP2 EPU Round 5 RAI Responses" dated July 28, 2010. The proprietary information in Enclosure 3 entitled, GEH Responses to NMP2 EPU Follow-up RAIs – Reactor Systems (Proprietary); is identified by a dark red dotted underline inside double square brackets, [[This sentence is an example.{3}]]. In each case, the superscript notation {3} refers to Paragraph (3) of this affidavit, which provides the basis for the proprietary determination.

(3) In making this application for withholding of proprietary information of which it is the owner or licensee, GEH relies upon the exemption from disclosure set forth in the Freedom of Information Act ("FOIA"), 5 USC Sec. 552(b)(4), and the Trade Secrets Act, 18 USC Sec. 1905, and NRC regulations 10 CFR 9.17(a)(4), and 2.390(a)(4) for trade secrets (Exemption 4). The material for which exemption from disclosure is here sought also qualifies under the narrower definition of trade secret, within the meanings assigned to those terms for purposes of FOIA Exemption 4 in, respectively, Critical Mass Energy Project v. Nuclear Regulatory Commission, 975 F2d 871 (DC Cir. 1992), and Public Citizen Health Research Group v. FDA, 704 F2d 1280 (DC Cir. 1983).

(4) The information sought to be withheld is considered to be proprietary for the reasons set forth in paragraphs (4)a. and (4)b. Some examples of categories of information that fit into the definition of proprietary information are:

a. Information that discloses a process, method, or apparatus, including supporting data and analyses, where prevention of its use by GEH's competitors without license from GEH constitutes a competitive economic advantage over other companies;

b. Information that, if used by a competitor, would reduce their expenditure of resources or improve their competitive position in the design, manufacture, shipment, installation, assurance of quality, or licensing of a similar product;

c. Information that reveals aspects of past, present, or future GEH customer-funded development plans and programs, resulting in potential products to GEH;

d. Information that discloses trade secret and/or potentially patentable subject matter for which it may be desirable to obtain patent protection.

(5) To address 10 CFR 2.390(b)(4), the information sought to be withheld is being submitted to NRC in confidence. The information is of a sort customarily held in confidence by GEH, and is in fact so held. The information sought to be withheld has, to the best of my knowledge and belief, consistently been held in confidence by GEH, not been disclosed publicly, and not been made available in public sources. All disclosures to third parties, including any required transmittals to the NRC, have been made, or must be made, pursuant to regulatory provisions or proprietary and/or confidentiality agreements that provide for maintaining the information in confidence. The initial designation of this information as proprietary information, and the subsequent steps taken to prevent its unauthorized disclosure, are as set forth in the following paragraphs (6) and (7).

(6) Initial approval of proprietary treatment of a document is made by the manager of the originating component, who is the person most likely to be acquainted with the value and sensitivity of the information in relation to industry knowledge, or who is the person most likely to be subject to the terms under which it was licensed to GEH. Access to such documents within GEH is limited to a "need to know" basis.

(7) The procedure for approval of external release of such a document typically requires review by the staff manager, project manager, principal scientist, or other equivalent authority for technical content, competitive effect, and determination of the accuracy of the proprietary designation. Disclosures outside GEH are limited to regulatory bodies, customers, and potential customers, and their agents, suppliers, and licensees, and others with a legitimate need for the information, and then only in accordance with appropriate regulatory provisions or proprietary and/or confidentiality agreements.

(8) The information identified in paragraph (2) above is classified as proprietary because it contains results of an analysis performed by GEH to support Nine Mile Point-2 Extended Power Uprate (EPU) license application. This analysis is part of the GEH EPU methodology. Development of the extended power uprate methodology and the supporting analysis techniques and information, and their application to the design, modification, and processes were achieved at a significant cost to GEH.

The development of the evaluation methodology along with the interpretation and application of the analytical results is derived from the extensive experience database that constitutes a major GEH asset.

(9) Public disclosure of the information sought to be withheld is likely to cause substantial harm to GEH's competitive position and foreclose or reduce the availability of profit-making opportunities. The information is part of GEH's comprehensive BWR safety and technology base, and its commercial value extends beyond the original development cost. The value of the technology base goes beyond the extensive physical database and analytical methodology and includes development of the expertise to determine and apply the appropriate evaluation process. In addition, the technology base includes the value derived from providing analyses done with NRC-approved methods.

The research, development, engineering, analytical and NRC review costs comprise a substantial investment of time and money by GEH. The precise value of the expertise to devise an evaluation process and apply the correct analytical methodology is difficult to quantify, but it clearly is substantial. GEH's competitive advantage will be lost if its competitors are able to use the results of the GEH experience to normalize or verify their own process or if they are able to claim an equivalent understanding by demonstrating that they can arrive at the same or similar conclusions.

The value of this information to GEH would be lost if the information were disclosed to the public. Making such information available to competitors without their having been required to undertake a similar expenditure of resources would unfairly provide competitors with a windfall, and deprive GEH of the opportunity to exercise its competitive advantage to seek an adequate return on its large investment in developing and obtaining these very valuable analytical tools.

I declare under penalty of perjury that the foregoing affidavit and the matters stated therein are true and correct to the best of my knowledge, information, and belief.

Executed on this 28th day of July 2010.

James F. Harrison

James F. Harrison
Vice President, Fuels Licensing
Regulatory Affairs
GE-Hitachi Nuclear Energy Americas LLC
3901 Castle Hayne Rd.
Wilmington, NC 28401

ATTACHMENT 7

AFFIDAVIT JUSTIFYING WITHHOLDING PROPRIETARY INFORMATION FROM GLOBAL NUCLEAR FUEL - AMERICAS LLC

Nine Mile Point Nuclear Station, LLC
July 30, 2010

Global Nuclear Fuel - Americas LLC

AFFIDAVIT

I, Anthony P. Reese, state as follows:

(1) I am Manager, Reload Design and Analysis, Global Nuclear Fuel–Americas, LLC ("GNF-A"), and have been delegated the function of reviewing the information described in paragraph (2) which is sought to be withheld, and have been authorized to apply for its withholding.

(2) The information sought to be withheld is contained in letter GE-PPO-1GYEF-KG1-546, G. Carlisle, GEH to Theresa Darling, Constellation Energy Nuclear Group, "NMP2 EPU Round 5 RAI Responses" dated July 28, 2010. GNF-A proprietary information in Enclosure 4 report labeled 0000-0032-0998-R2, and entitled "MCNP01A Low Enriched UO2 Pin Lattice in Water Critical Benchmark Evaluations Using ENDF/B-V Nuclear Cross-Section Data, Revision 1," dated June 2010, is identified by a dark red dotted underline inside double square brackets. [[This sentence is an example.{3}]] In each case, the superscript notation {3} refers to Paragraph (3) of this affidavit that provides the basis for the proprietary determination.

(3) In making this application for withholding of proprietary information of which it is the owner or licensee, GNF-A relies upon the exemption from disclosure set forth in the Freedom of Information Act (FOIA), 5 USC Sec. 552(b)(4), and the Trade Secrets Act, 18 USC Sec. 1905, and NRC regulations 10 CFR 9.17(a)(4), and 2.390(a)(4) for trade secrets (Exemption 4). The material for which exemption from disclosure is here sought also qualifies under the narrower definition of trade secret, within the meanings assigned to those terms for purposes of FOIA Exemption 4 in, respectively, Critical Mass Energy Project v. Nuclear Regulatory Commission, 975 F2d 871 (DC Cir. 1992), and Public Citizen Health Research Group v. FDA, 704 F2d 1280 (DC Cir. 1983).

(4) The information sought to be withheld is considered to be proprietary for the reasons set forth in paragraphs (4)a. and (4)b. Some examples of categories of information that fit into the definition of proprietary information are:

a. Information that discloses a process, method, or apparatus, including supporting data and analyses, where prevention of its use by GNF-A's competitors without license from GNF-A constitutes a competitive economic advantage over GNF-A and/or other companies.

b. Information that, if used by a competitor, would reduce their expenditure of resources or improve their competitive position in the design, manufacture, shipment, installation, assurance of quality, or licensing of a similar product.

c. Information that reveals aspects of past, present, or future GNF-A customer-funded development plans and programs, that may include potential products of GNF-A.

d. Information that discloses trade secret and/or potentially patentable subject matter for which it may be desirable to obtain patent protection.

(5) To address 10 CFR 2.390(b)(4), the information sought to be withheld is being submitted to the NRC in confidence. The information is of a sort customarily held in confidence by GNF-A, and is in fact so held. The information sought to be withheld has, to the best of my knowledge and belief, consistently been held in confidence by GNF-A, not been disclosed publicly, and not been made available in public sources. All disclosures to third parties, including any required transmittals to the NRC, have been made, or must be made, pursuant to regulatory provisions or proprietary and/or confidentiality agreements that provide for maintaining the information in confidence. The initial designation of this information as proprietary information, and the subsequent steps taken to prevent its unauthorized disclosure are as set forth in the following paragraphs (6) and (7).

(6) Initial approval of proprietary treatment of a document is made by the manager of the originating component, who is the person most likely to be acquainted with the value and sensitivity of the information in relation to industry knowledge, or who is the person most likely to be subject to the terms under which it was licensed to GNF-A. Access to such documents within GNF-A is limited to a "need to know" basis.

(7) The procedure for approval of external release of such a document typically requires review by the staff manager, project manager, principal scientist, or other equivalent authority for technical content, competitive effect, and determination of the accuracy of the proprietary designation. Disclosures outside GNF-A are limited to regulatory bodies, customers, and potential customers, and their agents, suppliers, and licensees, and others with a legitimate need for the information, and then only in accordance with appropriate regulatory provisions or proprietary and/or confidentiality agreements.

(8) The information identified in paragraph (2) above is classified as proprietary because it contains details of GNF-A's fuel design and licensing methodology for the Boiling Water Reactor (BWR). Development of these methods, techniques, and information and their application for the design, modification, and analyses methodologies and processes was achieved at a significant cost to GNF-A. The development of the evaluation process along with the interpretation and application of the analytical results is derived from the extensive experience database that constitutes a major GNF-A asset.

(9) Public disclosure of the information sought to be withheld is likely to cause substantial harm to GNF-A's competitive position and foreclose or reduce the availability of profit-making opportunities. The fuel design and licensing methodology is part of GNF-A's comprehensive BWR safety and technology base, and its commercial value extends beyond the original development cost. The value of the technology base goes beyond the extensive physical database and analytical methodology and includes development of the expertise to determine and apply the appropriate evaluation process. In addition, the technology base includes the value derived from providing analyses done with NRC-approved methods.

The research, development, engineering, analytical and NRC review costs comprise a substantial investment of time and money by GNF-A. The precise value of the expertise to devise an evaluation process and apply the correct analytical methodology is difficult to quantify, but it clearly is substantial. GNF-A's competitive advantage will be lost if its competitors are able to use the results of the GNF-A experience to normalize or verify their own process or if they are able to claim an equivalent understanding by demonstrating that they can arrive at the same or similar conclusions.

The value of this information to GNF-A would be lost if the information were disclosed to the public. Making such information available to competitors without their having been required to undertake a similar expenditure of resources would unfairly provide competitors with a windfall, and deprive GNF-A of the opportunity to exercise its competitive advantage to seek an adequate return on its large investment in developing and obtaining these very valuable analytical tools.

I declare under penalty of perjury that the foregoing affidavit and the matters stated therein are true and correct to the best of my knowledge, information, and belief.

Executed on this 28th day of July 2010.

Anthony P. Reese
Manager, Reload Design and Analysis
Global Nuclear Fuel – Americas, LLC
3901 Castle Hayne Rd.
Wilmington, NC 28401

ATTACHMENT 8

AFFIDAVIT JUSTIFYING WITHHOLDING PROPRIETARY INFORMATION FROM CONTINUUM DYNAMICS INC.

Nine Mile Point Nuclear Station, LLC
July 30, 2010

Continuum Dynamics, Inc.

(609) 538-0444 (609) 538-0464 fax 34 Lexington Avenue Ewing, NJ 08618-2302

AFFIDAVIT

Re: C.D.I. Report No. 10-12P – "Design and Stress Evaluation of Nine Mile Point Unit 2 Steam Dryer Modifications for EPU Operation," Revision 0; and Structural Integrity Report No. 1000814.401 "Flaw Evaluation of Indications in the Nine Mile Point Unit 2 Steam Dryer Vertical Support Plates Considering Extended Power Uprate Flow Induced Vibration Loading," Revision 0

I, Alan J. Bilanin, being duly sworn, depose and state as follows:

1. I hold the position of President and Senior Associate of Continuum Dynamics, Inc. (hereinafter referred to as C.D.I.), and I am authorized to make the request for withholding from Public Record the Information contained in the documents described in Paragraph 2. This Affidavit is submitted to the Nuclear Regulatory Commission (NRC) pursuant to 10 CFR 2.390(a)(4) based on the fact that the attached information consists of trade secret(s) of C.D.I. and that the NRC will receive the information from C.D.I. under privilege and in confidence.

2. The Information sought to be withheld, as transmitted to Constellation Energy Group as attachments to C.D.I. Letter No. 10123 dated 28 July 2010, C.D.I. Report No. 10-12P "Design and Stress Evaluation of Nine Mile Point Unit 2 Steam Dryer Modifications for EPU Operation," Revision 0, and Structural Integrity Report No. 1000814.401 "Flaw Evaluation of Indications in the Nine Mile Point Unit 2 Steam Dryer Vertical Support Plates Considering Extended Power Uprate Flow Induced Vibration Loading," Revision 0

3. The Information summarizes:

   (a) a process or method, including supporting data and analysis, where prevention of its use by C.D.I.'s competitors without license from C.D.I. constitutes a competitive advantage over other companies;
   (b) Information which, if used by a competitor, would reduce his expenditure of resources or improve his competitive position in the design, manufacture, shipment, installation, assurance of quality, or licensing of a similar product;
   (c) Information which discloses patentable subject matter for which it may be desirable to obtain patent protection.

   The information sought to be withheld is considered to be proprietary for the reasons set forth in paragraphs 3(a), 3(b) and 3(c) above.

4. The Information has been held in confidence by C.D.I., its owner. The Information has consistently been held in confidence by C.D.I. and no public disclosure has been made and it is not available to the public. All disclosures to third parties, which have been limited, have been made pursuant to the terms and conditions contained in C.D.I.'s Nondisclosure Secrecy Agreement which must be fully executed prior to disclosure.

5. The Information is a type customarily held in confidence by C.D.I. and there is a rational basis therefore. The Information is a type, which C.D.I. considers trade secret and is held in confidence by C.D.I. because it constitutes a source of competitive advantage in the competition and performance of such work in the industry. Public disclosure of the Information is likely to cause substantial harm to C.D.I.'s competitive position and foreclose or reduce the availability of profit-making opportunities.

I declare under penalty of perjury that the foregoing affidavit and the matters stated therein are true and correct to be the best of my knowledge, information and belief.

Executed on this 28 day of July 2010.

Alan J. Bilanin

Alan J. Bilanin
Continuum Dynamics, Inc.

Subscribed and sworn before me this day: July 28, 2010

Eileen P. Burmeister

Eileen P. Burmeister, Notary Public

EILEEN P. BURMEISTER
NOTARY PUBLIC OF NEW JERSEY
MY COMM. EXPIRES MAY 6, 2012